Highly Strained Four-membered Hetero-metallacycles of Group 4 Metallocenes

Dissertation

zur Erlangung des akademischen Grades
"Doktor der Naturwissenschaften" (Dr. rer. nat.)
vorgelegt an der
Mathematisch-Naturwissenschaftlichen Fakultät
der Universität Rostock

von

Dipl.-Chem. Martin Hähnel

geb. am 26.04.1985 in Zwickau

Rostock, den 28. August 2013

urn:nbn:de:gbv:28-diss2014-0065-8

Gutachter:

1. Gutachter: Prof. Dr. Uwe Rosenthal, Leibniz-Institut für Katalyse e.V. an der Universität Rostock

2. Gutachter: Prof. Dr. Axel Schulz, Universität Rostock

3. Gutachter: Prof. Dr. Laurel L. Schafer, University of British Columbia, Vancouver (Kanada)

Datum der Verteidigung: 28. Januar 2014

Auf den nun folgenden Seiten soll all den Bemühungen Rechnung getragen werden, ohne die eine erfolgreiche Arbeit so nicht möglich gewesen wäre. Diese entstand auf Anregung und unter Anleitung von Prof. Dr. Uwe Rosenthal von November 2010 bis August 2013 am Leibniz-Institut für Katalyse e. V. an der Universität Rostock.

Aus diesem Grund gilt mein besonderer und auch erster Dank meinem Betreuer, Prof. Dr. Uwe Rosenthal, nicht nur für die spannende und herausfordernde Themenstellung, sondern vor allem für die stete Balance zwischen gewährtem Freiraum und notwendiger Hilfestellung. Nur so konnte ich diese Arbeit mit meinen Ideen gestalten, ohne dabei das Ziel aus dem Blick zu verlieren. Darüber hinaus möchte ich mich für alle anregenden Diskussionen und Denkanstöße über die Chemie auf der einen und das ganz alltägliche Leben auf der anderen Seite herzlichst bedanken.

Mein überaus herzlicher Dank gebührt zudem Dr. Torsten Beweries, sowohl für die stete Diskussionsbereitschaft, auch wenn die Zeit gerade knapp war, als auch für das mannigfaltige Korrekturlesen verschiedener Manuskripte und die damit einhergehende Weitergabe des Wissens und seiner Erfahrung beim Thema:
"Wie schreibe ich gute englische Texte?"

Meiner Themenleiterin, Dr. Perdita Arndt, danke ich für die vielfältig gewährte Unterstützung sowohl in den vergangen Jahren in Rostock als auch beim Erstellen dieser Arbeit, wobei der ehemaligen Kollegin Regina Jesse sowie der aktuellen Kollegin Kathleen Schubert ein großer Dank für die Hilfe und Zusammenarbeit im Labor gebührt. Zusammen mit den weiteren Arbeitsgruppenmitgliedern – Dr. Vladimir V. Burlakov, Dr. Katharina Kaleta, Lisanne Becker und Kai Altenburger – danke ich sowohl für die freundliche Arbeitsatmosphäre in Labor und Büro nebst den vielen fruchtbaren Diskussionen als auch fruchtlosen, aber erheiternden Späßen und Unterhaltungen.

Dieses besonders angenehme Arbeitsumfeld wurde nicht zuletzt von Dr. Anke Spannenberg geprägt, ohne deren beherztes "Wollen wir?" ich wohl jetzt noch in der Rostocker Mensa verweilen würde. Dafür, sowie für die überaus große Geduld und Mühe beim Messen kleiner Kristalle, sei ihr herzlichst gedankt.

Ein nicht unerheblicher Teil dieser Arbeit entstand in einer Kooperation mit der Arbeitsgruppe um Laurel L. Schafer (Vancouver) während eines Auslandsaufenthaltes in Kanada. Besonders ihr, Jacky C.-H. Yim und Jean Michel Lauzon danke ich für die freundliche Aufnahme in ihre Arbeitsgruppe sowie die kollegiale Zusammenarbeit auf dem Gebiet der Amidatliganden. Ein weiteres herzliches Dankeschön gebührt Philippa Payne und Peter Christensen für die vielen schönen Stunden im Tiefschnee von Whistler Mountain.

Für die erfolgreiche Zusammenarbeit mit Prof. Dr. Axel Schulz, Dr. Alexander Villiger und Martin Ruhmann auf dem Gebiet der Carbodiimide bin ich ebenfalls sehr dankbar.

Für die zu diesem Thema durchgeführten quantenchemischen Rechnungen danke ich PD Dr. Haijun Jiao vom Institut als auch Prof. Dr. Eluvathingal D. Jemmis und Subhendu Roy (Indien).

Jacqueline B. Priebe aus der Arbeitsgruppe von Prof. Dr. Angelika Brückner danke ich besonders für die Aufnahme und Simulation der EPR-Spektren und der damit einhergehenden sehr angenehmen und ertragreichen Zusammenarbeit auf dem Gebiet der paramagnetischen Verbindungen.

Dr. Sven Hansen gilt mein Dank für die quantenchemischen Rechnungen auf dem Gebiet der Bis(phosphino)amide sowie der Bis(phosphino)methanide. Außerdem danke ich ihm außerordentlich für die gute und erheiternde Zeit nach der Arbeit, welche zumeist auf der Bereitstellung von Grill, Bier und Thüringer Rostbratwürsten basierte. Menschen, mit denen man die Zeit nach Feierabend teilt, sind immer einer gesonderten Erwähnung wert. Darum sei an dieser Stelle auch Dr. Monty Kessler für die vielen humorvollen Späße, das gemeinsame Fahrrad fahren und Fahrrad reparieren sowie die Zeiten an Grill und Kicker ebenfalls auf das Herzlichste gedankt.

Für den freundlichen und dennoch offenen Umgang in der der Arbeitsgruppe danke ich Fabian Fischer, Marc Gongoll, Dr. Marko Hapke, Phillip Jungk, Dr. Marcus Klahn, Dr. Karolin Kral, Dr. Bernd H. Müller, Dr. Normen Peulecke, Indre Thiel, Johannes Thomas, Dr. Nico Weding sowie Ute von Zweydorff.

Allen Mitarbeitern der analytischen Abteilung unter Leitung von PD Dr. Wolfgang Baumann danke ich für die gewissenhafte Durchführung aller erforderlichen Messungen.

Ohne Menschen, die mein Interesse an der Chemie geweckt und mich dem Studium ein gewaltiges Stück nähergebracht haben, wäre diese Arbeit nie entstanden. Daher danke ich besonders meiner Oma Gerda Hähnel und meiner Chemielehrerin Frau Marika Franzke für die Einführung in die Welt der Moleküle.

Abschließend danke ich meiner Familie, wobei ich besonders meine zukünftige Frau Janne besonders herausheben möchte. Danke!

Meiner Oma Gerda (†)

„Wenn einer, der mit Mühe kaum

Gekrochen ist auf einen Baum,

Schon meint, dass er ein Vogel wär,

So irrt sich der."

Wilhelm Busch

Table of Content

Abbreviations

anal.	analysis
ATR	attenuated total reflection
az	azaindolato
calcd.	Calculated
Bu	butyl
CI	chemical ionization
Cp	η^5-cyclopentadienyl- (C_5H_5)
Cp*	η^5-pentamethylcyclopentadienyl- (C_5Me_5)
Cy	cyclohexyl
d	doublet
Dipp	diisopropylphenyl
dec.	decomposition
dd	doublet of doublets
DFT	density functional theory
DME	dimethoxyethane
dpp-bian	1,2-bis[(2,6)-diisopropylphenyl)-imino]acenaphthene
EA	elemental analysis
EI	electron ionization
ebthi	*rac*-1,2-bis-(η^5-4,5,6,7-tetra-hydro-inden-1-yl)ethane
EPR	electron paramagnetic resonance
Et	ethyl
FT	fourier transformation
HMDS	hexamethyldisilazane, bis(trimethylsilyl)amide
HOMO	highest occupied molecular orbital
HSAB	hard and soft (Lewis) acids and bases
i	iso
IR	infrared
m	multiplet (NMR), medium (IR)
M	molecule
Me	methyl
Mes	mesityl, 2,4,6-trimethylphenyl

Mp	melting point
MS	mass spectrometry
m/z	mass to charge ratio
NBO	natural bond orbital
NHC	*N*-heterocyclic carbene
NICS	nucleus-independent chemical shift
NMR	nuclear magnetic resonance
NOESY	nuclear overhauser enhancement spectroscopy
NOON	natural orbital occupation numbers
Ph	phenyl
pmdta	*N*,*N*,*N*′,*N*′,*N*′′-pentamethyldiethylenetriamine
ppm	parts per million
Pr	propyl
py	pyridine
quart	quartet
quint	quintet
R	organic substituent
r_{cov}	covalent radius
s	singlet (NMR), strong (IR)
SCF	self-consistent field
shf	super hyperfine coupling
sept	septet
t	triplet
t	tertiary
THF	free tetrahydrofuran
thf	coordinated tetrahydrofuran
tmeda	tetramethylethylenediamine
p-Tol	para-tolyl
vs	very strong (IR)
VT	variable temperature
vw	very weak (IR)
w	weak (IR)

1. Introduction

Transition metal catalyzed processes are of tremendous importance in various industrial transformations.[1] Due to increasing focus on the environmental impact of such industrial processes, both chemical producers and government regulators are interested in maximizing resource and energy efficiency.[2] Therefore, many catalytic applications have passed through a refining process involving improved catalytic activities at milder conditions. As one example for such reactions, the alkyne metathesis has passed through this process, leading to efficient transformation rates at room temperature, cheap and air stable catalysts and a wide tolerance towards functional groups.[3] Moreover, the use of defined group 6 alkylidyne complexes (e.g. (t-BuO)$_3$W≡CCMe$_3$) resulted in both, better catalytic activity and insights into the mechanism of such transformations.[4] With the study of the mechanism, the importance of metallacycles as key intermediates in the catalytic cycle became of distinguished interest. As a result, the catalytic cycle of the alkyne metathesis reaction is well described nowadays. Surprisingly, a highly strained four membered metallacyclobuta-2,3-diene could be identified as a result of a decomposition pathway of the alkylidyne catalyst.[5]

In many other industrial processes, metallacycles of group 4 metals, especially titanium and zirconium, are found to be such important key intermediates. Their intense study led to detailed insights into the catalytic cycle, corroborating the mechanism with isolated complexes as catalytic intermediates.[6] As a result, processes like the metallocene based Ziegler-Natta polymerization of alkenes were improved continuously to become more and more efficient.[7] Besides the processes involving "all-C" carbon based metallacycles, catalytic transformations based on heterometallacycles are of both, academic and industrial interest. Among these, hydroamination is especially important for pharmaceutical industry, using this functionalization of unsaturated carbon-carbon bonds via formal addition of a hydrogen-nitrogen bond.[8] In the catalytic cycle, a [2+2] cycloaddition of the alkene or alkyne with the [M=N] species occurs, resulting in a nitrogen containing four-membered metallacycle as key intermediate of this reaction.[9] Subsequent reaction with a primary amine and elimination of the product complete the

catalytic cycle. Such insights into the catalytic cycle are of high importance for improving the reaction conditions by simply knowing the mechanisms.

Besides group 6 metallacyclobuta-2,3-diene complexes, mentioned above, highly strained four-membered metallacycles are insufficiently described compounds. Due to the increased ring strain and the resulting high reactivity towards various substrates, their isolation remains challenging. In contrast, three- and five-membered metallacycles of group 4 metallocenes are well known compounds.[10]

This work focuses on synthesis, characterization and reactivity of highly strained four-membered metallacycles of group 4 metallocenes, depicted in Table 1. "All-C"[a]- as well as heterometallacycles are described.

Generally, the cyclic structures discussed in this work, can be classified into two groups. Group one features four-membered metallacyclobuta-2,3-dienes, containing the allenic X=C=X unit in the ring. The second group contains cycles, which bear an allylic unit to stabilize the metal fragment. At the beginning of each chapter, the corresponding compounds of each category are described in detail.

[a] "All-C"-metallacycles contain only carbon atoms besides the metal in the cyclic unit.

Table 1. Carbon-, nitrogen-, phosphorus-, sulfur- and oxygen-containing four-membered metallacycles. Cycles highlighted in grey are not part of this work.

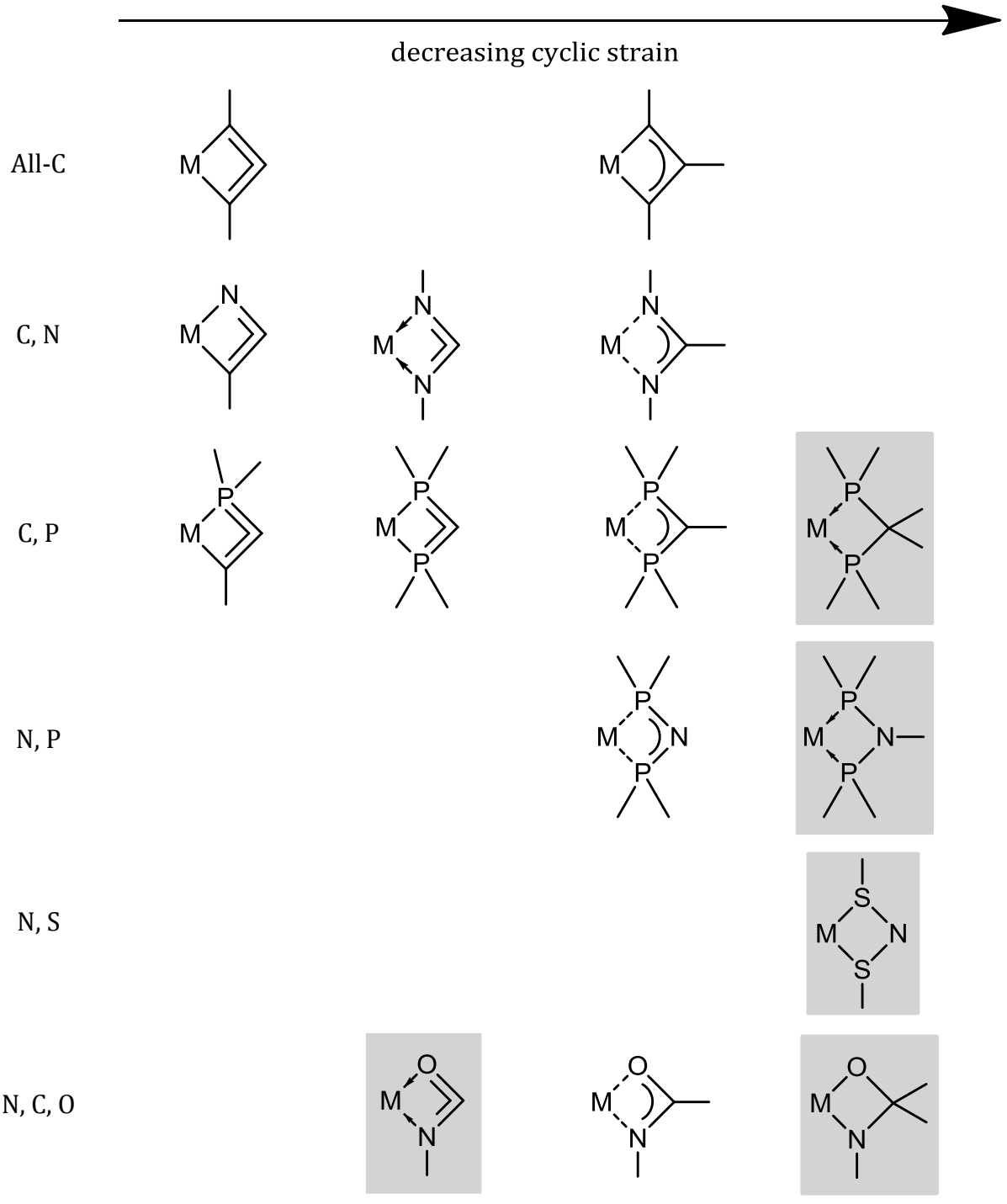

In this work, various metallocene compounds are used as precursors. These are depicted in Scheme 1. Complexes **1**-**4** are metallocene bis(trimethylsilyl)acetylene complexes, that are able to liberate the metallocene fragment after dissociation under mild

conditions. The metallocene complexes **5**-**8**, containing chlorido ligands are also used in this work, in most cases for salt metathesis reactions. Especially Schwartz' reagent (**8**) exhibits ideal properties for both salt metathesis as well as protonolysis reaction.

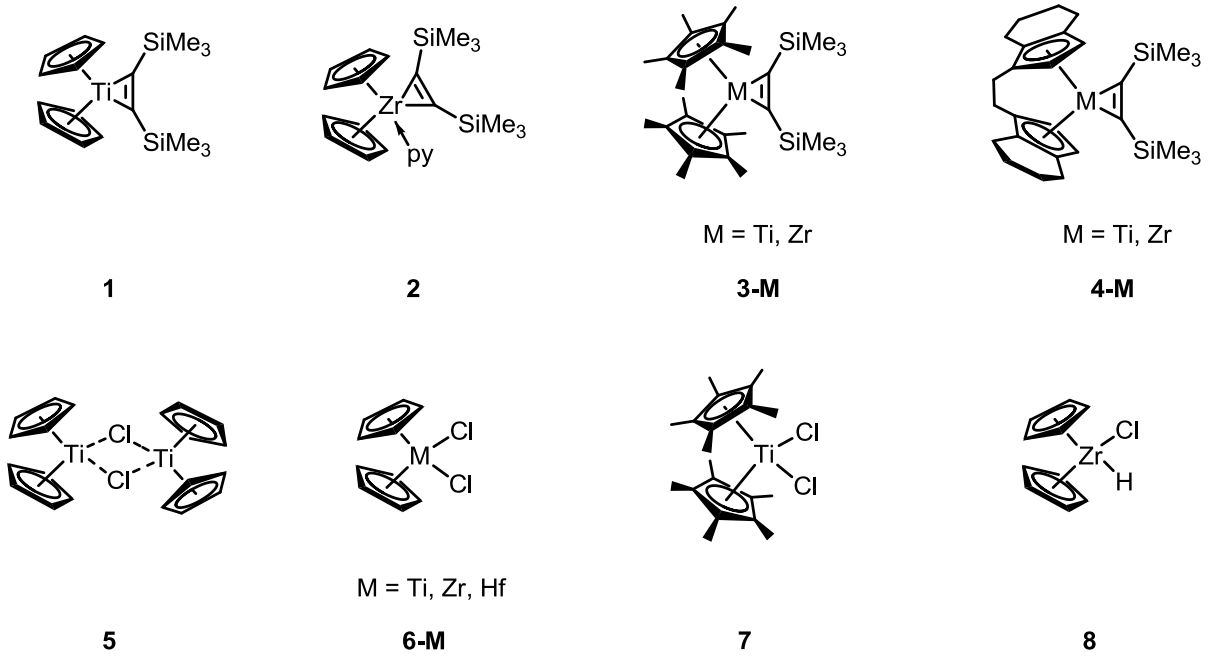

Scheme 1. Metallocene complexes used in this work.

While the oxidation state of these chlorido containing starting materials can be easily assigned (**5**: +III, **6**-**8**: +IV), the description of binding modes and subsequent oxidation states of the bis(trimethylsilyl)acetylene complexes **1**-**4** are more sophisticated. The different resonance forms of complexes **1**-**4** are depicted in Scheme 2.[11]

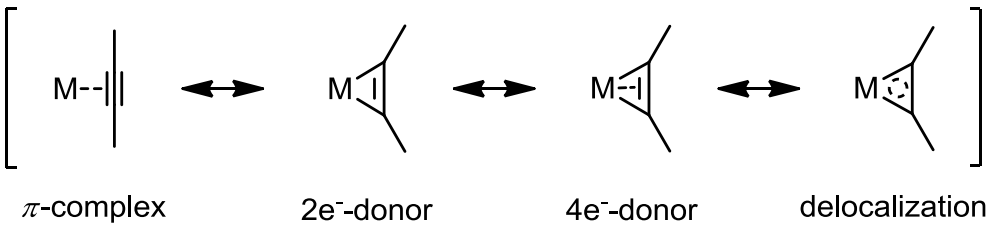

Scheme 2. Different resonance forms of metallocene alkyne complexes 1-4.

Four possible resonance forms have to be considered for the binding modes of the metallocene alkyne complexes. Depending on different analytical methods, all of these binding modes can be confirmed. For this reason, X-ray analysis, NMR- and

IR-spectroscopy as well as theoretical investigations are essential to understand the experimental results. Noteworthy, the oxidation state of the metal strongly depends on the used resonance form. While the π-complex requires the oxidation state +II for the metal center, in other resonance forms the metal has to be fully oxidized, exhibiting the oxidation state +IV. However, depending on the widely spread reactivity, discussed in the following chapters, one of the possible oxidation states might appear more convenient.

This work focuses on the chemistry of four-membered metallacycles. However, various non-cyclic complexes are described as well as result of unexpected reactivities. It can be classified into five main parts. The first chapter deals with the synthesis of "all-C" metallacycles, followed by a chapter with various carbon and nitrogen containing ligands, based on the concept that heteroatoms might stabilize highly strained structures. Subsequent exchange of the carbon atoms lead to carbon free metallacycles. In the chapter about the bis(diphenylphosphino)methanide ligands, the similarity of the isolobal fragments N→CR towards the phosphorus and nitrogen containing ligand bis(diphenylphosphino)amide is discussed. The fourth chapter deals with bis(diphenyl-phosphino)acetylene as ligand while the fifth part of this work reveals the flexibility of carbon, nitrogen and oxygen containing amidato ligands towards four-membered metallacycles.

2. Results and Discussion

2.1. Synthetic attempts of four-membered "all-C"-metallacycles

Up to this point, group 4 chemistry of highly strained four-membered "all-C"-metallacycles is very limited. This might be attributed to the fact, that appropriate ligand precursors are hardly accessible. In contrast, the corresponding highly strained five-membered metallacycles are synthesized by coordination reactions, starting from easily available neutral compounds. Exemplarily, coordination of 1,3-butadiynes results in the formation of the highly strained metallacyclopenta-2,3,4-trienes (Scheme 3, **A**).[10] Using but-1-ene-3-ynes results in the formation of the well known metallacyclopenta-2,3-dienes (**B**) occurs under mild conditions.[12]

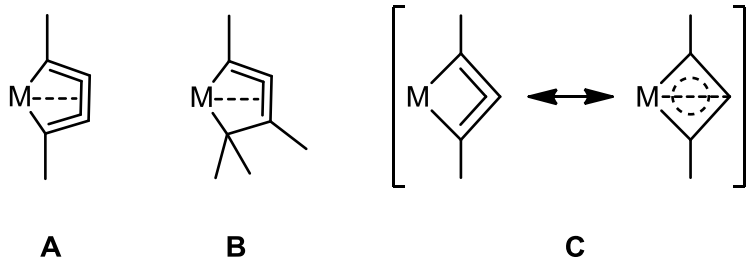

Scheme 3. Unusual "all-C"-metallacycles.

Noteworthy, the four-membered structures **C** are well known for group 6 metals. These highly strained complexes result as a coupling of a carbyne complex [M≡CR] with a terminal alkyne upon deprotonation.[5,13,14] Moreover, in alkyne metathesis such complexes are observed as decomposition products of the alkylidyne catalyst upon reaction with a terminal alkyne.[5] Adapting this synthetic pathway to group 4 metals is not feasible as complexes with the [M≡CR] fragment are unstable and have not been isolated yet. However, complexes containing the [Ti≡CR] unit have been observed as intermediates in various reactions by the group of Mindiola.[15]

Attempts to obtain group 4 metallacyclobuta-2,3-diene complexes (Scheme 3, **C**) have been conducted before,[16] starting from synthetically challenging allenes or silyl enol ethers. [17] Subsequent lithiation and salt metathesis with Cp_2MCl_2 (**6-M**) as well as protonolysis attempts with Cp_2TiMe_2 did not result in formation of the desired complex.[16]

Interestingly, it has been shown that commercially available propargylic systems such as 1-phenyl-but-1-yne are able to rearrange upon lithiation to form monometallated allenes via 1,3-lithium shift.[18] Moreover, also dimetallation has been described for such propargylic species, leading to ideal precursors for subsequent salt metathesis reactions.[19] Lithiation of 1-phenyl-but-1-yne in THF at -20 °C with two equivalents of *n*-butyllithium was performed for 2 h, followed by subsequent salt metathesis with Cp_2TiCl_2 (**6-Ti**), according to Scheme 4.

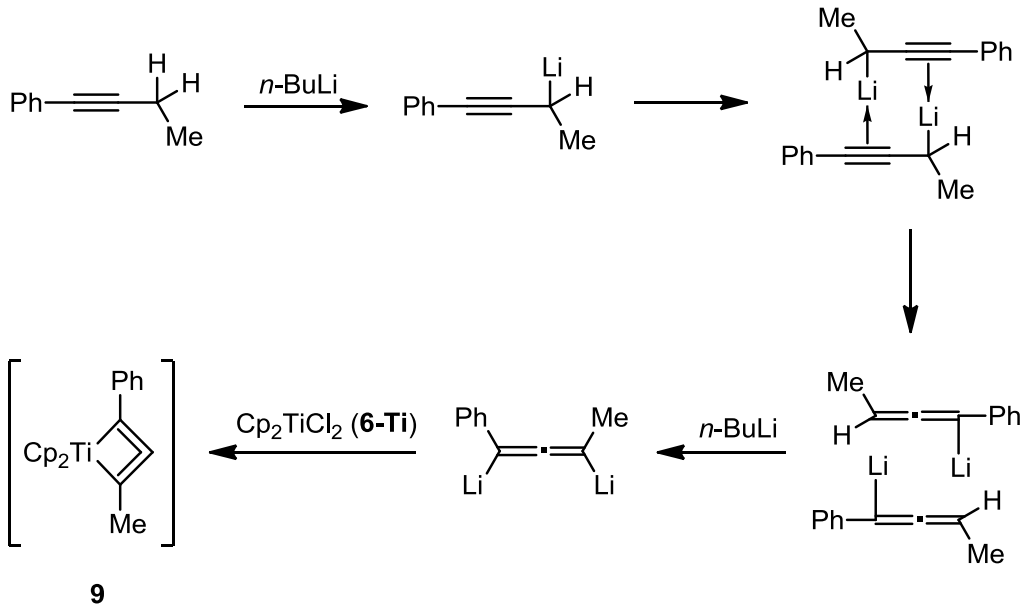

Scheme 4. 1,3-Lithium shift of lithiated 1-phenyl-but-1-yne, followed by second lithiation and salt metathesis with Cp_2TiCl_2 (6-Ti).

The reaction resulted in the formation a dark brown powder. ^{1}H NMR analysis revealed resonances, that can be assigned to the four-membered metallacyclobuta-2,3-diene complex **9**. The inequivalent Cp resonances appear at 5.66 and 5.56 ppm, while the Me group exhibits a singlet at 2.17 ppm. However, due to the high ring strain, complex **9** is very unstable, therefore no crystals, suitable for X-ray analysis could be obtained. Nevertheless complex **9** was characterized by mass spectrometry. Its molecular ion peak can be found at *m*/*z* 306. Moreover, the calculated isotopic pattern is keenly consistent with the observed one, strongly corroborating the existence of the metallacyclobuta-2,3-diene. Complex **9** is very unstable in solution and decomposes within hours. As decomposition products, CpH could be identified using NMR spectroscopy. These observations are consistent with theoretical predictions, revealing that these metallacycloallenes are only stabilized by two additional electrons, for example of

nitrogen substituents instead of the methyl and phenyl groups.[20] Furthermore, substitution of one or two carbon atoms of the metallacycle by these electron rich nitrogen atoms should also lead to a stabilization.

2.2. Complexes with Nitrogen and Carbon containing Ligands

Emanating from the fact that highly strained metallacycles can be stabilized by incorporation of heteroatoms into to the cyclic unit,[20] group 15 elements with their additional lone pair are of tremendous interest. Among these, especially nitrogen containing ligands are easily accessible and offer a wide diversity of properties. The scope of nitrogen and carbon containing ligands is of overwhelming variety. As this work generally focuses on chemistry of four-membered metallacycles, substrates able to form such species were chosen for intense investigations, thus leading to new insights into the bonding situation of such highly strained compounds.

The saturated metallacyclodiazabutanes (**D**) and metallacycloazabutanes (**G**) do not exhibit cyclic ring strain. However, complexes with such ligands were described for group 4 metals before. Bergman et al. synthesized $Cp_2Zr[\kappa^2$-*N*,*N*-(*p*-Tol)N-C(H)(Ph)-N(*p*-Tol)] (type **D**).[21] Both cyclic C-N bond lengths are in the range of a typical single bond.[22] The structural motif **G** was also described by the group of Bergman for a zirconocene complex,[23] displaying only single bonds in the central metallacycle. Another example was synthesized by the group of Beckhaus via formal [2 + 2] cycloaddition reaction of a carbodiimide to a titanaallene intermediate $[Cp^*_2Ti{=}C{=}CH_2]$.[24]

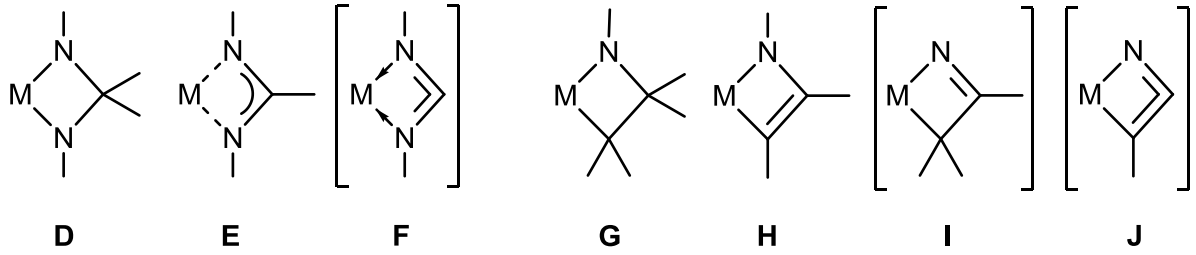

Scheme 5. Selected examples of nitrogen containing four-membered metallacycles.

Four-membered metallacycles **E** are well known for group 4 metals although the incorporation of one double bond into the cyclic system leads to an increasing ring strain. Especially metallocene complexes are known with either amidinato or guanidinato ligands. Gambarotta and co-workers described the structure of $Cp_2Zr(Cl)[\kappa^2$-*N*,*N*-[Cy-N-C(H)-N-Cy] (Cy = cyclohexyl) as an example for **E** with an amidinato ligand.[25] The titanocene^{III} complex $Cp_2Ti[\kappa^2$-*N*,*N*-(*i*-Pr)-N-C(N(*i*-Pr)$_2$)-

N-(*i*-Pr)], reported by Wasslen et al. features the above mentioned guanidinato ligand.[26] However, complexes displaying the structural motif **I** without any substituent at the N-atom and a C=N double bond are hitherto unknown. Contrarily, complexes with only one nitrogen atom and a C=C double bond in the cyclic system (**H**) are easily accessible.[27] These compounds are either synthesized via [2+2] cycloaddition of an alkyne at a metal-imido species M=NR or by insertion reaction of a nitrogen containing substrate (azido- or diazo-compound) into the M-C bond of a metallacyclopropene. Finally, metallacyclodiazabutadi-2,3-enes (**F**) and metallacycloazabutadi-2,3-enes (**J**) were hitherto not isolated. Therefore, this chapter focuses on the various synthetic attempts to isolate such highly strained species.

2.2.1. Complexes of Carbodiimides

2.2.1.1. State of the Art

In the last decades, the chemistry of carbodiimides was intensively investigated as generally, carbodiimides serve as substrates in different wide spread metal complex reactions. Examples for group 4 metallocenes include Floriani's report of the reaction of RN=C=NR' (R, R' = *p*-Tol) with $Cp_2Ti(CO)_2$. In this case, the carbodiimide is coupled reductively to form a twofold chelating ligand. The product obtained can be described as a tetraazadimetallabicycle.[28] Moreover, the above mentioned reaction of a titanaallene intermediate $Cp^*_2Ti{=}C{=}CH_2$ with carbodiimides RN=C=NR' (R, R' = *p*-Tol, Cy) yields products, which display a four-membered azatitanacyclobutane moiety.[24] In the reaction of $Cp_2Zr{=}N(t\text{-Bu})$ and carbodiimides, discovered by Bergman and co-workers, a guanidinate ligand $[(t\text{-Bu})N\text{-}C(=NR)\text{-}NR]^{2-}$ is formed via [2+2] cycloaddition, binding to the zirconocene^{IV} center in a κ^2-*N*,*N*-fashion.[29] Moreover, reactions of $Cp_2Ti(\eta^2\text{-}Me_3SiC_2SiMe_3)$ (**1**) with various small carbodiimides have been intensively investigated, resulting in the formation of unusual nitrogen-containing four- and five-membered metallacycles. An overview of the products for the latter reaction type is depicted in Scheme 6.

Depending on the substituents, in most of the cases a coupling of two carbodiimide moieties occurs to result in either diamido- or diamidinato-ligands. Noteworthy, the four-membered diamidinato complex features the coordination mode **E**. With *i*-Pr

substituents, a coupling of the carbodiimides with the bis(trimethylsilyl)acetylene and subsequent migration of one of the $SiMe_3$ groups was observed.[30] Using cyclohexyl substituents, a second complexation of the carbodiimide via the central carbon atom with an additional titanocene fragment atom takes place under particular conditions. Performing the same reaction at elevated temperatures resulted in the formation of the diamidinato coupling product.[31] However, the $SiMe_3$-substituted carbodiimide forms a trimethylsilyl substituted titanocene^{III} guanidine species in this reaction.[16] The ligand contains an additional $N(SiMe_3)_2$ fragment at the central carbon atom, most likely as a result from the tautomeric equilibrium between the carbodiimide RN=C=NR and the cyanamide R_2N-CN.[32]

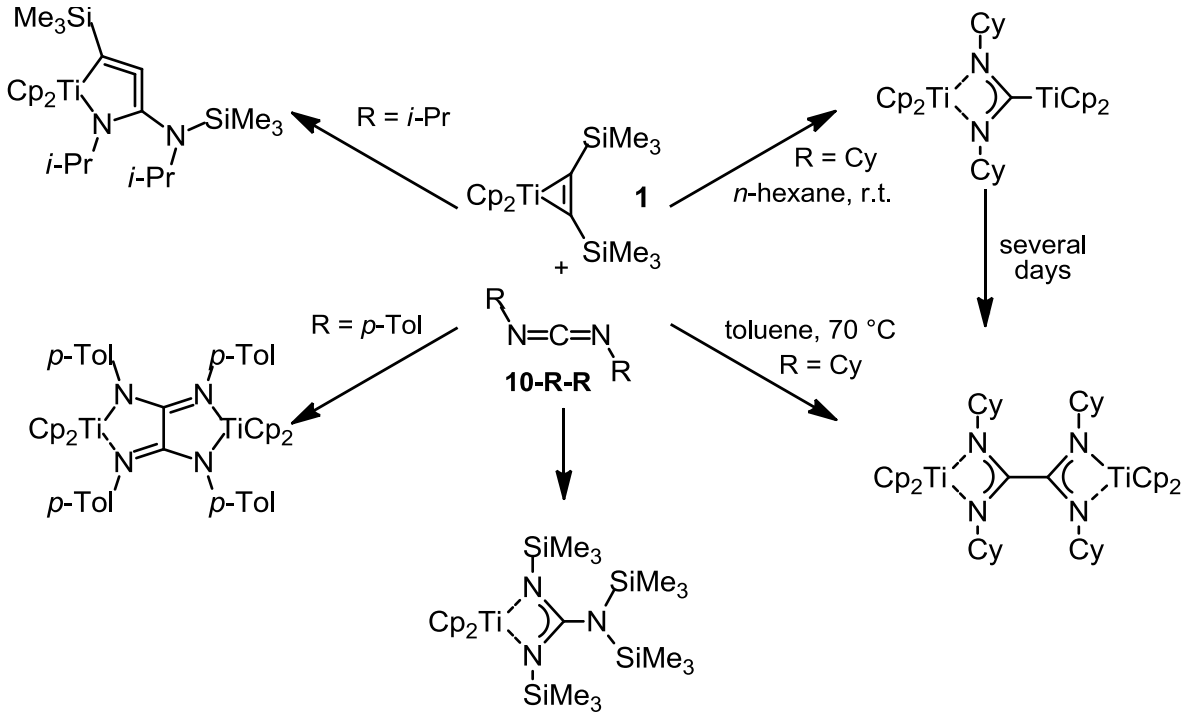

Scheme 6. Products obtained in the reaction of the titanocene alkyne complex with small carbodiimides.

As rather small variations at the substituents or reaction conditions already lead to tremendous differences regarding the products, steric changes on both titanocene precursor and carbodiimides were performed to get novel insights into the electronic nature of the highly strained four-membered heterometallacycle **F** (Scheme 5).

2.2.1.2. Complexation vs. C–N Bond Activation

Reaction of the mesityl substituted carbodiimide **10-Mes-Mes**[33] with **1** in *n*-hexane gives a mixture of two unusual und unexpected products. The main product is a titanocene guanidine complex (**11**) (Scheme 7), very similar to the above described complex. Interestingly, in **11** one hydrogen atom is bound to the exocyclic nitrogen atom to give an amine functionality. The origin of the proton is subject to speculations – abstraction from a solvent molecule is one possibility. Another likely explanation could however be found in the structure of the second product **12**, which consists of a coupled cyclopentadiene-[C=N-Mes]-moiety, which is coordinated to a titanocene fragment. Additionally, another [CN-Mes] serves as an additional ligand to stabilize the complex. Thus, abstraction of a proton from a free cyclopentadienyl fragment took place; unfortunately the exact stoichiometry of the reaction as well as the nature of the organometallic by-product could not be revealed.

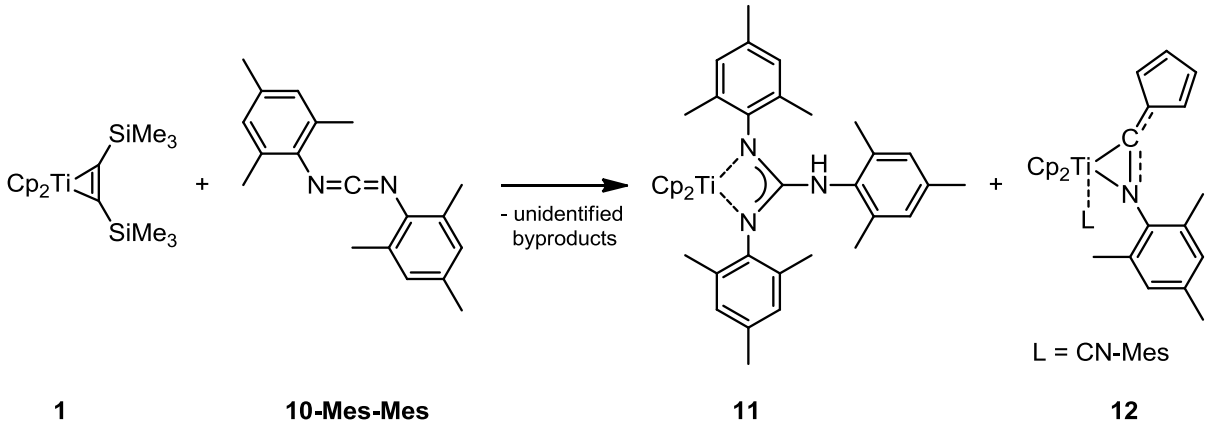

Scheme 7. Reaction of complex 1 with carbodiimide 10-Mes-Mes.

Due to the paramagnetic nature of complex **11**, no valuable NMR data could be obtained. Therefore, it was characterized by mass spectrometry, the molecular ion peak was detected at m/z 590. The molecular structure is depicted in Figure 1.

The Ti center is coordinated by two Cp units and the guanidinate ligand in a distorted tetrahedral geometry, thus forming a four-membered planar metallacycle (deviation from the plane Ti1–N1–C1–N3 of 0.002 Å). The Ti–N distances are in the same range as observed before.[27] However, it should be noted that Ti1–N1 (2.1821(16) Å) is slightly shorter than Ti1–N3 (2.2285(15) Å), most likely due to the unsymmetrical guanidine ligand. In complex **12** (Figure 2), the unusual structural motif of a fulvene bound to titanocene and a [CN-Mes] fragment is present. In ^{1}H NMR experiments, four resonances

(ddd) are observed, thus indicating asymmetry due to the restricted rotation of the cyclopentadiene group at C1. Structural data (C1−C2 1.398(3) Å) further corroborate the presence of a fulvene unit with partial double bond character.

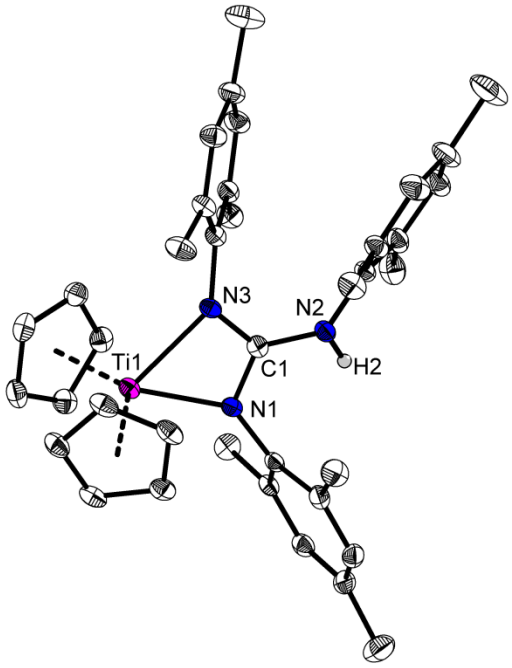

Figure 1. Molecular structure of complex 11. Hydrogen atoms except H2 are omitted for clarity. The thermal ellipsoids correspond to 30 % probability.

The titanocene unit is surrounded by two CN groups [CN-Mes], one being an η^1-end-on bound isocyanide group and the second CN unit being coordinated η^2-side-on, thus leading to the formation of a three-membered metallacycle, which is also found in the well-known metallacyclopropenes or other metallacycles. The latter CN fragment is further substituted by the fulvene unit. Ti1−C1 and Ti1−N1 bond lengths are in the range of single bonds (Σr_{cov} = 2.11 Å and 2.07 Å, respectively[34]) with the latter being slightly elongated. C1−N1 corresponds to a typical double bond and the fulvene bond C1−C2 is best described as an elongated double bond, indicating delocalization of electrons in the side-on coordinated ligand. This is further supported by the almost coplanar arrangement of the cyclopentadiene group with the titanacycle (angle of 1.2(2)°). Noteworthy, transition metal complexes with such fulvene coordination modes find almost no precedent in literature. The only example was published by Poveda and Carmona and co-workers, who prepared unusual palladium- and platinum fulvene-substituted complexes with an uncoordinated NH unit and found a C−C bond distance

(fulvene ring carbon to α carbon at fulvene ring) of 1.37(1) Å in Pd[C(NH*t*-Bu)=C(C_4H_3Me)][CH($SiMe_3$)$_2$](CN*t*-Bu)(PMe_3), which is in the same range as found for the titanocene complex **12**.[35] Moreover, Erker et al. reported on formimidoyl-functionalized lithium cyclopentadienides of the type Li[C_5H_4-CH=NAr] (Ar = *p*-Tol, 2,6-Me-C_6H_3, 2,6-*i*-Pr-C_6H_3),[36] displaying a nitrogen-bound metal center and a free CH group.

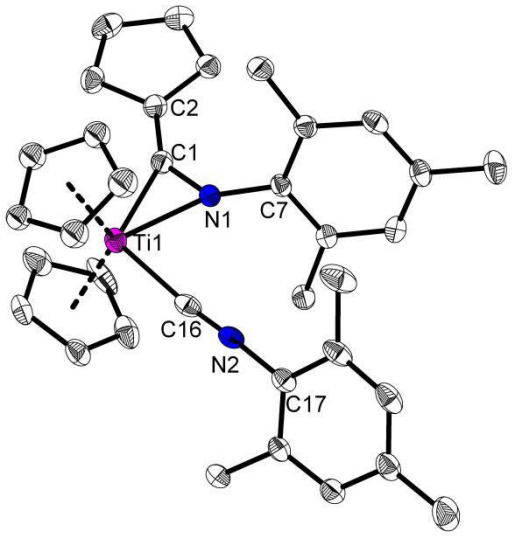

Figure 2. Molecular structure of complex 12. Hydrogen atoms and the second position of one disordered Cp ligand are omitted for clarity. The thermal ellipsoids correspond to 30 % probability.

The singlet state of complex **12** is calculated to be more stable than the triplet state by 36.0 kcal/mol. The metal is in the oxidation state of +IV in complex **12**. The important MOs of complex **12** are shown in Scheme 8. The bond lengths of the Ti1–C1 (2.106 Å) and Ti1–N1 bonds (2.117 Å) suggest stronger complexation of the RCNR' moiety to the Cp_2Ti fragment; HOMO-2, HOMO-3 and HOMO-12 account for this interaction. On the other hand, the Ti1–C16 bonding appears to be a dative contact (2.170 Å), which involves interaction between the orbital of the cyano group with the metal d orbital (HOMO-23, Scheme 8). Considerable double bond character in the calculated C1–C2 (1.388 Å) as well as in C1–N1 (1.291 Å) bonds of the coordinated RCNR' moiety is supportive of π-conjugation along the N1–C1–C2 unit in complex **12**.

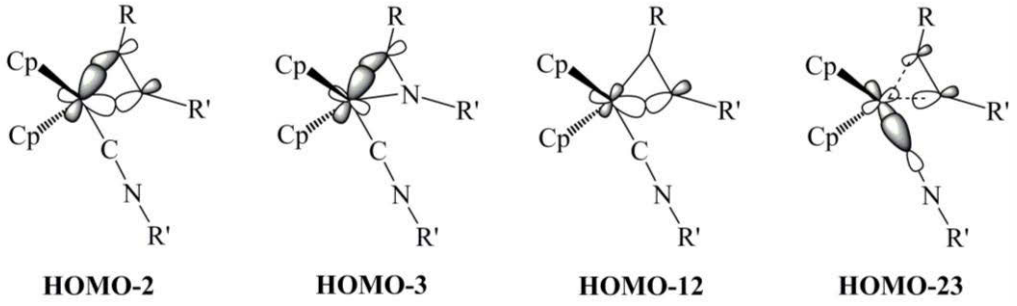

Scheme 8. Important molecular orbitals of the complex 12 (R = C_5H_4, R' = Mes).

Performing the reaction of the same carbodiimide **10-Mes-Mes** with the sterically more demanding permethylated titanocene bis(trimethylsilyl)acetylene complex **3-Ti**, unexpected formation of the diamagnetic bis(isocyanide) complex **13** as another C–N bond activation product takes place (Scheme 9).

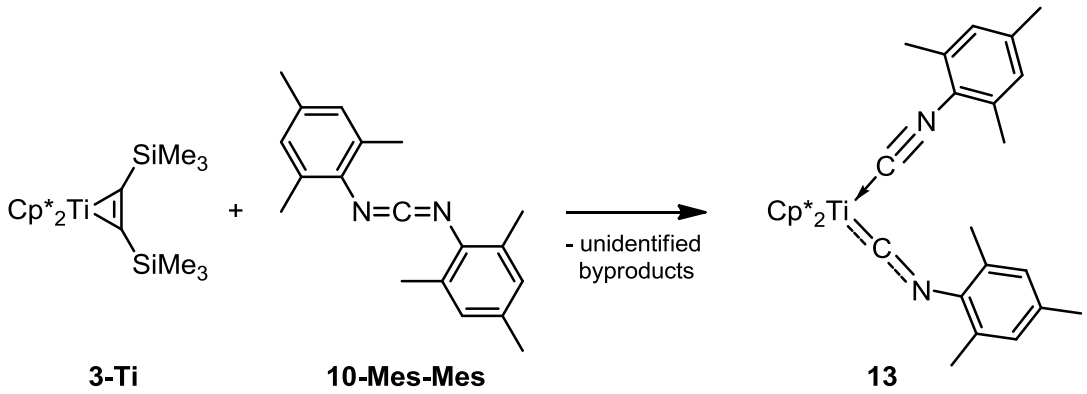

Scheme 9. Formation of 13 in the reaction of 3-Ti with 10-Mes-Mes.

^{1}H NMR analysis revealed that in solution both isocyanide groups are magnetically equivalent, giving only one set of resonances at 2.08 and 2.46 ppm for the methyl groups at the aromatic rings as well as at 6.68 ppm for the CH protons, respectively. However, single crystal X-ray analysis of complex **13** showed that two different isocyanide ligands are present in the molecule in the solid state (Figure 3). C–N bond lengths are different (C1–N1 1.217(3), C2–N2 1.175(3) Å) and one of the CN-Ar fragments displays a significant deviation from linearity of the C–N–C_{Ar} unit (C1–N1–C3 142.4(2)°), revealing a mostly sp^2-hybridized nitrogen atom.

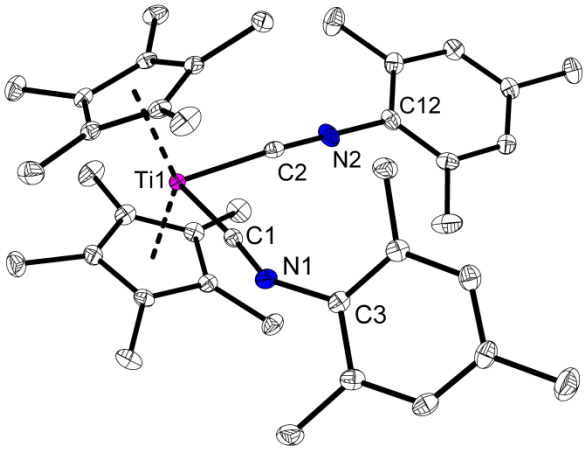

Figure 3. Molecular structure of complex 13. Hydrogen atoms are omitted for clarity. The thermal ellipsoids correspond to 30 % probability.

A similar complex displaying two inequivalent isocyanide groups was reported by Sita and co-workers. Reaction of dinuclear end-on-bridged dinitrogen complexes {Cp*M[N(*i*-Pr)C(Me)N(*i*-Pr)]}$_2$(μ-η^1:η^1-N_2) (M = Mo, W) with the isocyanide ArNC (Ar = 2,6-Me-C_6H_3) yielded mononuclear species of the type Cp*M[N(*i*-Pr)C(Me)N(*i*-Pr)]-(C=NAr)(C≡NAr).[37] Notably, titanocene bis(isocyanide) complexes are known (e.g. Cp'$_2$Ti(CNAr)$_2$ (Cp'$_2$ = η^5-$Me_2Si(C_5H_4)_2$, Ar = 2,6-Me-C_6H_3)[38]), however such strong deviations from linearity in the C–N–C_R unit as found in complex **13** is unknown. Previously, such significant bond angle distortions for isocyanide ligands have been assigned to a strong π acceptor character of the ligand, thus resulting in back-donation of electron density from the metal center into the antibonding π*-orbital of the isocyanide triple bond.[39] Due to the presence of an electron donating Cp* ligand and a formal Ti^{II} species, this could also be the case in complex **13**. Regarding this fact, the different reactivity of **1** and **3-Ti** towards **10-Mes-Mes** can be assigned to both different steric demand of the Cp ligands as well as slightly different electronic nature of the metallocene fragment.

In the reaction of **1** with the even more sterically demanding carbodiimide **10-Dipp-Dipp**,[33] C–N bond activation takes place to yield a titanocene^{IV} imido complex (**14a**) according to Scheme 10. The residual CN-Dipp moiety serves as an additional ligand to stabilize the metal imido fragment. Performing the same reaction with the permethylated titanocene complex **3** results in the formation of the similar imido complex (**14b**),

however, due to the higher steric demand of the metallocene unit in this case no additional ligand is required to stabilize the metal center.

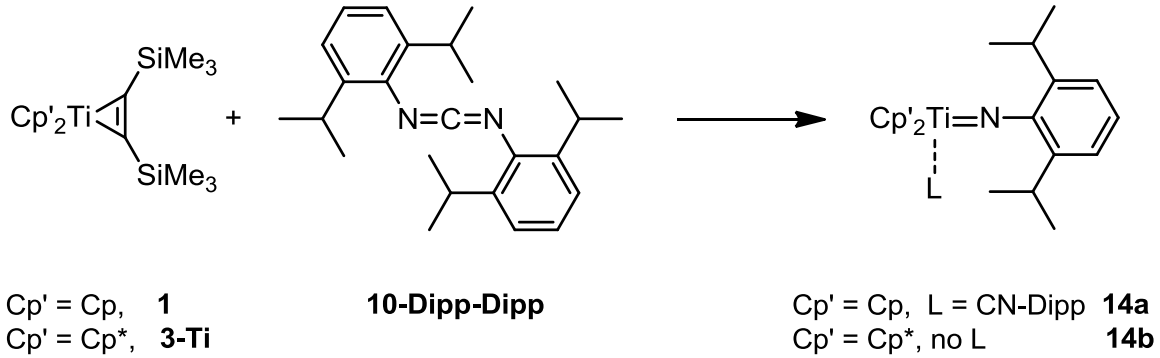

Scheme 10. Formation of titanocene imido complexes 14a and 14b.

The ^{1}H NMR spectra of both complexes **14a** and **14b** are very similar, displaying sharp resonances of either Cp or Cp* groups at 5.99 and 1.86 ppm, respectively. The methine resonances of the imido ligand appear equivalent for both complexes, thus indicating C_{2v} symmetry in solution. The IR spectrum of **14a** consists of an intense band at 2160 cm^{-1}, which can be assigned to the C≡N stretch of the isocyanide ligand, similar to the C≡N resonance in $Cp_2Zr(\eta^1\text{-}CN\textit{t}\text{-}Bu)(\eta^2\text{-}Me_3SiC_2SiMe_3)$ at 2124 cm^{-1}. [40]

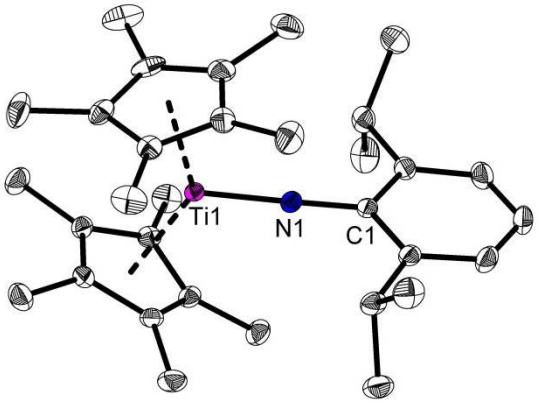

Figure 4. Molecular structure of complex 14b. Hydrogen atoms are omitted for clarity. The thermal ellipsoids correspond to 30 % probability.

Due to low quality of the single crystals of **14a**, no X-ray crystal structure analysis could be performed. However, crystals of **14b** suitable for X-ray analysis were obtained from a saturated toluene solution at room temperature. The molecular structure is depicted in Figure 4. The bent titanocene unit is coordinated with an imido group to result in a

distorted trigonal planar geometry around the Ti center. The Ti1–N1 bond length (1.764(1) Å) is in the range of a double bond (Σr_{cov} = 1.77 Å[34]) and in good agreement to values found before for other structurally similar titanocene imido complexes (e.g. 1.722(4) Å in $[C_5H_3(SiMe_3)_2]_2Ti{=}NSiMe_3$ and 1.765(3) Å in $Cp^*_2Ti{=}NPh$).[41] The Ti1–N1–C1 unit is found to be almost linear (178.40(13)°), which is in agreement with NMR data described above.

In all of these reactions, the initial step is most likely the substitution of the bis(trimethylsilyl)acetylene spectator ligand by the carbodiimide to form the unstable four-membered heterometallacycle **F** via a dissociative mechanism.[6] However, the formation of the experimentally observed complexes suggests a strong biradical character of this intermediate according to Scheme 11. Further electronic structure and bonding analysis of the intermediate four-membered heterometallacycle revealed open-shell singlet state (OSSS) character together with a delicate and unique Ti–C interaction (Scheme 11, middle).

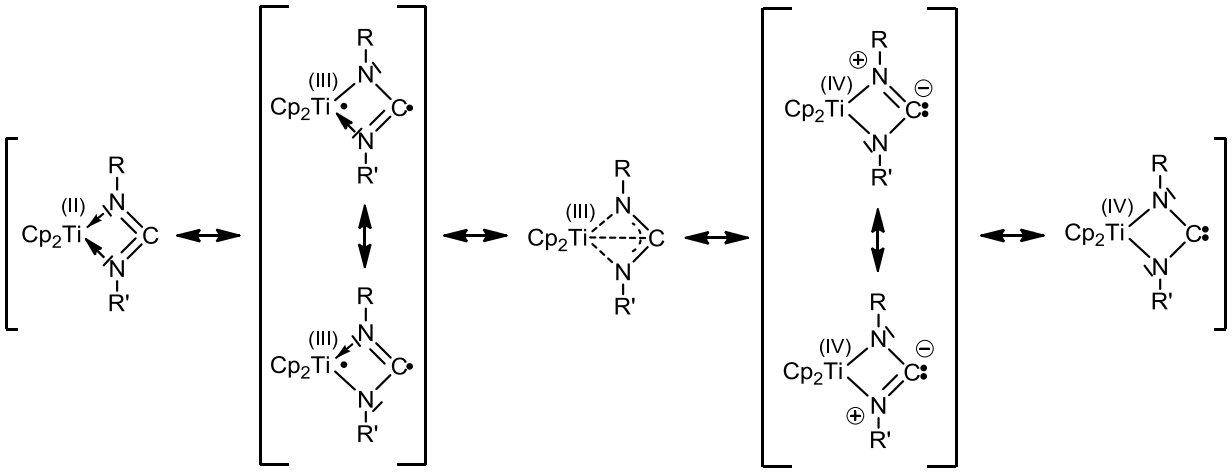

Scheme 11. Resonance forms of the metallacyclic intermediate F with R/R' = alkyl or aryl substituents.

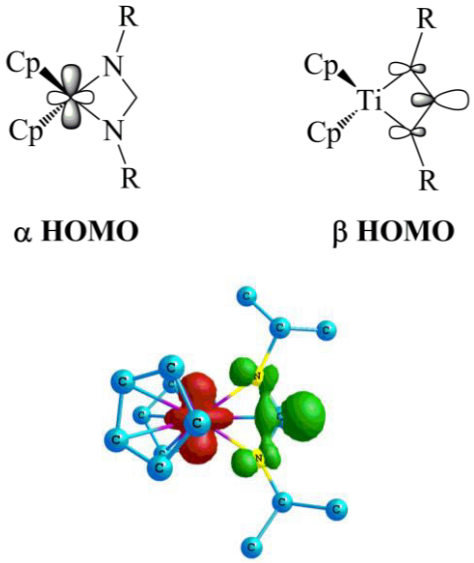

Scheme 12. Schematic representations of α and β HOMO (R = *i*-Pr)(top) and calculated SCF spin density plot of the metallacyclic intermediate C (bottom); (H atoms are removed for clarity).

One of the single electrons of the "biradicaloid" species is located at the Ti center (α HOMO) while the second single electron is found to be at the ligand (β HOMO) (Scheme 12). However, an interaction of these single electrons might result in a peculiar Ti–C interaction. Calculated Ti–C bond lengths (2.316 Å – 2.462 Å) are not far from the Ti–C σ bond distance of 2.160 Å in the calculated Cp_2TiMe_2 complex. Therefore the Ti–C interaction can be termed as a “stretched” chemical bond, leading to a significant stabilization via "internal" complexation by coincidental decrease of the biradicaloid character. It should be noted, that the intensity of the biradical character depends on both steric and electronic effects. This intensity gets reflected by the NOON (natural orbital occupation numbers) value (100 % for a perfect biradical). Therefore the sterically demanding and electron donating Mes group (highest NOON value; 55.8 %) subsequently lead to the longest Ti–C interaction (2.462 Å).

The NHC-type resonating structures with a Ti^{IV} center seem to have less contribution to the overall description of the molecule. This electronic assignment of intermediate **F** also draws support from the fact that most of the experimentally observed complexes are found to contain a Ti^{III} center, which is well in line with resonating biradicaloid structures. However, the experimentally observed complexes are stabilized via external complexation as mentioned above. Depending on the extent of biradical character in the heterometallacycle **F**, the β HOMO (or α HOMO) reacts differently. Generally, a less

biradical character leads to coordination with another molecule to form four-membered diamidinato complexes, while higher biradical character tends to activate the C−N bond of the carbodiimide to give various activated complexes (**11** and **13**). It is important to note that the “stretched” Ti-C bond ("internal" complexation) of the monometallic heterometallacycle **F** disappears in complexes with "external" complexation which further strengthen the presented interpretation.

2.2.2. Complexes of γ-Methylene Nitriles

2.2.2.1. State of the Art

The application of γ-methylene nitriles N≡C-CH_2R (R = alkyl, aryl) as ligands in synthetic chemistry is mainly based on its neutral form to generate a dative bond of the lone pair of the N-atom with the metal center (Scheme 13). Such complexes are known for group 4 metals. For example, Mindiola and co-workers described a Ti imido triflate complex with additional coordination of a neutral mesitylacetonitrile ligand.[42]

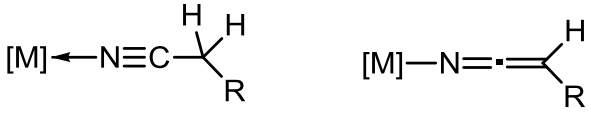

Scheme 13. γ-methylene nitriles as neutral and anionic ligands.

However, its deprotonated form is also known as an anionic ligand to form keteniminate complexes. The only complex with a group 4 metal was described by Lorber and co-workers, featuring a Zr-N=C=C(H)-C(Me)=N(H)-Zr bridge between two Zr centers.[43] Besides this singly deprotonated γ-methylene nitrile complex, keteniminate compounds were described in our group before. Upon C-H-activation of diphenylacetonitrile, the keteniminato complex $Cp^*_2Ti(N=C=CPh_2)_2$ was synthesized. Noteworthy, by using the ebthi ligand instead of Cp*, a coupling occurred to form a four-membered heterometallacycle.[44] As ideal precursors for the highly strained structures **L** (Chapter 2.2, Scheme 5), the complexes should feature both, one remaining γ-H atom together with a halide ligand at the metal center for subsequent salt metathesis. Surprisingly, such complexes are not only unknown for group 4 metals but have not been described generally.

2.2.2.2. Titanium and Zirconium Keteniminate Complexes

On the basis of the 1,3-propargylic shift of lithiated γ-methylene alkynes, described in Chapter 2.1, this concept was extended to γ-methylene nitriles as possible precursor ligands for highly strained structures according to motif **J**. Hereby, the sterically demanding mesitylacetonitrile was chosen as precursor.

Deprotonation reaction with *n*-butyllithium resulted in the 1,3-Li propargylic shift according to Scheme 14. After deprotonation, most likely a dimeric species is formed by interaction of the lone pair of the N atom with the Li atom of a second molecule, finally resulting in Li-keteniminato species.[45]

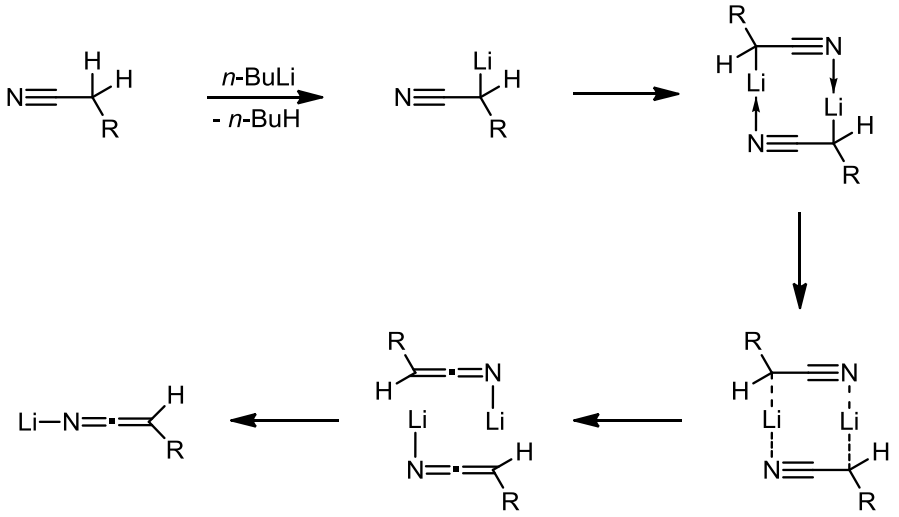

Scheme 14. 1,3-Li shift of lithiated γ-methylene nitriles via intermolecular transportation involving a dimeric aggregate.

Subsequent salt metathesis reaction of this species with $Cp^*_2TiCl_2$ (**7**) yielded the titanocene keteniminato complex **15** according to Scheme 15. Noteworthy, the salt metathesis occurred in a clean 1:1 stoichiometric ratio, no bis(keteniminato) complex was observed. In ^1H NMR spectrum, the resonance of the remaining methine proton is observed at 3.81 ppm. The corresponding ^{13}C resonance appears at 43.2 ppm, while the C1 signal appears downfield at 171.9 ppm, similar to these of other keteniminato complexes.[44,46]

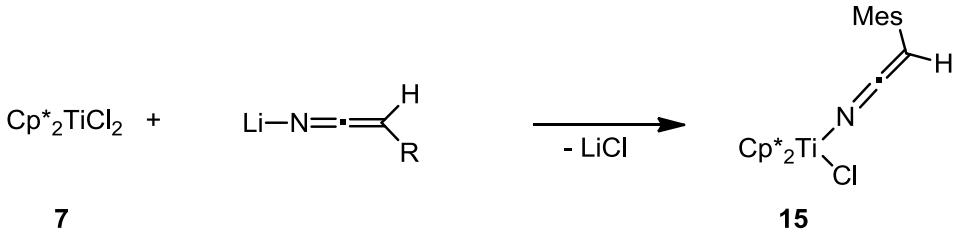

Scheme 15. Synthesis of complex 15.

The molecular structure of complex **15** is depicted in Figure 5, featuring a Ti center in a distorted tetrahedral geometry with the N1-Ti1-Cl1 angle (91.79(9)°) varying significantly from the ideal tetrahedral angle. This deviation is most likely caused by the big steric demand of the Cp* ligands. The keteniminato unit is almost linear (angle N1-C1-C2: 177.4(3)°) as expected for an *sp*-hybridized C1 atom. Subsequently, the N1-C1 and C1-C2 bond lengths correspond to typical allenic double bonds,[22] as observed in group 4 keteniminato complexes before.[46]

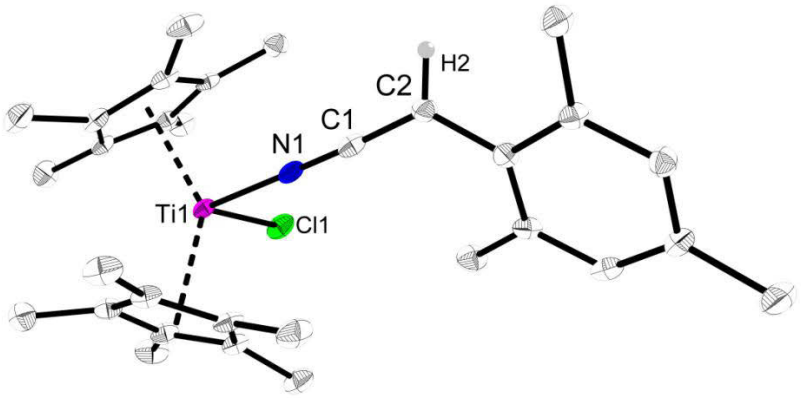

Figure 5. Molecular structure of 15 in the solid state. Hydrogen atoms except H2 are omitted for clarity. The thermal ellipsoids correspond to 30 % probability.

Although group 4 keteniminato complexes were described before, complex **15** is a rare example of such species bearing a proton at C2. Moreover, this complex also features a chlorido ligand at the Ti center as ideal preconditions for accessing the highly strained structure **J** by formal abstraction of HCl from **15**. Therefore, a second deprotonation attempt with several strong bases was performed (Scheme 16).

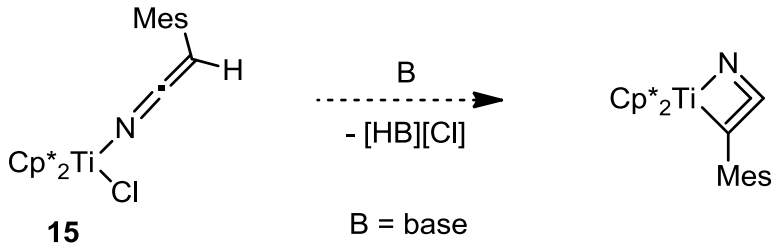

Scheme 16. Dehydrohalogenation attempt of 15 to yield a heterometallacyclobuta-2,3-diene.

However, using *n*-butyllithium or *t*-butyllithium as bases even at -78 °C resulted in formation of a dark brown solution. EPR analysis revealed the existence of various paramagnetic products. Therefore, no dedicated products could be isolated.

Performing the salt metathesis reaction of the "in-situ" generated Li keteniminato complexes with Cp_2ZrCl_2 (**6-Zr**), however, did not result in the formation of the expected zirconocene mono-keteniminato complex. Instead, a reaction in a 1:2 stoichiometric ratio occurred to result in the new coupling product **16** and unreacted starting material **6-Zr**.

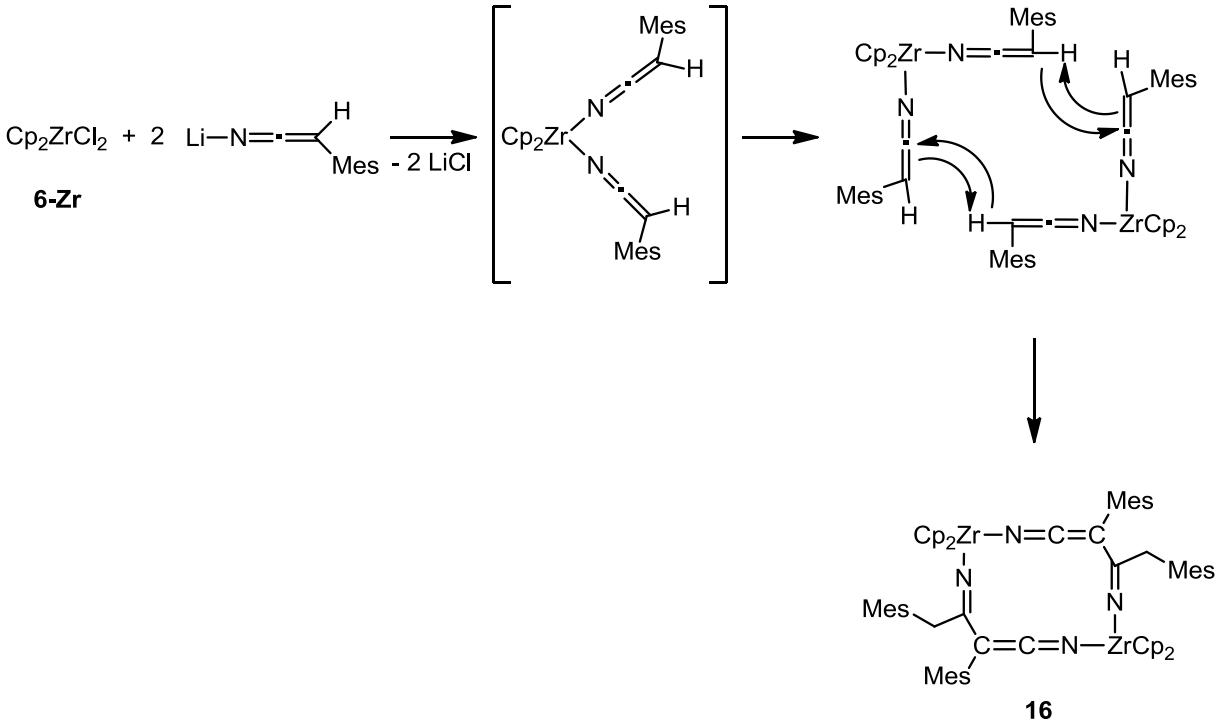

Scheme 17. Possible mechanism for the formation of complex 16 via zirconocene bis(keteniminate) complex.

In the reaction an intermolecular and unsymmetrical coupling of the central *sp*-hybridized C-atom of one keteniminato ligand with the *sp*²-hybridized C-atom of a second keteniminato ligand occurred, together with a proton transfer to result in the dimeric coupling product **16**. Most likely, the zirconocene bis(keteniminato) complex is formed as the initial step as an intermediate according to Scheme 17. Due to the remaining acidic γ-proton, one of the keteniminato ligands may act as a protonation agent while the other one acts as a proton acceptor. Subsequently, a C-C-bond formation takes place between the γ-C and the β-C in an intermolecular manner to form a bidentate ligand with both, keteniminato and imido functionality.

In the ^{1}H NMR spectrum, only one Cp resonance occurs at 5.77 ppm. The signal of the resulting methylene unit from the coupling appears at 3.20 ppm as a singlet while the mesityl substituents show different resonances for both aromatic and methyl groups. The molecular structure of complex **16** is depicted in Figure 6.

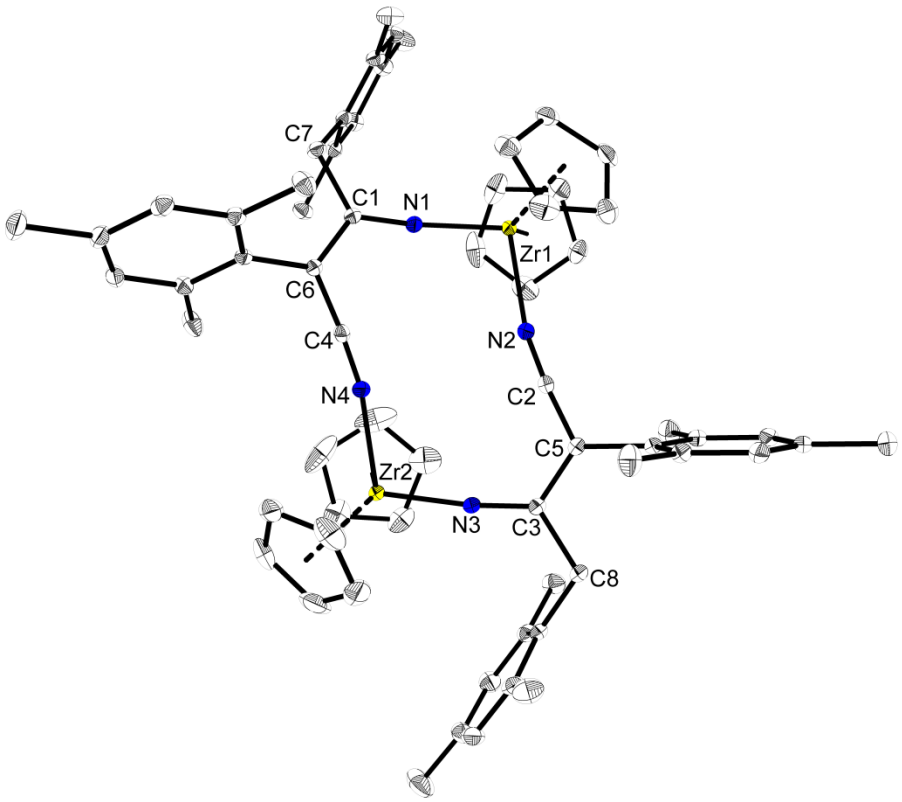

Figure 6. Molecular structure of 16 in the solid state. Hydrogen atoms are omitted for clarity. The thermal ellipsoids correspond to 30 % probability.

The Zr centers are surrounded by two Cp units, one keteniminato group and an imido group in a distorted tetrahedral geometry. While the keteniminato units are almost linear (angles N2-C2-C5: 174.25(17)°; N4-C4-C6: 175.83(16)°), the newly formed imido units are planar (sum of angles: 359.99° for C1 and C3), clearly indicating an sp^2-hybridization of their central carbon atoms C1 and C3. The created C-C-bonds (C1-C6 1.4197(19) Å; C3-C5 1.418(2) Å) exhibit adequate double bond character. Moreover, the Zr-imido (av. 1.950(1) Å) bonds are shorter than the Zr-keteniminato (av. 2.211 Å) bonds, indicating a stronger binding. Based upon these structural data, both resonance forms shown in Scheme 18 have a significant contribution on the appearance of complex **16**.

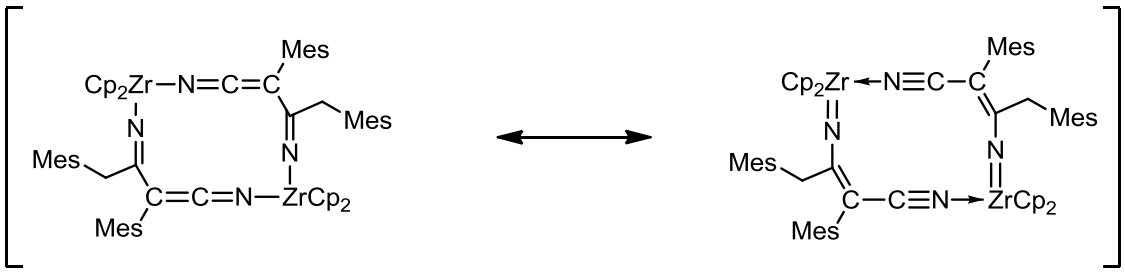

Scheme 18. Resonance forms of complex 16.

Although coupling of nitriles is well known for a variety of different transition metals, such coupling products were not described before. However, complexes with a five-membered [NCCCN] bridge have been observed. Besides the already mentioned Zr complex,[43] another main group complex is described. The reaction of Sr(dpp-bian)(thf)$_4$ (dpp-bian = 1,2-bis[(2,6)-diisopropylphenyl)-imino]acenaphthene) with acetonitrile resulted in such bridging complex.[47] The coordination of the first nitrile, followed by a deprotonation yielded a keteniminate. Subsequent bond formation between the α-carbon of a second CH_3CN and the β-carbon atom of the keteniminate unit resulted in the five membered bridge M-N(H)-C(Me)=C(H)-C≡N-M. In contrast to complex **16**, the Sr complex features an amide bond, resulting from a protonation of one nitrogen atom.

On the basis of these results, it can be stated that titanocene complexes are able to form mono keteniminato chlorido complexes while the corresponding zirconocene complexes prefer bis(keteniminato) complexes. Therefore, only the titanocene complexes are

suited as precursors for the formation of highly strained structures, even if these reactions did not succeed so far. However, the zirconocene complexes are not useful for such reactions. Nevertheless interesting coupling reactions result from the tendency to form bis(keteniminato) complexes leading to new insights into C-C-bond formations of γ-methylene nitriles.

2.2.3. Complexes with 7-Azaindolato ligands

2.2.3.1. State of the Art

Up to this point, chemistry of 7-azaindolato ligands is rarely described. Although this ligand can act in various interesting coordination modes, including mono- and dinuclear binding, only two complexes have been structurally characterized so far. These lanthanide complexes $Cp^*_2Yb(az)$ and $(DME)_2Yb(az)_2$ (az = 7-azaindolato), were both described by the group of Deacon.[48] They feature mononuclear coordination in a κ^2-*N*,*N*-fashion, thus forming four-membered heterometallacycles according to coordination mode **E** (Chapter Scheme 5). Other possible coordination modes were not described yet. (Scheme 19)

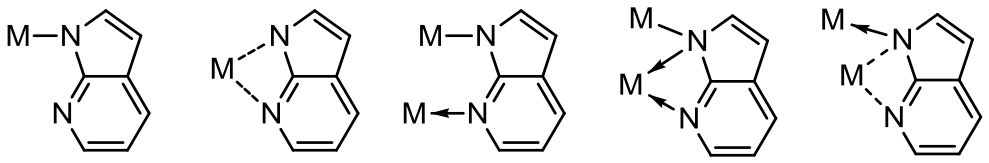

Scheme 19. Different mono- and dinuclear coordination modes of the 7-azaindolato ligand.

Noteworthy, the molecular structures of both Yb complexes exhibit strongly disordered 7-azainolato ligands. This disordering results from the similarity of the five- and the six-membered ring of the ligand, leading to an overlay of five- and six-membered ring of the 7-azaindolato ligand in the solid state. Hence, they cannot be separated and lead to the described disordering.

Therefore, in this chapter both unsubstituted 7-azaindole and 8-*t*-Bu-7-azaindole are used as ligand precursor. Due to the different steric demand of the *t*-Bu group, different coordination modes as well as omitting the above described disordering were proposed,

thus leading to a comparison of both ligands. Moreover, the depicted coordination modes of this ligand (Scheme 19) offer the possibility to form the four-membered heterometallacycle **E** (Scheme 5) by binding of both N-atoms to one metal center.

2.2.3.2. 7-Azaindolato complexes

In order to conduct salt metathesis reactions, deprotonation of 7-Azaindole with *n*-butyllithium in tmeda was performed, thus resulting in formation of the corresponding lithium complex. Surprisingly, single crystals of the deprotonation product, suitable for X-ray analysis were obtained. In the solid state complex **17** exhibits a dimeric structure according to Scheme 20.

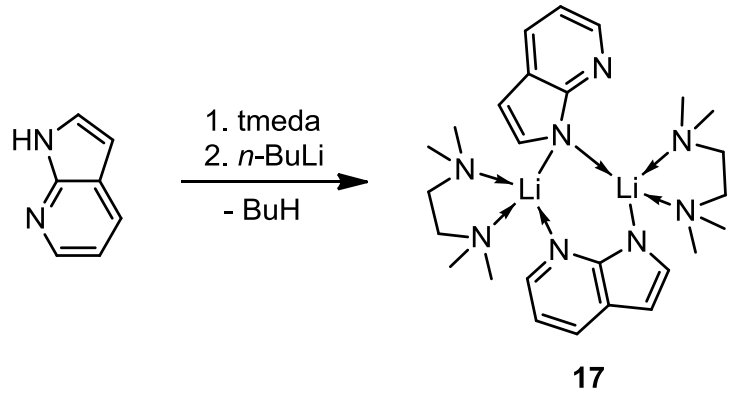

17

Scheme 20. Formation of the dimeric complex 17.

The molecular structure of **17** is depicted in Figure 7. In the dimeric complex, two different coordination modes of the 7-azaindolato ligand are present. While one ligand acts as a bridging ligand via both amido unit and the coordinating lone pair of pyridine unit, the second unsubstituted 7-azaindolato ligand features the bridging only over the amido unit in a μ^2-*N*,*N*-fashion. Moreover, each Li atom is coordinated by one chelating tmeda molecule , thus resulting in a distorted tetrahedral geometry for both Li atoms.

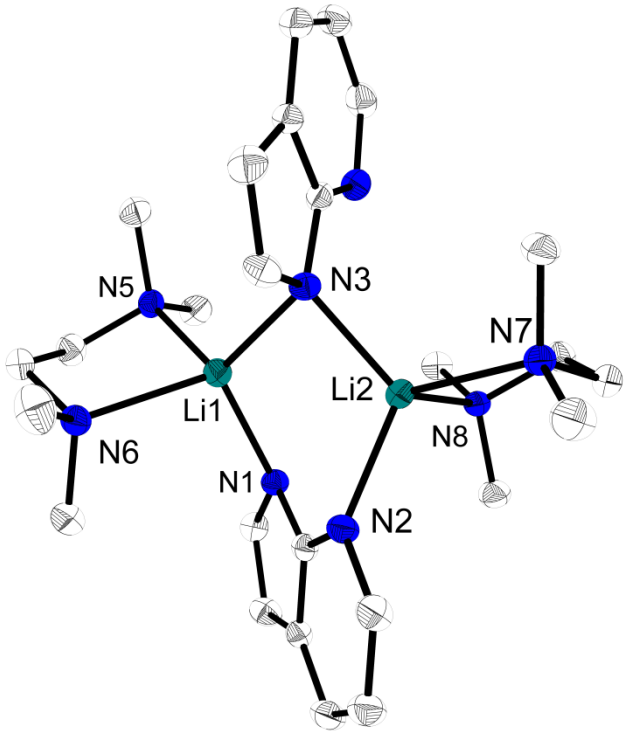

Figure 7. Molecular structure of 17 in the solid state. Hydrogen atoms are omitted for clarity. The thermal ellipsoids correspond to 30 % probability.

Performing the deprotonation reaction with the *t*-Bu substituted 7-azaindole at the same conditions, a mononuclear complex according to Scheme 21 is obtained.

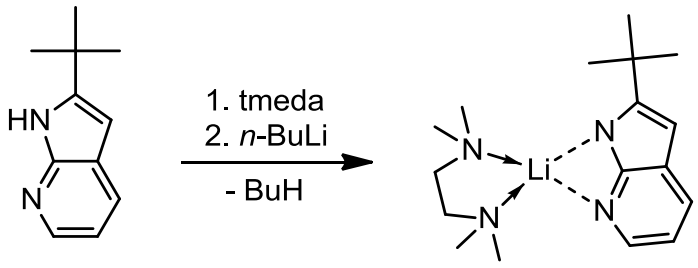

18

Scheme 21. Formation of the monomeric complex 18 by using substituted 7-azaindole.

The molecular structure of **18** in the solid state, shown in Figure 10, exhibits a Li center in a distorted tetrahedral geometry. The 7-azaindolato ligand features a chelating κ^2-*N*,*N* coordination mode over both N-atoms, thus forming a four-membered heterometallacycle. As observed in complex **17**, the Li center is stabilized by one chelating tmeda ligand.

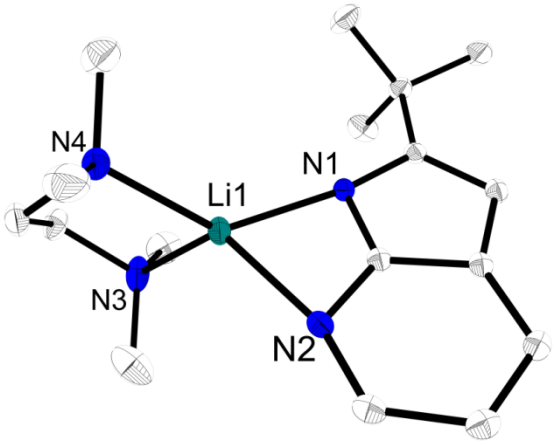

Figure 8. Molecular structure of 18 in the solid state. Hydrogen atoms and the disordered part of the tmeda ligand are omitted for clarity. The thermal ellipsoids correspond to 30 % probability.

These different results impressively show the influence of the sterically demanding *t*-Bu group, effectively preventing the dimerization as observed in complex **17**. In order to obtain different titanocene complexes with differently substituted 7-azaindolato ligands, complexes **17** and **18** were tested in salt metathesis reactions with $(Cp_2TiCl)_2$ (**5**) and Cp^*_2TiCl. However, other synthetic pathways described below were found to be more suitable.

The synthesis of these different titanocene complexes with the 7-azaindolato ligand involves various reactions with different titanocene precursors. Reaction of the sterically demanding $Cp^*_2Ti(\eta^2\text{-}Me_3SiC_2SiMe_3)$ (**3-Ti**) with unsubstituted 7-azaindole resulted in formation of the deep red titanocene^{III} complex **19** via oxidation of the former titanocene^{II} center according to Scheme 22. The final disposition of the hydrogen remains unclear, as both, elimination of the alkyne and reduction to H_2 as well as formation of the 1,2-bis(trimethylsilyl)ethene are known.

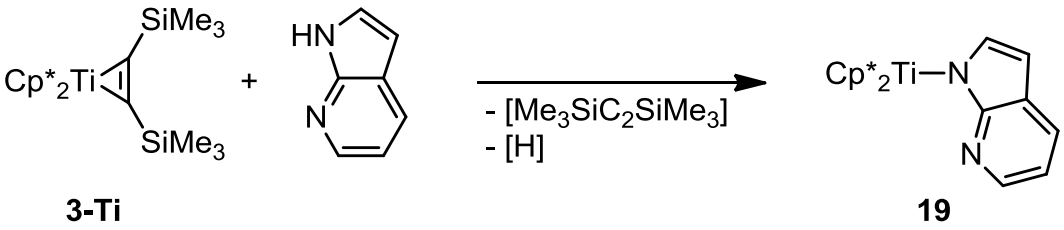

3-Ti **19**

Scheme 22. Synthesis of complex 19 via oxidation.

Due to the already discussed tendency of this ligand to be disordered in the solid state, only single crystals of poor quality could be obtained. The structural motif of complex **19** is depicted in Figure 9. Although the unsubstituted 7-azaindolato ligand was used, no chelating κ^2-*N*,*N* coordination mode could be observed. In complex **19** the Ti center is surrounded by two Cp* units and the amido function of the 7-azaindolato ligand in a trigonal planar fashion.

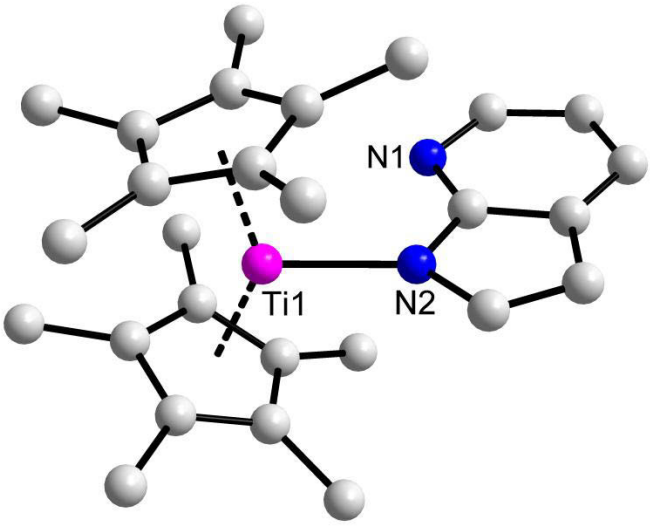

Figure 9. Structural motif of complex 19 in the solid state. Hydrogen atoms and the second molecule of the asymmetric unit are omitted for clarity.

Noteworthy, reaction of $Cp_2Ti(\eta^2\text{-}Me_3SiC_2SiMe_3)$ (**1**) with unsubstituted 7-azaindole yielded a dark paramagnetic powder. However, no crystals suitable for X-ray analysis could be obtained, therefore this reaction is not shown. Performing the reaction of **1** with the *t*-Bu substituted 7-azaindole, reaction only occurs at elevated temperature, leading to a mixture of products. Moreover, using **3-Ti**, no reaction occurred at all.

Therefore, salt metathesis reactions were performed. Noteworthy, the deprotonation can also be achieved by using di(alkyl)magnesium reagents. Using Et-Mg-*n*-Bu, followed by subsequent reaction with $(Cp_2TiCl)_2$ (**5**) resulted in formation of the dark green paramagnetic complex **20** according to Scheme 23.

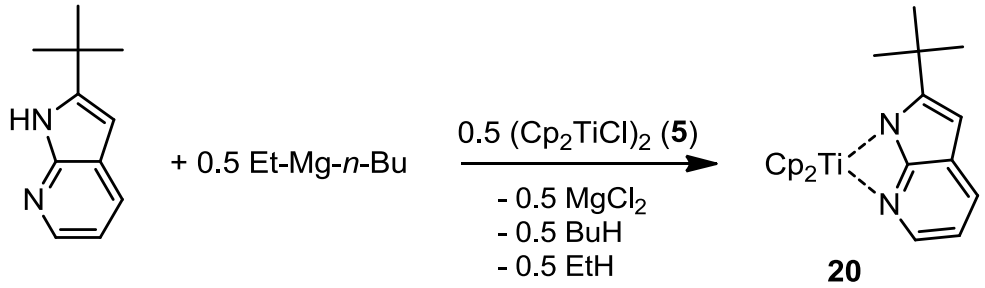

Scheme 23. Synthesis of complex 20 via salt metathesis.

The molecular structure of complex **20** is depicted in Figure 10. The Ti center is surrounded by two Cp units and the *t*-Bu substituted 7-azainolato ligand. Despite the use of the sterically demanding ligand, the coordination to the metal center occurs in a chelating κ^2-*N*,*N* fashion, thus leading to the formation of a four-membered heterometallacycle. The chelating effect is most likely attributed to the small steric demand of the Cp rings, especially compared to the sterically demanding Cp* ligands of complex **19**, which disfavor κ^2-binding.

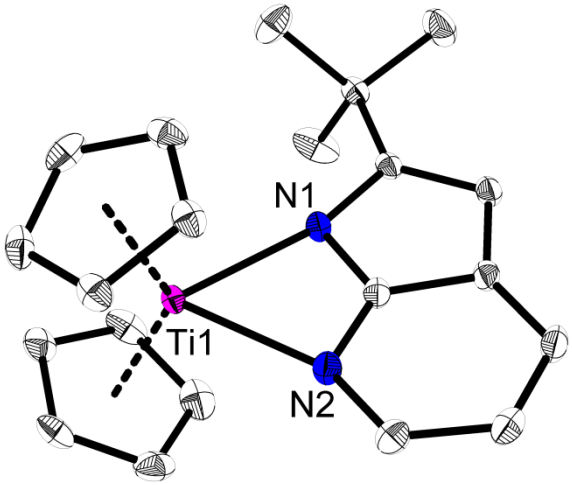

Figure 10. Molecular structure of 20 in the solid state. Hydrogen atoms and the second molecule of the asymmetric unit omitted for clarity. The thermal ellipsoids correspond to 30 % probability.

The averaged Ti-N1 (2.225 Å) and Ti-N2 (2.229 Å) bonds are very similar, corroborating the resonance forms depicted in Scheme 24. Therefore, complex **20** can be considered as an example of a four-membered heterometallacycle according to coordination mode **G** (Scheme 5).

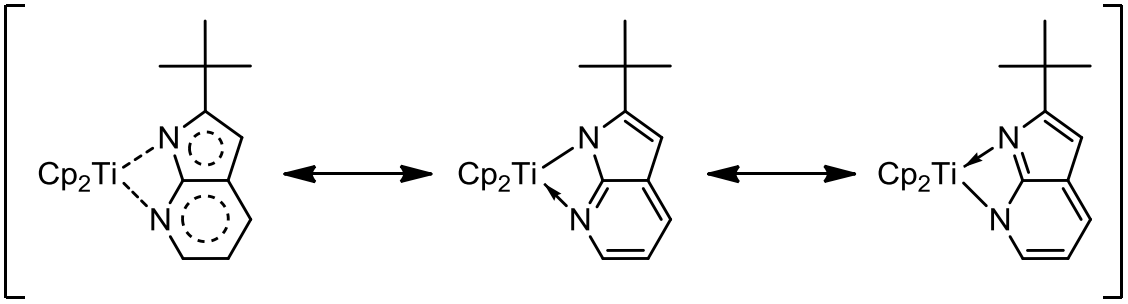

Scheme 24. Possible resonance forms of complex 20.

Independently from the deprotonation reagent, no salt metathesis reaction occurred by using the sterically demanding Cp^*_2TiCl. Also a variation of the reaction conditions such as time, temperature and solvent did not result in a significant change. NMR analysis of the reaction mixtures only revealed unreacted starting material. Most likely, the steric demand of both the Cp* ligands and *t*-Bu group prevents the reaction.

The expected differences in the coordination of unsubstituted and substituted 7-azaindolato ligands are only obvious in the case of the Li complexes **17** and **18**. For the titanocene complexes **19** and **20**, the coordination is strongly affected by the different cyclopentadienyl ligands, while the substitution of the 7-azaindolato ligands does not affect the coordination. Therefore, only the use of unsubstituted Cp ligands resulted in the formation of the desired four-membered heterometallacycle **E** (Chapter 2.2, Scheme 5). However, by using a sterically demanding substituent at 7-azaindolato ligand, the overlay of five- and six-membered ring of the 7-azaindolato ligand in the solid state could be prevented.

2.3. Phosphorus and Nitrogen Containing Metallacycles

2.3.1. State of the Art

In order to extend the scope of carbon-free heterometallacycles, chemistry of phosphorus and nitrogen containing ligands was investigated intensively. Previous studies on group 4 metallocene sulfurdiimide complexes have shown promising results.[49] Moreover, it has been well documented that *N*,*N*-bis(diphenylphosphino)amide can act as a ligand in three different binding modes (Scheme 25).

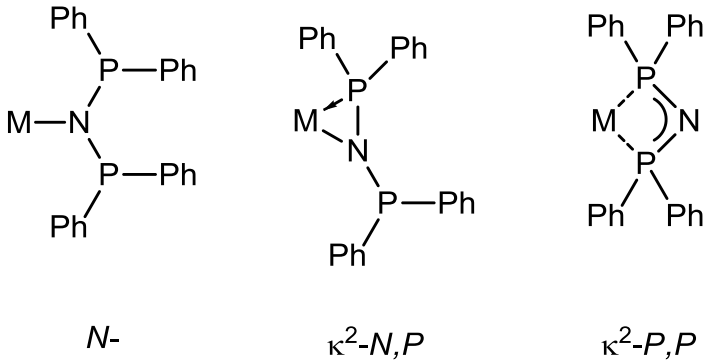

Scheme 25. Different binding modes of *N*,*N*-bis(diphenylphosphino)amide ligand.

N-binding is only known for the main group metals Cs[50] and K.[51] However, in the K complex additional interactions of the metal center with Ph groups of the ligand were observed. Formation of three-membered heterometallacycles as an result of *N*-binding with additional *P*-coordination (κ²-*N*,*P*) is described for numerous rare earth[52,53,54,55] and some alkaline earth metal complexes[54,55,56] as well as for the sodium complex (pmdta)Na[N(PPh$_2$)$_2$].[57] Cp$_2$Zr(Cl)[κ²-*N*,*P*-N(PPh$_2$)$_2$] as the only transition metal complex with κ²-*N*,*P* coordination mode was synthesized by Roesky and co-workers.[58] Contrarily, κ²-*P*,*P* coordination mode is described for many transition metals such as Fe,[59,60] Ni,[61] Pd[62] and Pt.[60] In accordance with the HSAB concept, this coordination mode is favored for late transition metals as the complexation takes place via κ²-coordination with the relatively soft phosphorus atoms. Subsequently, κ²-*P*,*P* coordination is unknown for hard early transition metals.

2.3.2. Three-membered Metallacycles with *N,N*-Bis(diphenyl-phosphino)amide

Reaction of hafnocene dichloride with one equivalent of lithiated *N,N*-bis(diphenyl-phosphino)amine leads, not surprisingly, to formation of a hafnocene^{IV} amide complex which features additional coordination of one of the phosphorus atoms of the ligand (Scheme 26). Complex **21-Hf** is isostructural to the zirconocene complex $Cp_2Zr(Cl)[\kappa^2$-*N,P*-$N(PPh_2)_2]$ (**21-Zr**), which was described by Roesky et al.[58] In **21-Hf**, in solution two different phosphorus resonances were found at δ = 60.3 and -4.7 ppm with the downfield peak indicating a strong coordination of the phosphorus atom to the hafnium center, even in solution. At room temperature, rapid exchange of the coordinating phosphorus atom can be observed by ^{31}P-NOESY spectroscopy, indicating a "flapping" of the *N,N*-bis(diphenylphosphino)amide ligand at the metal centre. In ^{1}H NMR spectra, the resonance of the Cp rings appear as a triplet due to a ^{3}J-coupling ($^{3}J_{P,H}$ = 8.4 Hz) of the Cp protons with the coordinating phosphorus atom. At 348 K both ^{31}P-resonances disappear, indicating coalescence of the phosphorus atoms at elevated temperatures.

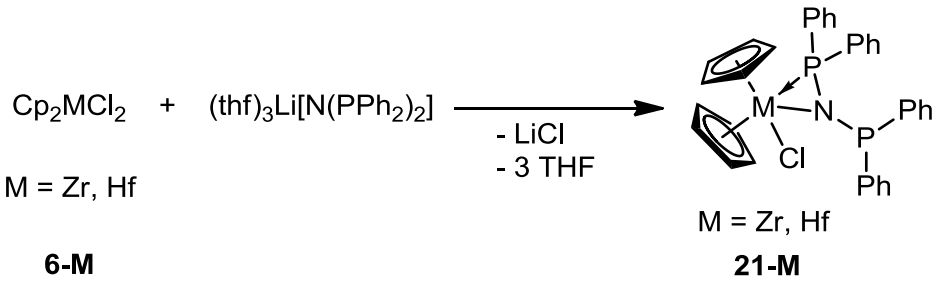

Scheme 26. Synthesis of complexes 21-Zr and 21-Hf.

Colourless crystals of **21-Hf** suitable for X-ray analysis were obtained from a saturated toluene solution at room temperature. The molecular structure of complex **21Hf** is shown in Figure 11. The hafnium center is coordinated by two Cp units, a chlorido ligand and the *N,N*-bis(diphenylphosphino)amide moiety via N1 and P1 in a κ^2-*N,P* -fashion, similar to the Zr complex **21-Zr**.[58] Hf1, N1 and P1 form a plane with the chlorido ligand being 0.26 Å above and the phosphorus atom P2 0.31 Å below this plane. A Hf1–P1 distance of 2.6248(6) Å was observed, smiliar to other hafnocene complexes with

additional phosphorus coordination (cf. $Cp_2Hf(PMe_3)(\eta^2\text{-}Me_3SiC_2SiMe_3)$: Hf-P 2.660(1) Å [63]).

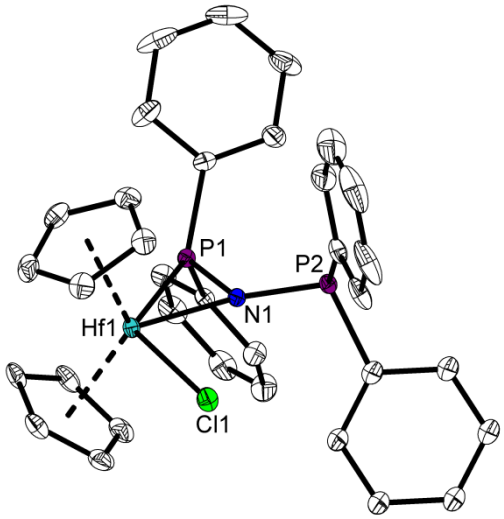

Figure 11. Molecular structure of 21-Hf in the solid state. Hydrogen atoms, the second position of the disordered Ph group and the solvent molecules (toluene) are omitted for clarity. The thermal ellipsoids correspond to 30 % probability.

2.3.3. Four-membered Metallacycles with *N,N*-Bis(diphenylphosphino)-amide

In order to elucidate the electronic influence of the oxidation state of the metal, Ti^{III} and Zr^{III} complexes were investigated as well. Therefore $(Cp_2TiCl)_2$ was used as an ideal $[Cp_2Ti]^{III}$ source. Reaction of *N,N*-bis(diphenylphosphino)amine with $(Cp_2TiCl)_2$ at elevated temperatures in THF resulted in the formation of the paramagnetic titanocene^{III} monochlorido complex **22** (Scheme 27). *N,N*-bis-(diphenylphosphino)amine acts as a donor ligand to fill up the deficient coordination number of the Cp_2TiCl fragment. Green crystals suitable for X-ray analysis were obtained from a saturated toluene solution at 8 °C. The molecular structure is depicted in Figure 12. The Ti center is surrounded by two Cp units, the chlorido ligand and the *P*-coordinating *N,N*-bis-(diphenylphosphino)amine in a distorted tetrahedral geometry with the Cl1-Ti1-P1 angle (81.033(15) °) being rather small. The Ti1−P1 distance was found to be 2.6224(5) Å, which is in the expected range compared to other trivalent titanocene^{III} complexes $Cp_2TiCl(PMe_2R)$ (R = Me[64], $SiMe_3$[65]). The structural parameters (N1-H1A···Cl1 unit:

N1-H1A 0.80(2), H1A···Cl1 2.62(2), N1···Cl1 3.283(2) Å; N1-H1A···Cl1 141(2)°) indicate a weak hydrogen bond between the chlorine and the hydrogen atom of the amino group.[66]

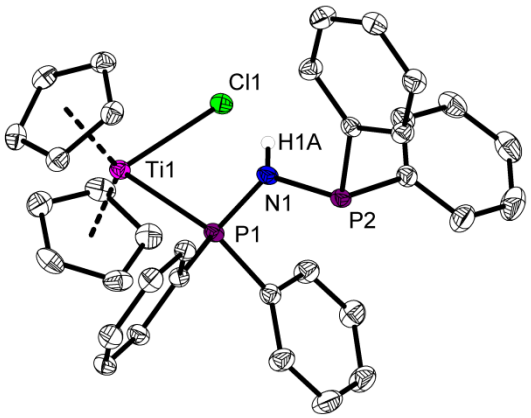

Figure 12. Molecular structure of 22 in the solid state. Hydrogen atoms except H1A are omitted for clarity. The thermal ellipsoids correspond to 30 % probability.

Interestingly, **22** reacted with *n*-butyllithium in THF in a well-predicted way to give complex **23-Ti** as the first highly strained four-membered metallacycle of an early transition metal with a *N,N*-bis(diphenylphosphino)amide ligand (Scheme 27).

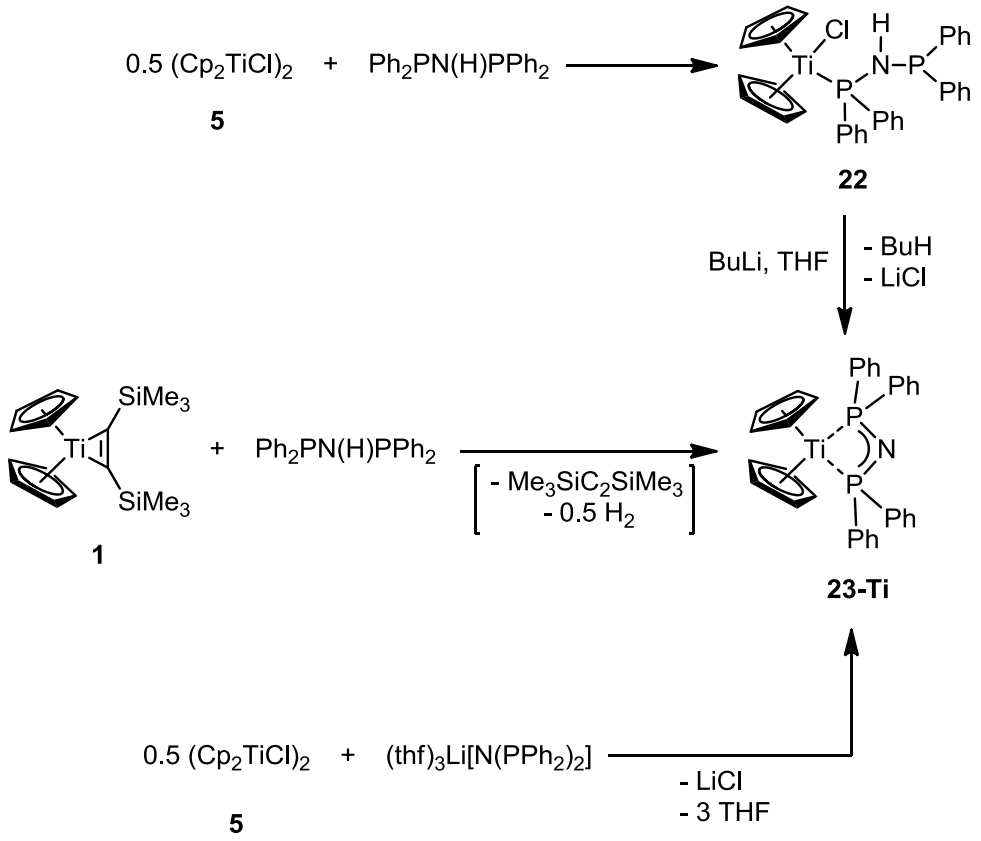

Scheme 27. Synthesis of the titanocene complexes 22 and 23-Ti on different pathways.

Formation of the dark green Ti^{III} metallacyclic amide $Cp_2Ti(\kappa^2\text{-}P,P\text{-}Ph_2P\text{-}N\text{-}PPh_2)$ (**23-Ti**) took place selectively and in high yields (85%), oxidation to Ti^{IV} was not observed. Attempts to use weaker bases such as triethylamine did not succeed. Additionally, reactions to obtain **23-Ti** on alternative pathways were investigated. Deprotonation of *N,N*-bis-(diphenylphosphino)amine with *n*-butyllithium, followed by subsequent salt metathesis reaction with $(Cp_2TiCl)_2$ also resulted in the formation of the four-membered heterometallacycle **23-Ti** according to Scheme 27. Surprisingly, **23-Ti** was also formed in the reaction of $Cp_2Ti(\eta^2\text{-}Me_3SiC_2SiMe_3)$ (**1**) in combination with the amine via a one electron oxidation of the Ti center. In all cases, formation of the heterometallacycle takes place in high yields (85 and 95%, respectively).

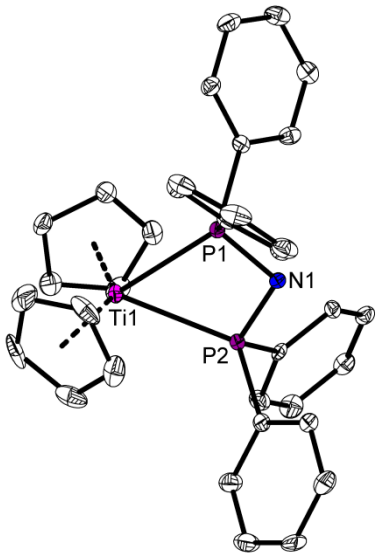

Figure 13. Molecular structure of 23-Ti in the solid state. Hydrogen atoms, the second molecule of the asymmetric unit and the solvent molecules (THF) are omitted for clarity. The thermal ellipsoids correspond to 30 % probability.

The molecular structure of complex **23-Ti** is shown in Figure 13. The titanium center is coordinated by two Cp ligands and the chelating PNP moiety in a strongly distorted tetrahedral geometry. The Ti–P distances (2.5997(6) Å - 2.6293(6) Å) are comparable to those in complex **22**. Due to the chelating effect of the ligand, the P–N–P angle (av. 104.7°) is rather small for an sp^2-hybridised nitrogen atom. The very small P–Ti–P angle (av. 60.1°) proves the high strain of the metallacycle, being even smaller than the P–M–P angle (64.5 – 67.4°) in other transition metal complexes.[60] This is notable, because the square planar or octahedral geometry of these complexes and the tetrahedral geometry of the titanium center suggest the opposite (ideal: square planar/octahedral 90°, tetrahedral 109.5°).

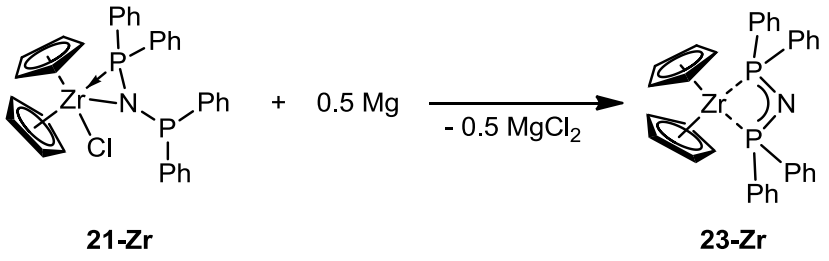

Scheme 28. Synthesis of 23-Zr via reduction of 21-Zr with Mg.

Performing the reaction of **21-Zr** with magnesium at elevated temperatures in THF resulted in the formation of a very rare Zr(III) complex, the four-membered metallacycle **23-Zr** (Scheme 28), which is isostructural to complex **23-Ti**. The reaction occurs even with an excess of Mg, impressively corroborating the stability of this Zr^{III} complex. This is noteworthy, because normally Zr^{III} compounds are very sensitive to possible reduction or disproportionation reactions.[67] Dark orange crystals of complex **23-Zr** can be obtained from concentrated toluene solution at -78 °C. The molecular structure of complex **23-Zr** is depicted in Figure 14. In contrast to the starting material, the Zr center features the κ^2-*P*,*P*-coordination in a strongly distorted tetrahedral geometry, forming the four-membered heterometallacycle.

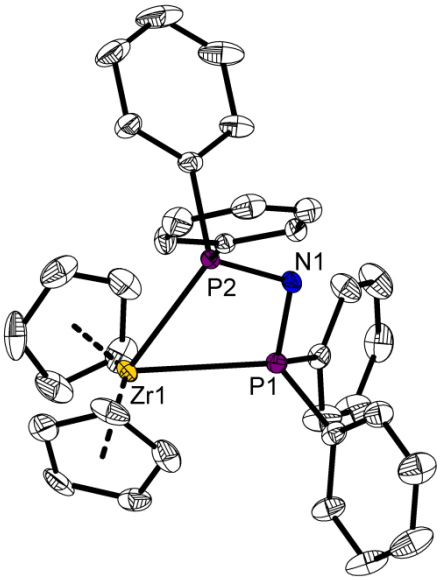

Figure 14. Molecular structure of 23-Zr in the solid state. Hydrogen atoms and the solvent molecules (toluene) are omitted for clarity. The thermal ellipsoids correspond to 30 % probability.

The P–N bond lengths in complex **23-Zr** are equivalent and the same as found in **23-Ti.** The P–Zr–P angle (57.69(2)°) represents the high strain of the heterometallacycle as shown in **23-Ti** and deviates highly from the ideal tetrahedral angle (109.47°). This different coordination behavior compared to **21-Zr** cannot be caused only by the steric demand of the chlorido ligand in **21-Zr** as its Zr center offers sufficient space for a κ^2-*P*,*P*-coordination as well. Regarding the HSAB concept, the reduced metal center in the oxidation state +III more likely prefers an interaction with the relatively soft

phosphorus atoms instead of a bonding with the hard nitrogen atom. Despite the small P–M–P angle and the resulting high ring strain of complexes **23-M**, especially the existence of **23-Zr** as rare Zr^{III} species proves their stability. All mesomeric resonance forms that might contribute to the stability of complexes **23-M** are depicted in Scheme 29.

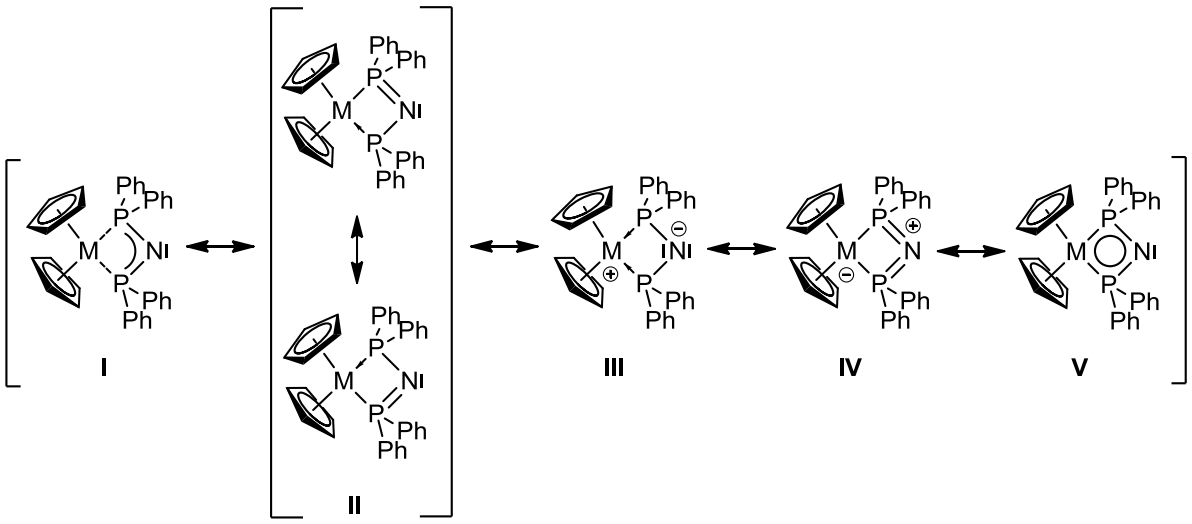

Scheme 29. Possible resonance forms of complexes 23-M.

In order to elucidate the influence of the metallacycle towards this stability, theoretical calculations have been conducted. The computed structural parameters for the thermodynamically most stable forms of both **23-Ti** and **23-Zr** are in good agreement with those found by X-ray analysis. The central heterometallacyclic unit is planar. In complex **23-Ti**, the Ti^{III} center exhibits a Mulliken spin density of 1.40 (Zr 1.04 in **23-Zr**, respectively). Examination of the charge distribution in the ligand by means of NBO analysis revealed that the negative charge is localized at the N-atom in all complexes **23-M**. The Wiberg bond index of the Ti-N bond in **23-Ti** is 0.60 (Zr 0.58 in **23-Zr**, respectively). The negative NICS values[68] (-6.06 ppm for **23-Ti**, -4.43 ppm for **23-Zr**) indicate in-plane aromaticity as an important contribution to the stability (Scheme 29, **V**) of the heterometallacycle, as observed before in a theoretical study of group 4 metallocene sulfurdiimide complexes[49] and group 4 metallocene bis(trimethylsilyl)acetylene complexes.[11] The NBO analysis suggests two highly polarized M–P σ bonds with occupancies of approximately 95 % and two P–N σ bonds, each having a high occupancy of 98 %. This, along with the Wiberg bond indices, reveals the presence of a four-membered σ skeleton for complexes **23-M**. An interannular

bonding contribution between the metal centre and the central N can be excluded by comparing the contact distances and the sum of the covalence radii (calculated contacts: Ti···N 3.30 Å and Zr···N 3.44 Å, respectively; Σr_{cov}: Ti–N 2.07 Å and Zr–N 2.25 Å, respectively[34]).

Surprisingly the similar reaction of **21-Hf** with Mg did not result in formation of the desired four-membered metallacycle, but anyhow in C-H bond activation to give a wide set of different products. Luckily, one of these products could be isolated as few colourless crystals of the hafnocene hydrido complex **24**, isostructural to the starting material **21-Hf** (Scheme 30).

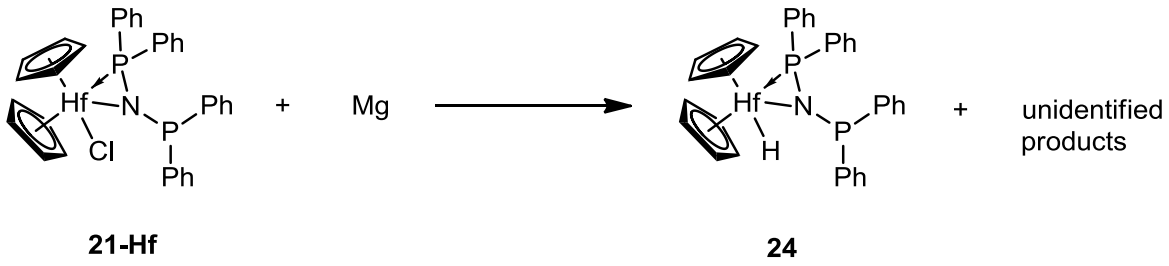

21-Hf **24**

Scheme 30. Unexpected formation of 24.

The hydrido resonance in the ^{1}H NMR spectrum appears as a doublet, due to a coupling with the coordinating phosphorus atom at 8.31 ppm ($^{3}J_{P,H}$ = 7.1 Hz). Tilley and co-workers described the hafnocene^{IV} hydrido complex CpCp*Hf[Si(SiMe$_3$)$_3$] with the hydrido resonance strongly shifted to higher field,[69] while other complexes with a similar shift are known as well.[70] The Cp resonances appear as a doublet with a small coupling constant J = 0.9 Hz, most likely due to a coupling with the metal hydride. However, in the hydrido resonance, this coupling is not resolved; its final origin remains uncertain. In ^{31}P NMR spectrum, one single resonance was found at δ -40.3 ppm. In contrast to the resonances of **21-Hf**, the existence of only one signal indicates, that the flapping of the phosphorus atoms at room temperature occurs faster than the NMR-timescale. Crystals suitable for X-ray analysis were obtained from a toluene solution. The molecular structure of **24** is depicted in Figure 15.

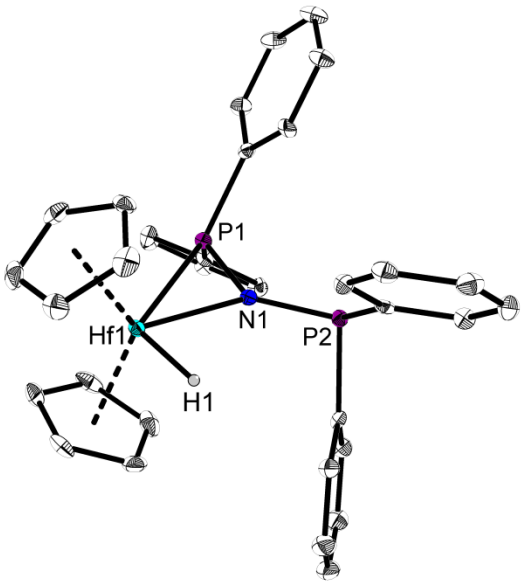

Figure 15. Molecular structure of 24 in the solid state. Hydrogen atoms except H1 are omitted for clarity. The thermal ellipsoids correspond to 30 % probability.

Despite the small steric demand of the hydrido ligand and the big Hf^{IV} center, the *N,N*-bis(diphenylphosphino)amide ligand coordinates in a κ^2-*N,P*-fashion similar to **21-Hf**. This observation proves the importance of a reduced metallocene^{III} center for the formation of a four-membered metallacycle using the [PNP] fragment.

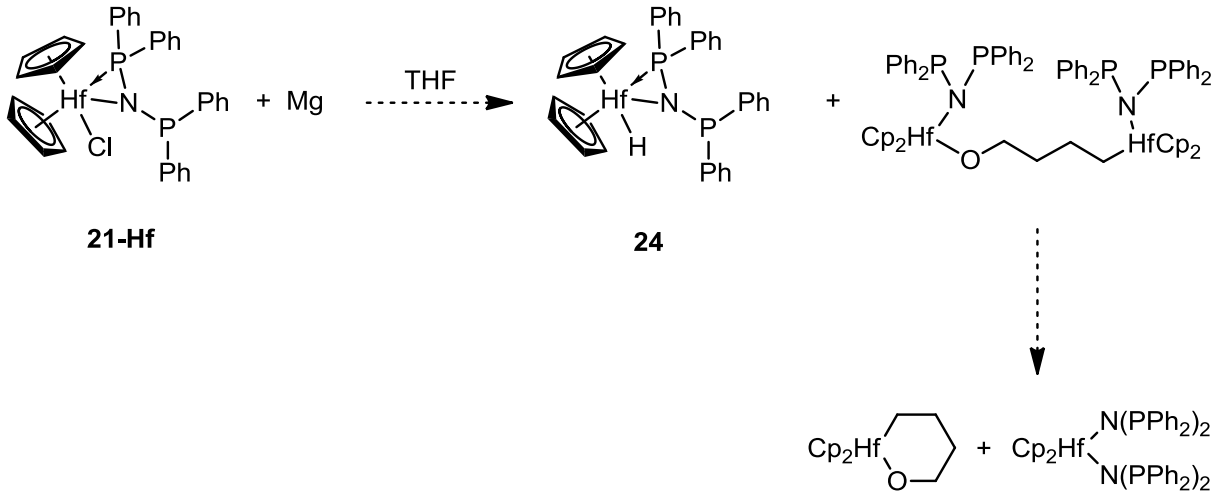

Scheme 31. Possible THF ring opening reaction of 21-Hf.

The origin of the hydrido ligand remains unclear. However, the ^{1}H NMR spectrum of the reaction mixture suggests activation of a THF molecule as found before in reactions of hafnocene and zirconocene compounds with Mg.[71] Attempts to avoid such undesired

solvent activation by using Li in toluene instead of Mg in THF failed. A possible THF-opening reaction is depicted in Scheme 31. Notably, no free *N,N*-bis(diphenylphosphino)amine was observed.

2.4. Phosphorus and Carbon Containing Four-membered Metallacycles

2.4.1. State of the Art

The chemistry of four-membered metallacycles with phosphorus and carbon containing ligand has been well documented over the last century. Thereby, most of these complexes contain a neutral $R_2P\text{-}C(R_2)\text{-}PR_2$ diphosphinomethane ligand with an sp^3-hybridized carbon atom, displaying a rather small ring strain (Scheme 32, **K**). Surprisingly, such complexes are unknown for group 4 metals. Generally, only a few complexes with early transition metals (Nb and Ta) are described.[72]

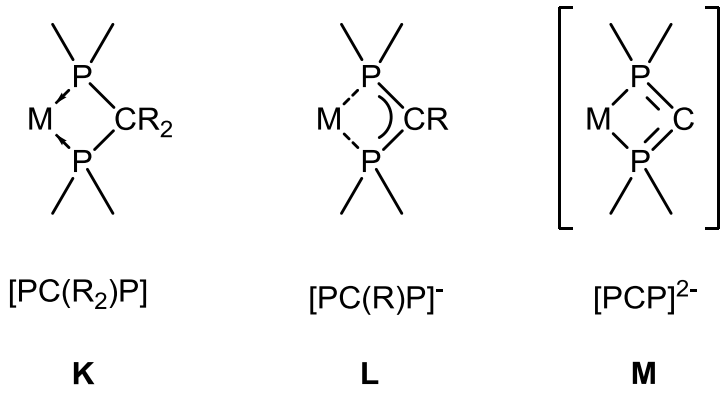

Scheme 32. Different four-membered metallacycles with a [PCP] fragment.

However, this class of ligands is known in various complexes of Cr[73] and Mo,[74] and late transition metals such as Fe,[75] Ru,[76] Ni,[77] Cu,[78] or even Au.[79] The monoanionic diphosphinomethanide ligand $[R_2P\text{-}C(R)\text{-}PR_2]^-$ (**L**) with a sp^2-hybridyzed carbon atom is isolobal to the $[R_2P\text{-}N\text{-}PR_2]^-$ ligand, discussed in Chapter 2.3 and therefore a matter of special interest. This type of ligand features a more distinct cyclic strain, thus less complexes are described with this class of ligand. Although different coordination modes such as *C*- or κ^2-*C*,*P*- binding are possible (similar to the [PNP] fragment), κ^2-*P*,*P* coordination is observed very often for this class of ligands. Contrarily to the neutral diphosphinomethane ligand, also hard early transition metal complexes are described. Karsch and co-workers described a Zr complex[80] and an Fe complex.[81] The V complex $[Li(thf)_4][V\{\kappa^2\text{-}P,P\text{-}Ph_2PC(H)PPh_2\}_3]$ was synthesized by Gambarotta et al.[82] Karsch et al. prepared both the zirconocene complex $[Cp_2Zr(Cl)\{\kappa^2\text{-}P,P\text{-}Ph_2P\text{-}C(SiMe_3)\text{-}PPh_2\}]$[83] and the ate complex $[Li(tmeda)_2][Zr(Cl)_2\{\kappa^2\text{-}P,P\text{-}Ph_2P\text{-}C(SiMe_3)\text{-}PPh_2\}_2]$.[84] Additionally,

this group obtained the titanocene complex [$Cp_2Ti\{\kappa^2$-*P*,*P*-$Me_2PC(SiMe_3)PMe_2\}$].[85] The dimeric ethylene-bridged complex [$Cp_2Zr(Cl)\{\kappa^2$-*P*,*P*-$(Ph_2P)_2C(C_2H_4)C(\kappa^2$-*P*,*P*-$PPh_2)_2\}Zr(Cl)Cp_2$] was described by Harrington's group.[86] In contrast to the HSAB concept, which predicts soft κ^2-*P*,*P* coordination to soft late transition metals, this bonding mode is also observed in these hard d^0 metal complexes, which would be expected to strongly favor a coordination mode including carbon bonding. The dianionic diphosphinomethandiide ligand (**M**) with an *sp*-hybridized carbon atom would contain two P^V atoms in the cyclic unit and the desired allene moiety to result in a highly strained cyclic system. Up to this point, such compounds have not been described.

2.4.2. Metallacycles with Bis(diphenylphosphino)methanide Ligands

Deprotonation reaction of diphosphinomethanes Ph_2P-C(H)(R)-PPh_2 (R = H, $SiMe_3$) with *n*-BuLi resulted in the in situ prepared analogous lithium-bis(diphenylphosphino)methanides.[87] Subsequent salt metathesis reaction with $(Cp_2TiCl)_2$ yielded the titanocene^{III} complexes **25a** and **25b** already at low temperatures in very good yields (Scheme 33).

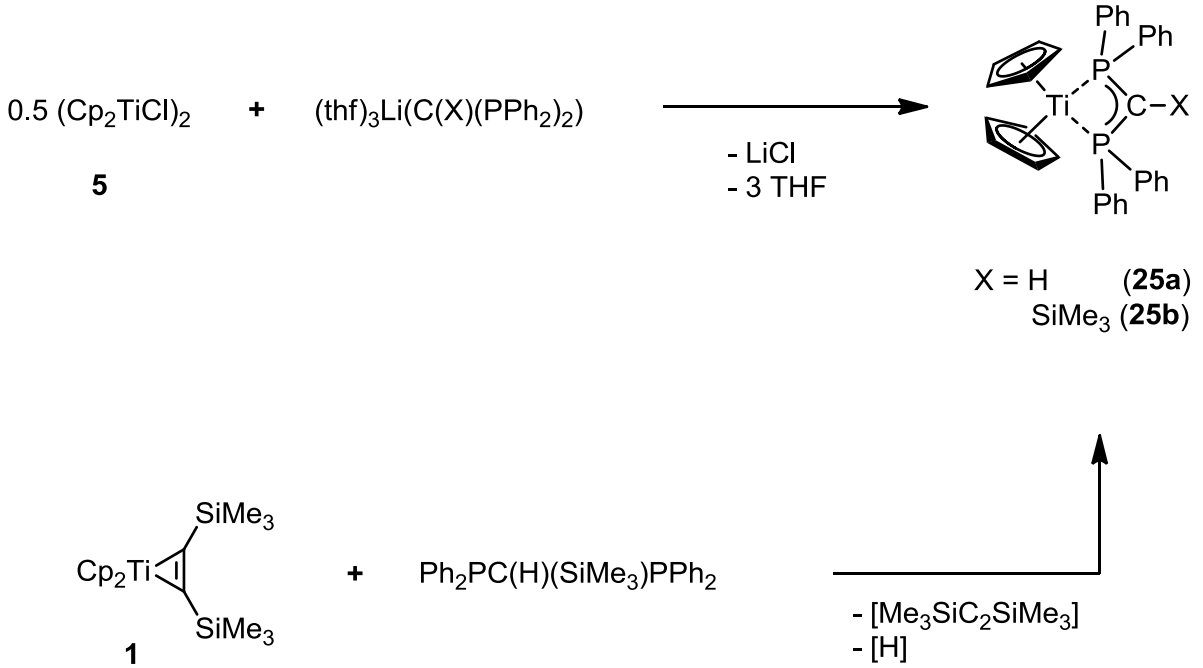

Scheme 33. Synthesis of the titanocene complexes 25a and 25b.

These paramagnetic complexes were characterized by mass spectrometry with the [M+H] peak of **25a** at *m/z* 562 and the molecular ion peak of **25b** at *m/z* 633. Reacting

the well-known titanocene source $Cp_2Ti(\eta^2\text{-}Me_3SiC_2SiMe_3)$ (**1**) with $Ph_2P\text{-}CH_2\text{-}PPh_2$, no formation of the desired product **25a** occurred. However, reaction of $Ph_2P\text{-}CH(SiMe_3)\text{-}PPh_2$ with **1** at elevated temperatures easily resulted in the formation of the desired metallacycle as an additional procedure to obtain **25b**. Most likely, the ligands firstly coordinates to the metal center, followed either by transfer of the proton to the bis(trimethylsilyl)acetylene or a reduction and the formation of dihydrogen.[10] However, the final disposition of the hydrogen remains unclear, as both, elimination of the alkyne and reduction to H_2 as well as formation of the 1,2-bis(trimethylsilyl)ethene were found before. The molecular structure of complex **25a** is depicted in Figure 16.

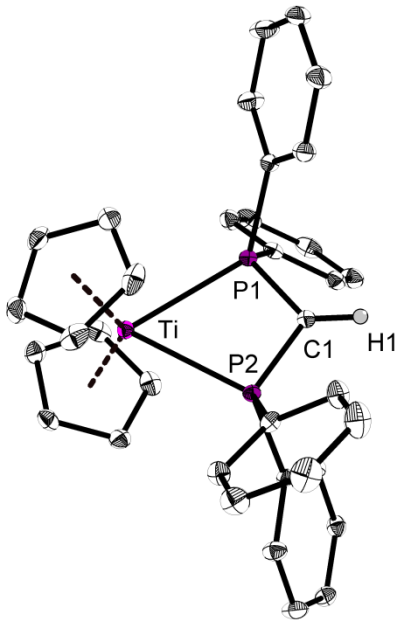

Figure 16. Molecular structure of 25a in the solid state. Hydrogen atoms except H1 are omitted for clarity. The thermal ellipsoids correspond to 30 % probability.

In accordance to the isolobal [PNP] complex, described above, the titanium center is coordinated by two Cp moieties and the chelating PC(H)P unit in a strongly distorted tetrahedral geometry. The P-Ti-P angle (63.201(13)°) is very small, similar to the already mentioned [PNP] complex (64.5-67.4°), indicating a high ring strain of the metallacycle. The P-C-P angle (106.71(8)°) is rather small for an sp^2-hybridised carbon atom, most likely due to the chelating effect of the ligand. The P-C1 bond length (av. 1.725 Å) are longer than an usual P-C(sp^2) double bond, but shortened compared to a typical P-C(sp^2) single bond.[22] This indicates a bond order between 1 and 2, according to the resonance forms, depicted in Scheme 34.

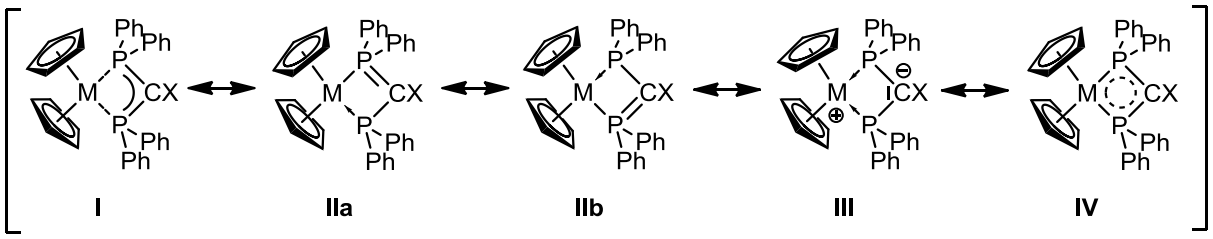

Scheme 34. Possible resonance forms of complexes 25a (X = H) and 25b (X = $SiMe_3$).

In order to get a detailed understanding of both, bonding situation and stabilizing mechanism, we also performed EPR experiments. The EPR spectrum of complex **25a** in solution is depicted in Figure 17.

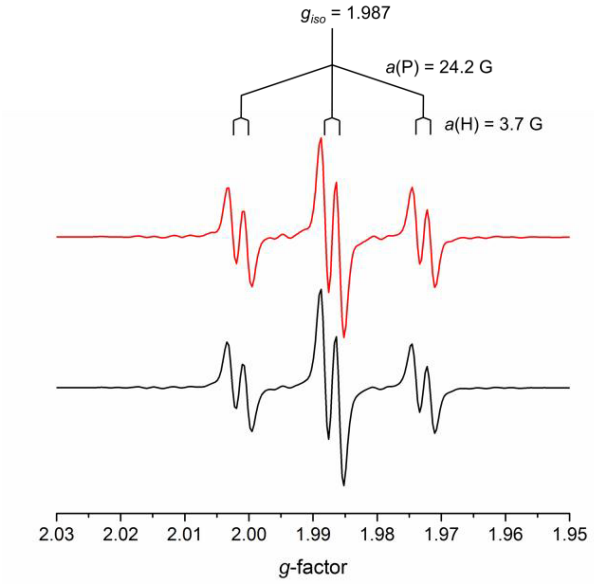

Figure 17. EPR spectrum of 25a in toluene solution at room temperature (black, bottom), simulated spectrum (red) on top.

Based on spectrum simulation the signal at g = 1.987 arises from a S = 1/2 single electron and can be assigned to a Ti^{III} center showing a superhyperfine (shf) structure from coupling to two equivalent nuclei of ^{31}P (I = 1/2, a(P) = 24.2 G) as well as to one ^{1}H nucleus (I = 1/2, a(H) = 3.73 G). A hyperfine (hf) structure with a(Ti) = 9.13 G resulting from the coupling to the isotope nuclei ^{47}Ti (I = 5/2, natural abundance: 7.40%) and ^{49}Ti (I = 7/2, natural abundance: 5.40%) is observable as weak signal features especially in the low- and high-field range. These data agree with the molecular structure of complex

25a, which exhibits coordination of two equivalent P atoms to the Ti^{III} center. Therefore, the coupling constants *a*(P) for both phosphorus nuclei show the same value.
Similar EPR parameters were obtained before by Dick and Stephan for titanocene phosphide systems as $Cp_2TiPPh_2(PMe_3)$ showing a *g*-factor of 1.991 and shfs to ^{31}P with *a*(P) = 26.2 and 2.3 G, respectively.[88] Since the distance between Ti^{III} and the ^{1}H nucleus in **25a** is markedly larger than the Ti-P distance, the Ti^{III}-^{1}H shf coupling is smaller compared to the Ti^{III}-^{31}P coupling.

Reaction of the lithiated bis(diphenylphosphino)methane with Schwartz reagent (**8**) resulted in formation of the four-membered metallacycle **26** according to Scheme 35. In ^{31}P NMR, the phosphorus resonances at -14.16 and -16.46 ppm appear as a doublet, due to a coupling (^{2}J = 144 Hz) with the second phosphorus atom of the ligand. In contrast to complex **25a**, the phosphorus atoms are not equivalent as a result of the broken symmetry caused by the ancillary hydrido ligand. Additionally, complex **26** was characterized by mass spectrometry, its molecular ion peak was found at *m/z* 603.

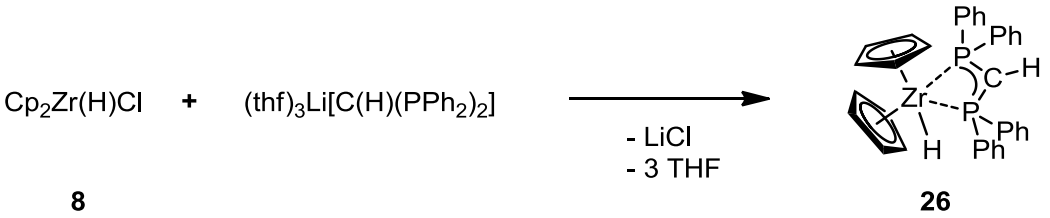

Scheme 35. Formation of the zirconocene hydrido complex 26.

The molecular structure of **26** is shown in Figure 18. The zirconium center is surrounded by two Cp units, the hydrogen atom H1A and the chelating [PCP] ligand in a κ^2-*P*,*P*-fashion. Zr1 and the phosphorus atoms P1 and P2 form a plane, the carbon atom C1 being 0.19 Å above this plane, resulting in a small distortion of the planarity of the central metallacycle. The hydrogen atom H1A is located 0.13 Å below this plane. As found for the Ti^{III} complex **25a**, the P-C1 bond lengths (av. 1.723 Å) show the same bond order between 1 and 2. The P1-Zr-P2 angle (59.203(11)°) is smaller than in complex **25a**, indicating an even higher ring strain of the metallacycle.

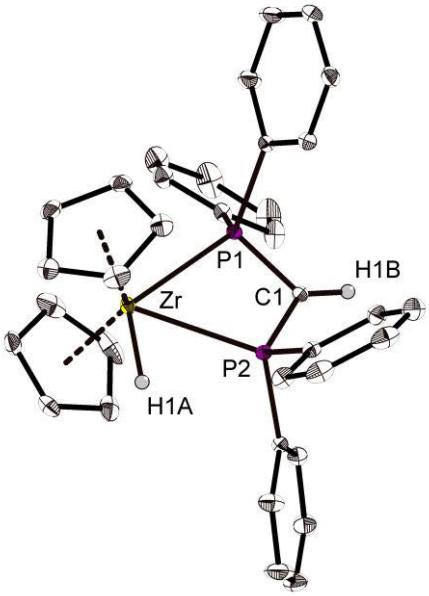

Figure 18. Molecular structure of 26 in the solid state. Hydrogen atoms except H1A and H1B are omitted for clarity. The thermal ellipsoids correspond to 30 % probability.

Reaction of both lithiated diphosphinomethanes $(thf)_3Li[Ph_2P\text{-}C(R)\text{-}PPh_2]$ (R = H, $SiMe_3$) with Cp_2HfCl_2 resulted in the formation of the desired products **27a** and **27b**, respectively (Scheme 36).

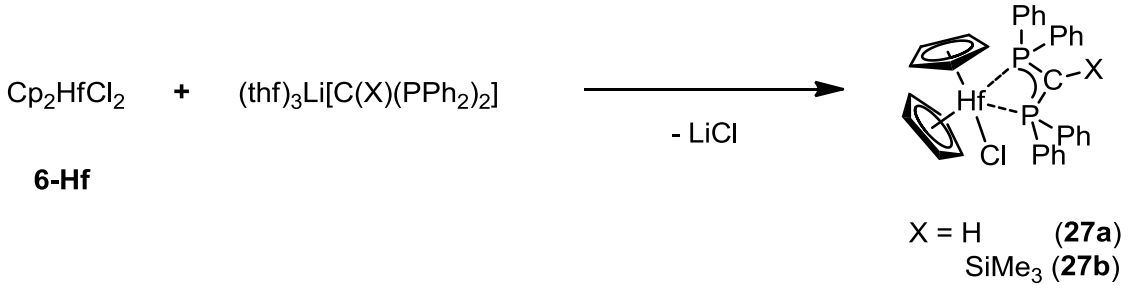

Scheme 36. Synthesis of the hafnocene chlorido complexes 27a and 27b.

The central four-membered rings of these complexes are similar to the fragment in the zirconocene complex **26**. In ^{31}P NMR spectra of complex **27a**, two phosphorus resonances were found at -4.55 and -10.57 ppm, appearing both as a doublet (^2J = 235 Hz), resulting from the coupling with the second phosphorus atom. For **27b**, the phosphorus resonances were found at 10.41 and 7.88 ppm as doublets (^2J = 219 Hz) These two sets of resonances indicate non-equivalence of the phosphorus atoms due to the chlorido ligand on the hafnium center as found in complex **26**. In the ^1H NMR spectra

of **27a**, the resonance of the Cp rings appears as a triplet, due to a ^3J coupling ($^3J_{H,P}$ = 1.2 Hz) of the Cp protons with the phosphorus atoms while in **27b**, the Cp signal appear as a doublet of doublets ($^3J_{H,P1}$ = 1.5 Hz, $^3J_{H,P2}$ = 0.7 Hz), resulting from two indifferent couplings with both of the phosphorus atoms.

Additionally, both complexes were characterized by mass spectrometry, the $[M\text{-}Cl]^+$ peak of **27a** was found at *m/z* 693, the $[M]^+$ peak of **27b** at *m/z* 800, respectively. The molecular structure of **27a** is depicted in Figure 19.

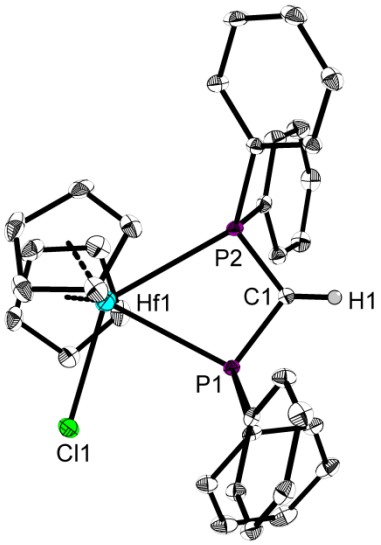

Figure 19. Molecular structure of 27a in the solid state. Hydrogen atoms except H1 are omitted for clarity. The thermal ellipsoids correspond to 30 % probability.

While the similar [PNP] complex in Chapter 2.3 features an κ^2-*P*,*N* coordination, the chelating ligand in complex **27a** binds over both phosphorus atoms in a κ^2-*P*,*P*-fashion to form a highly strained four-membered hetero-hafnacycle. However, in contrast to complex **26**, the carbon atom C1 deviates stronger from that plane (angle between the planes, defined by M1, P2, P1 and P1, C1, P2: **27a** 13.83(8)° and for comparison in **28**: 10.4(1)°), leading to a more bent cyclic unit. While the carbon atom C1 is located 0.24 Å above the plane, formed by Hf1, P2 and P1, the chlorido ligand is almost located in this plane (0.005 Å below). As discussed for complexes **25a** and **26**, the C1-P distances (1.717(2) Å) in complex **27a** correspond to an elongated P-C double bond as well as to a shortened P-C single bond,[22] indicating the bond order between 1 and 2.

2.4.3. Investigations to the Chemistry of Metallacycles with Bis(diphenylphosphino)methandiide Ligands

Complexes **26**, **27a** and **27b** were tested as precursors for access of hetero metallacyclobuta-2,3-diene (Scheme 32, **M**) by liberating H_2, HCl or Me_3SiCl according to Scheme 37. Complexes **26** and **27b** were heated up to 110 °C in toluene, however, no reaction occurred. Reaction of complex **27a** with both strong bases *n*-butyllithium and *t*-butyllithium unfortunately also did not result in the formation of the heterometallacyclobuta-2,3-diene complex. While reaction of **27a** with *n*-butyllithium did not occur, the use of *t*-butyllithium only resulted in the formation of a hardly soluble orange solid. NMR analysis did not reveal a specific product, most likely the decomposition of **27a** takes place to result in a mixture of different species. It has to be considered, that complexes **26**, **27a** and **27b** are very stable and therefore not useful as precursors for the synthesis of heterometallacyclobuta-2,3-dienes (Scheme 32, **M**).

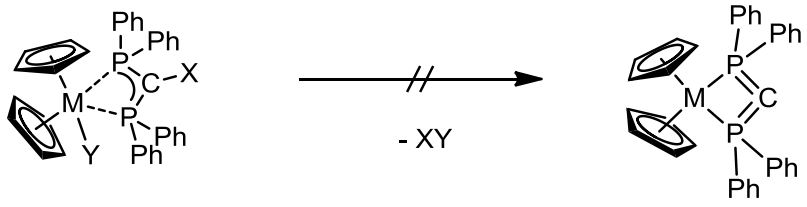

M = Zr, X = Y = H (**26**)
M = Hf, X = H, Y = Cl (**27a**)
M = Hf, X = $SiMe_3$, Y = Cl (**27b**)

Scheme 37. Attempts to formation of heterometallacyclobuta-2,3-dienes.

2.5. Metallacycles with Bis(diphenylphosphino)acetylene Ligands

2.5.1. State of the Art

Generally, the coordination chemistry of heterosubstituted alkynes EC≡CE (E = OR, NR_2, PR_2) at early transition metals is very limited. These limitations are most likely caused by the different electronic nature of the substituents on the central C_2-unit and the resulting stability of the alkynes. Nevertheless, some rare examples of nitrogen or boron containing alkynes have been described for group 4 metals.[89,90] In order to expand the scope of chemistry of phosphorus and carbon containing ligands that are able to form four-membered metallacycles, bis(diphenylphosphino)acetylene $Ph_2PC{\equiv}CPPh_2$ was chosen as a promising precursor for such metallacycles. Although the chemistry of acetylene ligands on group 4 metallocenes was intensively investigated in the last decades,[10] pnictogen substituted alkynes have been rarely used as ligands for these early transition metals to form mononuclear complexes.[89] This might be due to the different electronic nature of the pnictogen substituent, which discloses a wide range of different coordination modes with the lone pair of the pnictogen atom. Besides the realized η^2-C-C-binding mode (**N**) mononuclear binding should also occur with both phosphorus atoms (κ^2-*P*,*P*) (**O**), or over one phosphorus and one carbon atom in a κ^2-*C*,*P* fashion to form a four-membered metallacycle (**P**) (Scheme 38).

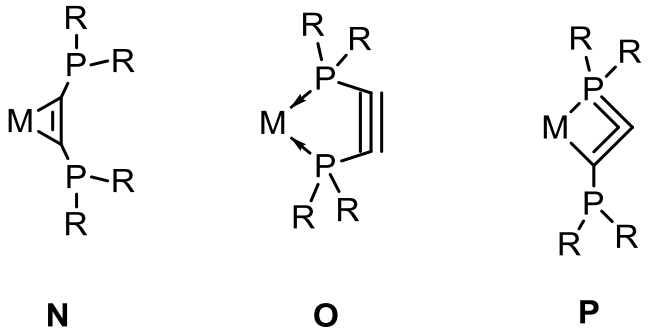

Scheme 38. Possible mononuclear coordination modes of the $R_2PC{\equiv}CPR_2$ ligand.

Due to these flexible coordination modes, only one example of a diphosphino substituted alkyne complex binding exclusively over the alkyne unit (**N**) is known. This niobium[I] compound $(CO)_2(PPhMe_2)_2(I)Nb(\eta^2\text{-}Ph_2PC_2PPh_2)$, was synthesized by Rehder and co-workers.[91] Besides, there are many examples of complexes coordinating a second or even a third metal fragment to this ligand $Ph_2PC{\equiv}CPPh_2$ by binding other metal fragments with the lone pairs of the phosphorus atoms (Scheme 38, **O**) or even two

metal fragments over the alkyne unit.[92,93] Coordination only over the phosphorous atoms has not been described so far. Noteworthy, there are examples for monophosphino substituted alkynes, which serve as excellent ligands also in case of group 4 metallocene complexes. Tilley and co-workers recently reported on the reactions of $R_2PC{\equiv}CR'$ (R = *i*-Pr, Et, Ph; R' = Ph, Mes) with the zirconocene source $Cp_2Zr(py)(\eta^2\text{-}Me_3SiC_2SiMe_3)$ to give three- and five-membered all-C-metallacycles.[94] However, incorporation of the electron rich phosphorus atom in the cyclic unit would lead to a significantly increasing stability of the ring system as already presented in previous chapters.[20] Furthermore, the incorporation of only one of the phosphorus atoms in the cyclic unit would result in the very interesting coordination mode (**P**), being a four-membered heterometallacyclobuta-2,3-diene.

2.5.2. "All-C" Metallacycles

Reaction of bis(diphenylphosphino)acetylene with the sterically demanding titanocene source $Cp^*_2Ti(\eta^2\text{-}Me_3SiC_2SiMe_3)$ (**3-Ti**) in toluene at elevated temperatures resulted in the formation of the alkyne complex $Cp^*_2Ti(\eta^2\text{-}Ph_2PC_2PPh_2)$ (**28**) in very good yields (Scheme 39).

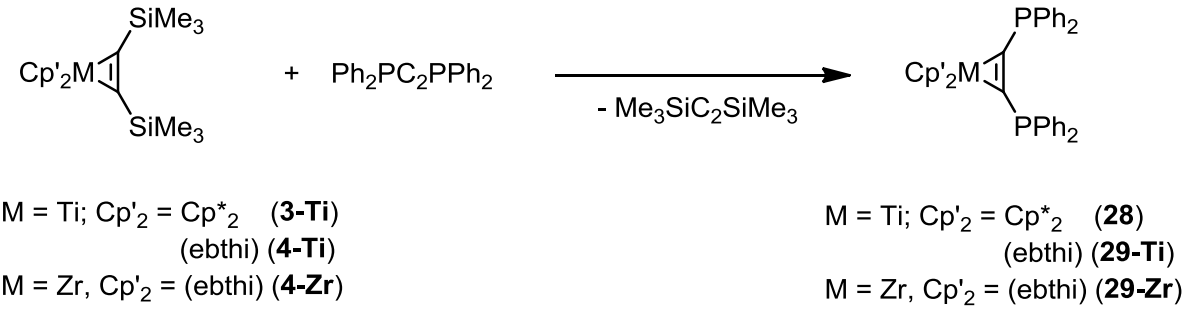

Scheme 39. Synthesis of complexes 28, 29-Ti and 29-Zr.

Complex **28** does not feature additional coordination of one of the phosphorus atoms, the ligand binds exclusively via the alkyne unit, yielding the well known metallacyclopropene fragment according to coordination mode (**N**). Performing the same reaction with the similar titanocene alkyne complex **4-Ti** results in the formation of the similar alkyne complex **29-Ti**, which also does not feature any additional coordination, even when being less sterically crowded than the permethylated complex **28**. ^{31}P NMR spectra of these complexes display only one single phosphorus resonance

at 7.14 ppm (**28**) and 2.06 ppm (**29-Ti**), respectively, indicating equivalence of both phosphorous atoms. The quaternary carbon signals of the coordinated alkyne appear as a doublet, due to a coupling with the adjacent phosphorus atoms at 213.4 (**28**) and 213.8 ppm (**29-Ti**), respectively. The coupling constants of 77.5 Hz (**28**) and 76.8 Hz (**29-Ti**) are very similar and in the expected range for a C-P ^{1}J coupling. A comparison of the corresponding quaternary ^{13}C signals of the uncoordinated alkynes of starting materials and products ($Ph_2PC{\equiv}CPPh_2$ 107.8 and $Me_3SiC{\equiv}CSiMe_3$ 114.0 ppm, respectively) reveals that the resonances of the free ligands are similar. The corresponding resonances of **3-Ti** and **4-Ti** (248.5 and 244.5 ppm, resp.),[95,96] lead to significant $\Delta\delta$ values (134.5 ppm for **3-Ti** and 130.5 ppm for **4-Ti**). However, in complexes **28** and **29-Ti** these $\Delta\delta$ values (105.6 ppm for **28** and 106.4 ppm for **29-Ti**) are smaller. The resulting differences (28.9 ppm for **3-Ti**/**28** and 24.1 ppm for **4-Ti**/**29-Ti**) can be attributed to a different binding of the bis(diphenylphosphino)acetylene to the metal center compared to the bis(trimethylsilyl)acetylene. In general, the less downfield shift indicates a weaker binding of the alkyne to the metal center, leading to more electron density in the C-C multiple bond. However, the lone pairs of the phosphorous atoms might interact with the alkyne unit to transfer electron density into the multiple bond system, leading to an upfield shift in the ^{13}C spectrum as a result of the hyperconjugation. This observation is in good agreement with the resonances of the phosphorus atoms (7.14 ppm for **28** and 2.06 ppm for **29-Ti**), which are slightly shifted downfield compared to the phosphorus resonance of the free alkyne (-31.58 ppm), indicating this electron transfer. Additionally, the IR spectrum of **28** (and **29-Ti**) show the C=C bond stretch at 1433 cm^{-1} (and 1430 cm^{-1}, resp.), a huge difference ($\Delta\nu$ = 664 cm^{-1} for **28** and 667 cm^{-1} for **29-Ti**) to the free ligand (ν = 2097 cm^{-1}).[97] The molecular structure of complex **28** is depicted in Figure 20.

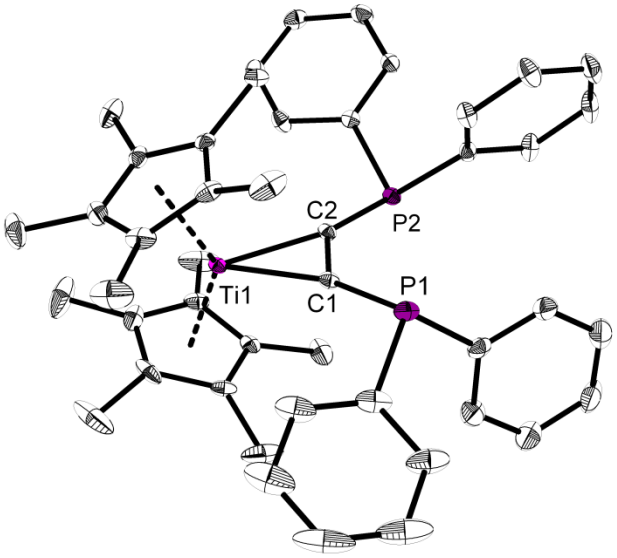

Figure 20. Molecular structure of 28 in the solid state. Hydrogen atoms and the second molecule of the asymmetric unit are omitted for clarity. The thermal ellipsoids correspond to 30 % probability.

Based on the resonance forms of such group 4 metallocene alkyne complexes in Chapter 1 (Scheme 2), the geometry of the titanium center, coordinated by two Cp* ligands and the alkyne unit, can be described either as strongly distorted tetrahedral or trigonal planar. All hereby described complexes are discussed as metallacyclopropenes and therefore, the geometry of the central metal atom is described as tetrahedral. Due to the small angle of the highly strained three-membered metallacycle, the tetrahedral geometry is strongly distorted. No additional ligand is observed, which can be attributed to the steric demand of the Cp* ligands. Not surprisingly, the Ti-C distances (2.129(2) Å and 2.115(2) Å) are similar to those of the starting complex **3-Ti**.[95] The C-C distance (1.317(3) Å) clearly indicates a double bond between the carbon atoms, subsidized by both PCC angles (131.42(14)° and 134.71(15)°) which refer to the sp^2-hybridisation of the carbon atoms.

The molecular structure of complex **29-Ti** is depicted in Figure 21, showing the same connectivity as in the already discussed complex **29-Ti**. The Ti-C distances are even shorter than in complex **28**, due to the decreased steric demand of the (ebthi) ligand. The C-C distance (1.309 (2) Å) is not significantly diiferent from that in **28**, indicating the same double bond character. Remarkable are the almost parallel Ph groups of the ligand, which indicate a π-stacking of these aromatic rings. The distance between both Ph-groups (distance between both centroids C_g-C_g 3.725(1) Å) is in the normal range of

such π-π interactions.[98] The angle between the planes defined by both Ph rings is very small (5.0°). The values for the angles between the ring normals and the vectors of the ring centroids (22.4 and 26.7°, respectively) are rather big, but in good agreement with other π-π-interactions.[98]

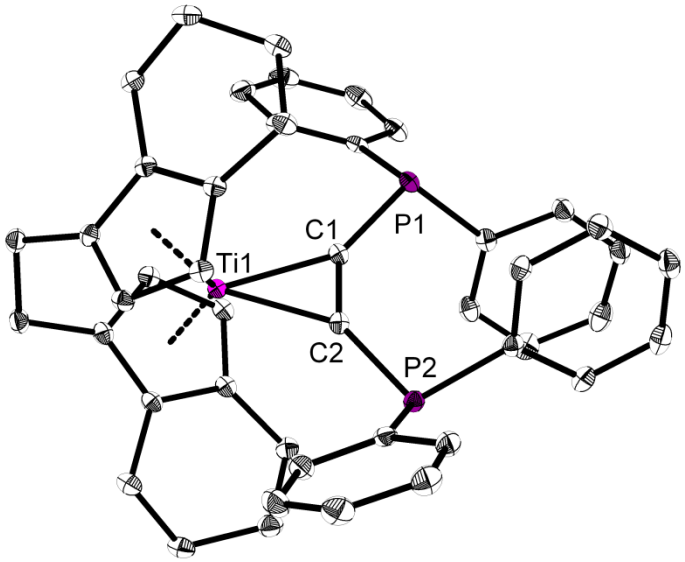

Figure 21. Molecular structure of 29-Ti in the solid state. Hydrogen atoms are omitted for clarity. The thermal ellipsoids correspond to 30 % probability.

In the reaction of the sterically demanding zirconocene alkyne complex **3-Zr** with bis(diphenylphosphino)acetylene no ligand exchange reaction occurred to yield the desired product. Also a variation of the reaction conditions regarding time, solvent or reaction temperature did not influence this reaction significantly and no product could be obtained.

Performing the reaction of the sterically less demanding zirconocene alkyne **4-Zr** with bis(diphenylphosphino)acetylene at room temperature in a 1:1 stoichiometric ratio, the already mentioned substitution reaction of the spectator ligand bis(trimethylsilyl)acetylene by the bis(diphenylphosphino)acetylene ligand occurs smoothly and results in the formation of the three-membered metallacycle **29-Zr**. In the ^{31}P-NMR spectrum, the resonance of the phosphorus atoms appears at 3.20 ppm as a singlet as both phosphorus atoms are equivalent. This resonance is very similar to the already described complexes **28** and **29-Ti**. The molecular structure of complex **29-Zr** is depicted in Figure 22.

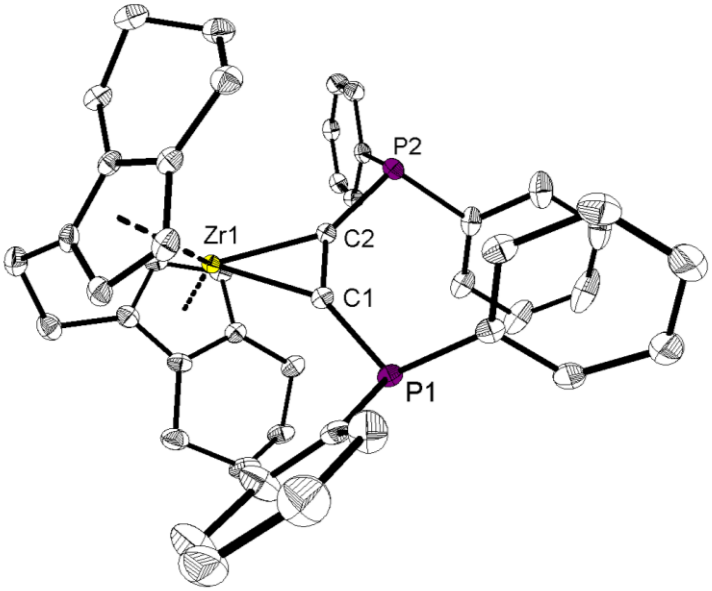

Figure 22. Molecular structure of 29-Zr in the solid state. Hydrogen atoms, the disordered part of the molecule and solvent molecules (toluene) are omitted for clarity. The thermal ellipsoids correspond to 30 % probability.

Generally, complex **29-Zr** is isostructural to the already discussed complex **29-Ti**. Noteworthy, a π-stacking as in **29-Ti** is observed between the parallel Ph groups of the ligand. The distance between both Ph-groups (C_g-C_g 3.623(1) Å, is in the normal range of such π-π-interactions.[98] This distance is close to the ideal π-π-interaction, observed in graphite (distance between the layers 3.35 Å).[99] The Ph rings are not ideally parallel displaced (9.5°) although the angle is rather small. The values for the angles between the ring normals and the vectors of the ring centroids (15.8 and 19.5°, respectively) are in the expected range for such a π-stacking.

2.5.3. Phosphorus Involving Metallacycles

Reaction of the zirconocene source $Cp_2Zr(py)(\eta^2\text{-}Me_3SiC_2SiMe_3)$ (**2**) with bis-(diphenylphosphino)acetylene in non-coordinating solvents resulted in the formation of the dinuclear complex **30a** according to Scheme 40. This external stabilization mode is already known from results mentioned above. Tilley and co-workers reported about the synthesis of various monosubstituted phosphinoacetylene zirconocene complexes, which are also stabilized by intermolecular interactions of the lone pairs of the

phosphorus atoms.[94] This dimerization with additional P-coordination leads to an increasing stability, it was impossible to receive the monomeric complex by adding THF or pyridine. Surprisingly, **2** does not react with two alkynes in a stoichiometric 1:2 ratio to give a five membered metallacyclopentadiene, neither does the dinuclear complex **30a** with an additional equivalent of alkyne. These reactions do not even occur at elevated temperature. Also the attempt to obtain the structural motif **31** by reacting two molecules of **2** with one alkyne resulted only in the formation of **30a** and **30b**.

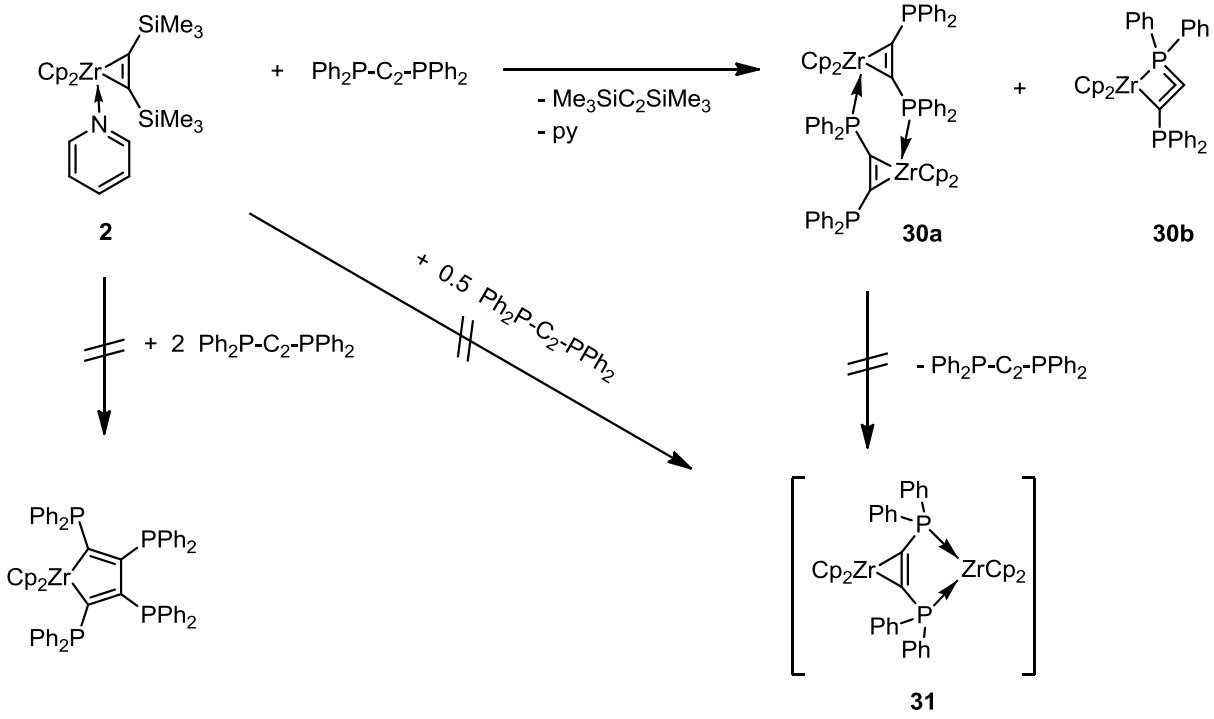

Scheme 40. Synthesis of the complexes 30a and 30b and stoichiometric variations.

In ^{31}P-NMR spectrum of **30a**, two different resonances appear at 15.3 and 8.4 ppm, showing the non-equivalent phosphorus atoms. This clearly indicates its dimeric nature also in solution. In the ^{1}H NMR spectrum, the resonance of the Cp rings appears at 5.52 ppm as a singlet. The corresponding resonance in the ^{13}C spectrum appears at 105.8 ppm.

However, in the ^{31}P NMR spectrum of the reaction mixture, besides the signals of the dinuclear complex **30a**, a different set of resonances appears. There are two independent doublets at 12.04 ppm and -15.72 ppm with a P-P coupling constant ^{3}J =

190.2 Hz, which is tentatively assigned to the structure of the four-membered metallacycle **30b**. Also in ^{1}H (5.88 ppm) and ^{13}C (111.8 ppm) spectra, the corresponding resonances of complex **30b** appear. To the best of our knowledge, this complex is the first metallacyclobuta-2,3-diene of a group 4 metal, very special because of the electron deficient character of the zirconium atom. By variations of the reaction conditions, the best ratio we could observe for **30a**:**30b** was 6:4. The possible resonance forms of **30b** are depicted in Scheme 41, being somehow similar to the allenyl/propargylic system of $Cp_2Zr(\eta^3\text{-}C(Ph)=C=CH_2)$, described by Wojcicki and co-workers.[100] In contrast to this work, the phosphorus atom bears an additional electron to permit the existence of the metallacycloallene. Moreover, the central cyclic fragment of the four-membered metallacycloallene complex **30b** is a hetero variation of the four-membered "all-C" metallacycle **9**, described in Chapter 2.1, corroborating the stabilizing effect of electron rich heteroatoms in the cyclic unit.

By heating the NMR tube up to 75 °C, it can be shown, that there is an equilibrium between both complexes **30a** and **30b** in solution. However, decomposition already takes place above 55 °C. Dissolving single crystals of complex **30a** in C_6D_6 in order to get a clean NMR spectrum also results in the formation of **30a** and **30b** in solution as in the both ^{31}P and ^{1}H NMR spectra the characteristic resonances for **30a** and **30b** appear.

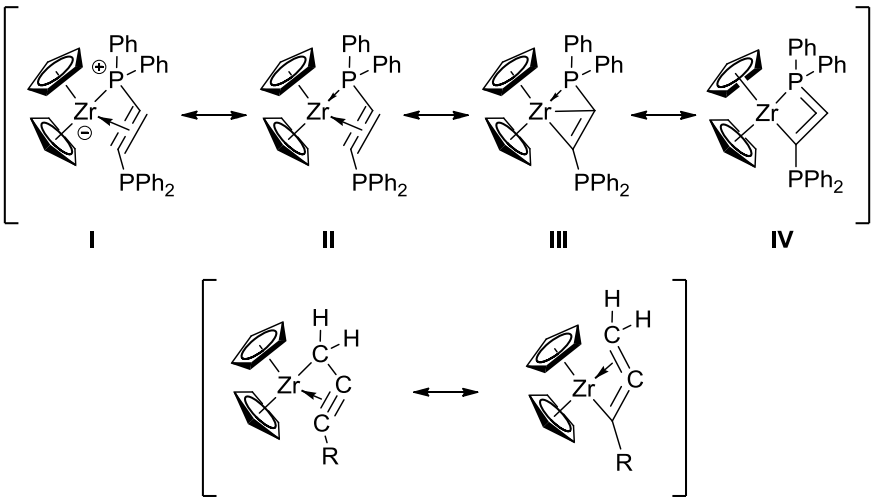

Scheme 41. Possible resonance forms of the monomeric complex 30b in solution (top) and similar allenyl/propargylic system of $Cp_2Zr(\eta^3\text{-}C(Ph)=C=CH_2)$, described by Wojcicki and co-workers (bottom).

For **30b**, four different resonance forms have to be considered, involving a Zr center in different oxidation states from +II to +IV. As NMR investigations have shown sharp signals for all resonances, the phosphonium-ate-complex with the Zr center in the oxidation state +III (**I**) only contributes to a small extent to the stabilization of the four-membered metallacycle **30b**.

The main difference of **30a** and **30b** in comparison to complexes **28**, **29-Ti** and **29-Zr** is the additional P-coordination which arises for **30a** from an (external) inter- and for **30b** from an (internal) intramolecular phosphorus coordination. At room temperature, an exchange of the coordinating phosphorus atoms of **30b** can be observed by ^{31}P NMR NOESY spectroscopy (although the cross peaks are weak), thus indicating a possible dynamic *flip-flop* interaction of both phosphorus atoms, as depicted in Scheme 42. This behaviour was also found before for Si-H-groups in $Cp_2Ti(\eta^2\text{-}HMe_2SiC_2SiMe_2H)$.[101] However, in ^{1}H NMR NOESY spectroscopy an additional unclear cross peak at 5.88/7.49 was observed.

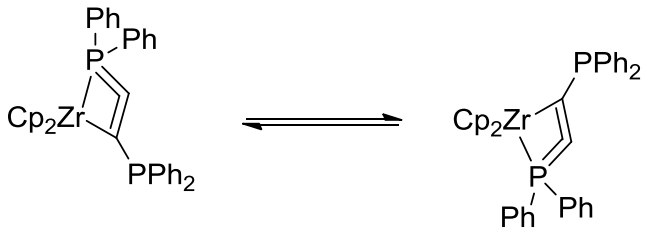

Scheme 42. Possible flip-flop interaction of both phosphorus atoms of 30b in solution.

The molecular structure of complex **30a** is depicted in Figure 23. The central structural motif is a six membered ring of two Zr-C-P fragments. Each zirconium center is coordinated by two Cp units, the alkyne fragment and the phosphorus atom of the second unit of the molecule. This additional coordination is necessary, due to both, small steric demand of the Cp ligands and the big zirconium center.

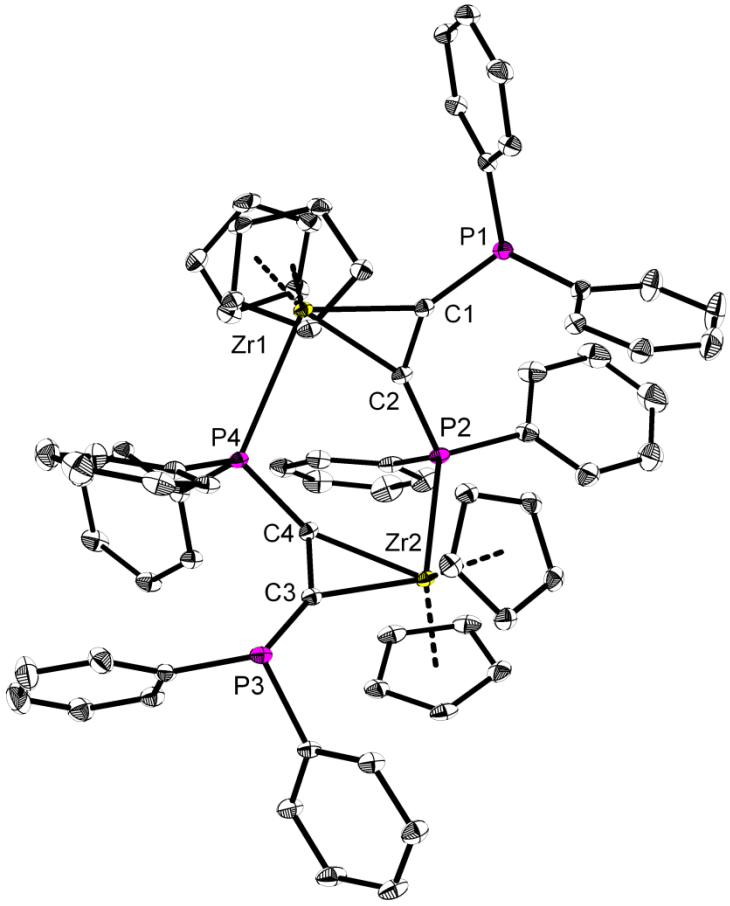

Figure 23. Molecular structure of 30a in the solid state. Hydrogen atoms and solvent molecules (toluene) are omitted for clarity. The thermal ellipsoids correspond to 30 % probability.

The existence of complex **30a** has shown, that bis(diphenylphosphino)acetylene $Ph_2PC{\equiv}CPPh_2$ is able to act not only as a ligand in mononuclear complexes, but can also involve its phosphorus atoms to form dinuclear complexes. Moreover, besides the three-membered metallacycle via the alkyne unit, a second coordination with both phosphorus atoms has been observed before to stabilize dinuclear complexes of group 6 metals with the central fragment $W[\eta^2\text{-}(Ph_2PC_2PPh_2)\text{-}\kappa^2\text{-}P,P']M]$ (M = Cr, Mo, W).[92]

Heating a toluene solution of complex **29-Zr** up to 100°C, the reaction mixture slowly turned from dark green to purple. Upon removal of the solvent, a dark purple solid was obtained. This compound can be attributed to the dinuclear complex **32**, according to Scheme 43. A reaction time of 3 hours was found to be the best, as a longer reaction time led to decomposition of the very unstable complex **32**. The resulting

bis(diphenylphosphino)acetylene was identified by both ^{1}H- and ^{31}P-NMR spectra. By performing the reaction with two equivalents of **4-Zr** and one equivalent of bis(diphenylphosphino)acetylene at elevated temperatures, the formation of complex **32** occurs directly. However, this pathway also leads to a higher amount of by-products.

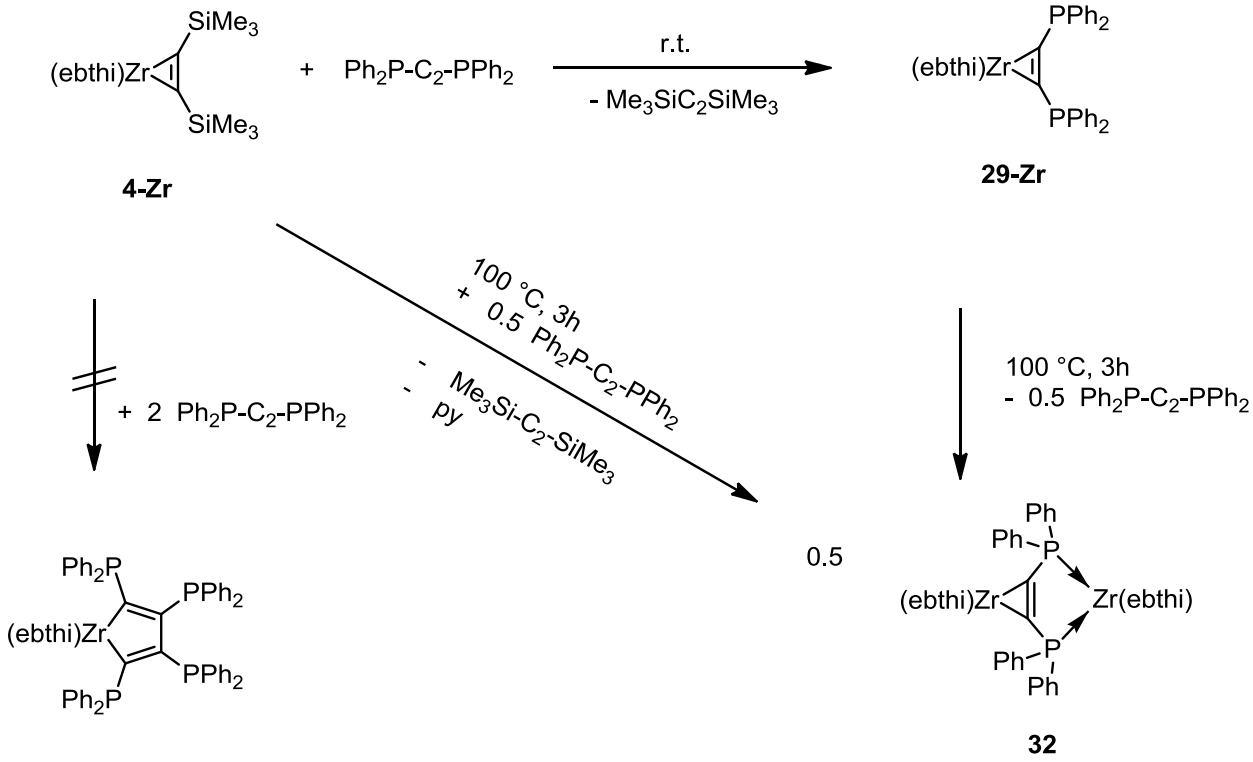

Scheme 43. Synthesis of complex 32 on different pathways.

NMR analysis of complex **32** shows a ^{31}P-NMR resonance at -168.67 ppm, clearly indicating a P-Zr bond.[102] Therefore, the two possible constitutional isomers α (cisoide) and β (transoide) together with both resonance forms are shown in Scheme 44. In the ^{1}H-NMR spectrum, two sets of (ebthi) signals appear. Therefore, the most probable structure of complex **32** is assigned to be isomer α. Additionally, complex **32** was characterized by mass spectrometry. The fragmentation pattern shows the [M-Ph] peak (m/z = 1025) and the [M-2Ph] peak (m/z = 948), clearly corroborating the dinuclear structure.

Unfortunately, complex **32** was found to be very unstable, even in the solid state. So up to this point, no crystals, suitable for X-ray analysis, could be obtained to confirm the suggested structure.

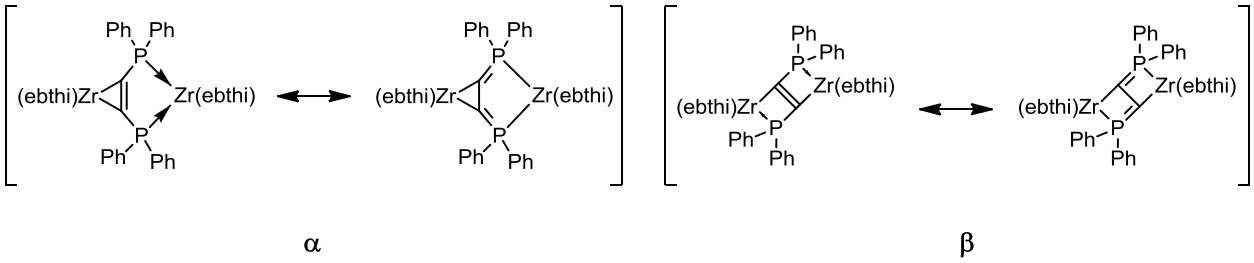

Scheme 44. Constitutional isomers of complex 32, both resonance forms are shown.

In order to obtain stable dinuclear complexes similar to **32** or the compounds described by Powell et al. (W(η²-($Ph_2PC_2PPh_2$)-κ²-*P*,*P*'}M] (M = Cr, Mo, W)[92]), reactions of **28** with two different late transition metal complexes of Co and Ni were performed. As precursors, CpCo(η⁴-H_2C=CH-C_2H_4-CH=CH_2)[103] and (PCy_3)$_2$Ni(η²-H_2C=CH_2)[104] were used as both complexes are able to liberate the spectator ligand under mild conditions to generate the reactive metal fragments [CpCo] and [Cy_3P_2Ni].

While reaction of **28** with CpCo(η⁴-H_2C=CH-C_2H_4-CH=CH_2) did not occur at all, the use of (Cy_3P)$_2$Ni(η²-H_2C=CH_2) to yield a heterobimetallic complex of an early and a late transition metal takes place already at room temperature. Unfortunately, the desired heterobimetallic complex is unstable, resulting in a C-P bond cleavage between the phosphino substituent and the central C_2 unit of the bis(diphenylphosphino)acetylene ligand. As the only characterized product, complex **33** was isolated in low yield of a few crystals. Its molecular structure is shown in Figure 24.

Each Ni atom is surrounded by one coordinating Cy_3P group, two bridging phosphorus atoms of two [Ph_2P]$^-$ groups and the second Ni molecule. Ni1, Ni2, P1 and P2 are almost planar with the phosphorus atoms P3 and P4 being slightly out of this plane (P3 0.3752(8) Å above, P4 0.3985(8) Å below). All P-Ni (P2-Ni, respectively) distances are similar and between 2.1563(7) and 2.1695(6) Å. The Ni1-Ni2 distance (2.3692(4) Å) is in the range of an expected Ni-Ni bond,[105] as found similar in other complexes, displaying this central structure motif.

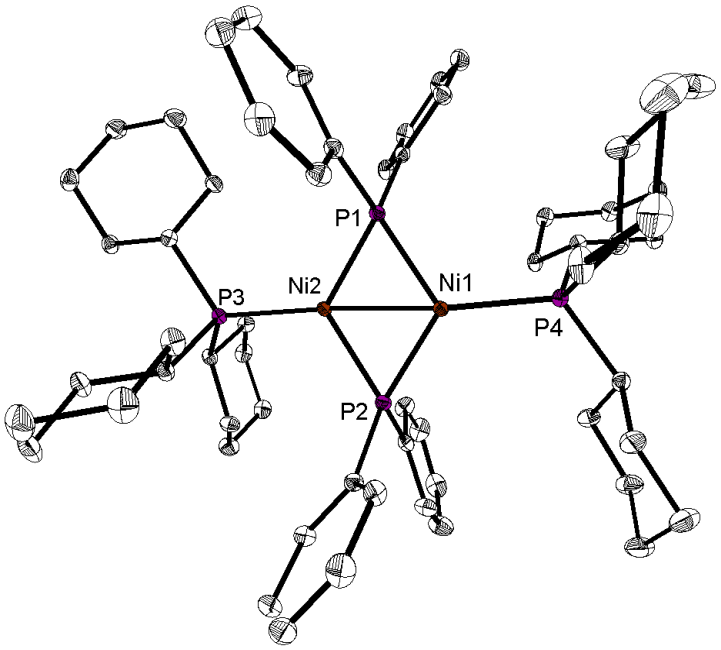

Figure 24. Molecular structure of 33 in the solid state. Hydrogen atoms and solvent molecules (THF) are omitted for clarity. The thermal ellipsoids correspond to 30 % probability.

Complex **33** is paramagnetic as expected for a square planar Ni^{I}-d^9 system. Therefore, the obtained NMR signals are broad. The reaction mixture shows a variety of different phosphorus resonances, indicating a complex reactivity leading to a diversity of different products. The resonances at 45.88 and 10.32 ppm can be assigned to complex **33**.

However, the existence of complex **33** is a good hint for the existence of the heterobimetallic complex as an intermediate according to Scheme 45. Most likely, after complexation of the Ni-fragment, the C-P bond cleavage occurs, resulting in a Ph_2P-Ni-PCy_3 fragment which gets stabilized by dimerization to complex **33**. The final disposition of the assumed [Cp^*_2Ti-C≡CPPh_2] fragment remains unclear.

Such C-E bond cleavage reactions of alkynes EC≡CE have been observed before for various substituents on various metals. Exemplarily, such Ph-C and Si-C bond cleavages are known for Pt complexes.[106,107] Moreover, Si-C cleavages are also described for the group 4 metals Ti and Hf.[108,109] Cleavage reactions of $Me_3SnC{\equiv}CSnMe_3$ and $PhCH_2SC{\equiv}CSCH_2Ph$ have also been described for group 4 metallocene complexes. The stannyl substituted alkyne complexes $Cp'_2Ti(\eta^2\text{-}Me_3SnC_2SnMe_3)$ (Cp' = Cp, $C_5H_3Me_2$) are found to be less stable than complex **28**, resulting in C-Sn bond cleavage to give $[Cp_2'Ti(\mu\text{-}\eta^2{:}\eta^1\text{-}C{\equiv}CSnMe_3]_2$.[110]

Moreover, reaction of $Cp_2Ti(\eta^2\text{-}Me_3SiC_2SiMe_3)$ (**1**) with bis(benzylsulfuryl)acetylene $PhCH_2SC{\equiv}CSCH_2Ph$ yields the complex $Cp_2Ti(SCH_2Ph)_2$ as well as the dinuclear species $(Cp_2Ti)_2(\mu\text{-}\kappa^2\text{-}\kappa^2\text{-}PhCH_2SC_4SCH_2Ph)$, displaying two $[Cp_2Ti]$ moieties bridged by a 1,4-bis(benzylsulfuryl)-1,3-butadiyne in *trans*-configuration.[111]

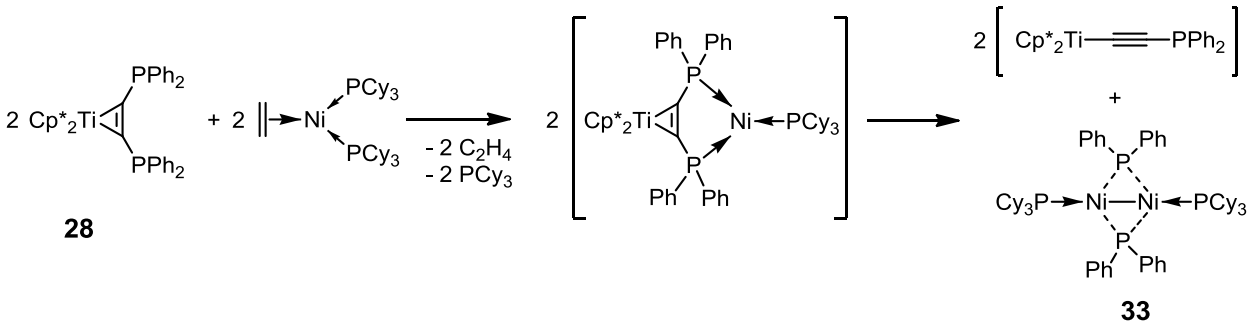

Scheme 45. Reaction of 28 with $(Cy_3P)_2Ni(\eta^2\text{-}H_2C{=}CH_2)$, yielding the Ni-Ni complex 33 together with unidentified byproducts.

2.6. Metallacycles with Carbon, Nitrogen and Oxygen Containing Ligands

2.6.1. State of the Art

Based on the amidinato heterometallacycles containing the structural motif **E** in Chapter 2.2 and the isolobal correlation O→NR, the exchange of both NR fragments by oxygen atoms lead carboxylato complexes, a class of ligands which is well known for group 4 metallocene complexes.[112] However, the replacement of only one NR fragment by an oxygen subsequently lead to amidato ligands as another important class of ligands.

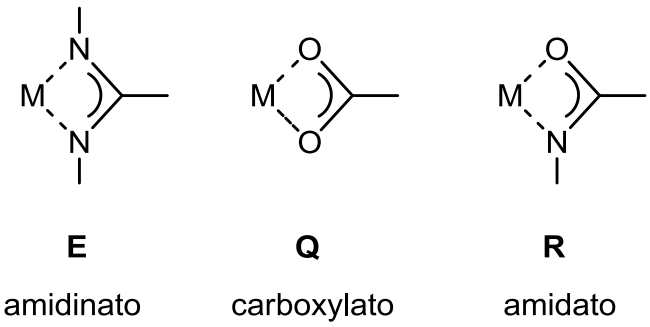

Scheme 46. Different isolobal ligands amidinato (E), carboxylato (Q) and amidato (R).

As this work focuses on the chemistry of four-membered heterometallacycles, amidates as carbon, nitrogen and oxygen containing ligands are of tremendous interest. This group of ligands is well known on group 4 metals,[113] however, its group 4 metallocene chemistry is, so far, very limited. Amidates can adopt three different binding modes (Scheme 47).[114] However, due to their oxophilicity the chelating κ^2-*N*,*O* and κ^1-*O* formations are preferred by early transition metals. Nevertheless, the κ^1-*N* arrangement also exists at Zr.[115] Other zirconocene amidato complexes are synthesized by insertion reactions of isocyanates into Zr-alkyl bonds, as described by Gambarotta,[116] Erker[117] and Yan.[118] These reactions result in formation of chelating κ^2-amidato complexes. Complexes with κ^1-*O* bonded ligand are favored for bulky substituents on the amidato ligand.[119]

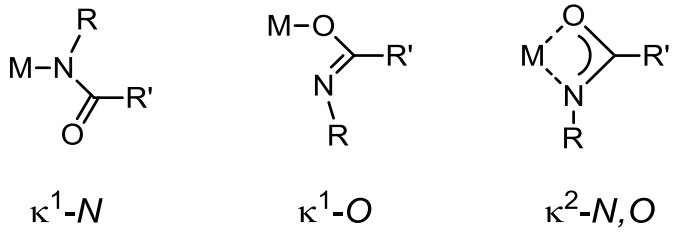

Scheme 47. Different mononuclear binding modes of amidato ligands.

2.6.2. Titanium Heterometallacycles with Amidato Ligands

In a cooperative study with Schafer and co-workers, reactions of [Cp'$_2$M] fragments (M = Ti, Zr; Cp' = Cp, Cp*) with various amides were investigated. Reaction of $Cp_2Ti(\eta^2\text{-}Me_3SiC_2SiMe_3)$ (**1**) with benzanilide resulted in formation of a dark green solid, from which green prisms of **34** could be obtained by recrystallization in toluene at -78 °C (Scheme 48). The analoguous but sterically more demanding complex **35** is formed under harsher conditions as dark blue crystals, due to the sterically shielded starting material **3-Ti**. Using **1** and the bigger *N*-(2,6-diisopropylphenyl)benzamide ligand, a similar reaction occurs to yield the dark green complex **36**. All three titanocene complexes **34**, **35**, **36** are paramagnetic Ti^{III} compounds, a result of a formal oxidation of the Ti^{II} center of **1**.

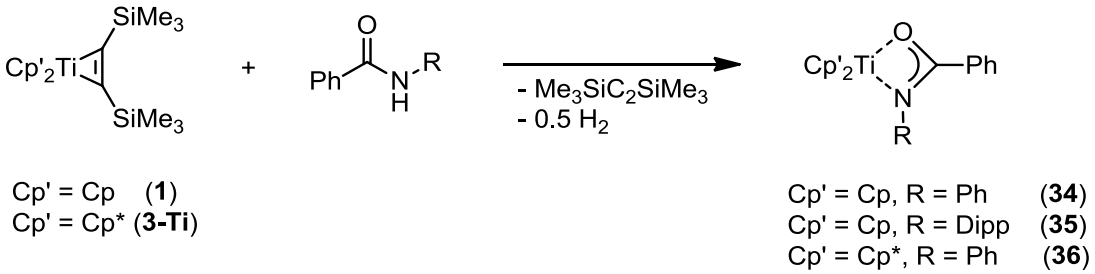

Scheme 48. Synthesis of complexes 34 and 35 and 36.

Reduction occurs at the amide proton, evolution of molecular H_2 was monitored by ^1H NMR spectroscopy. Its characteristic singlet appears at 4.47 ppm. Complexes **34**, **35** and **36** were structurally characterized by X-ray analysis. Their molecular structures are depicted in Figure 25. The chelating amidato ligands form a four-membered heterometallacycle, due to a κ^2-binding mode over N- and O-atom. The Ti-N distances of **34** (2.1703(15) Å), **35** (2.204(2) Å) and **36** (2.2427(10) Å) vary, due to the different steric demand of both amidato and Cp' ligand. On the other hand, the Ti-O bond lengths

of **34** (2.1456(13) Å), **35** (2.1615(18) Å) and **36** (2.1146(9) Å) are mainly influenced by the steric demand of the Cp' ligand and less from the *N*-substitution (Table 2).

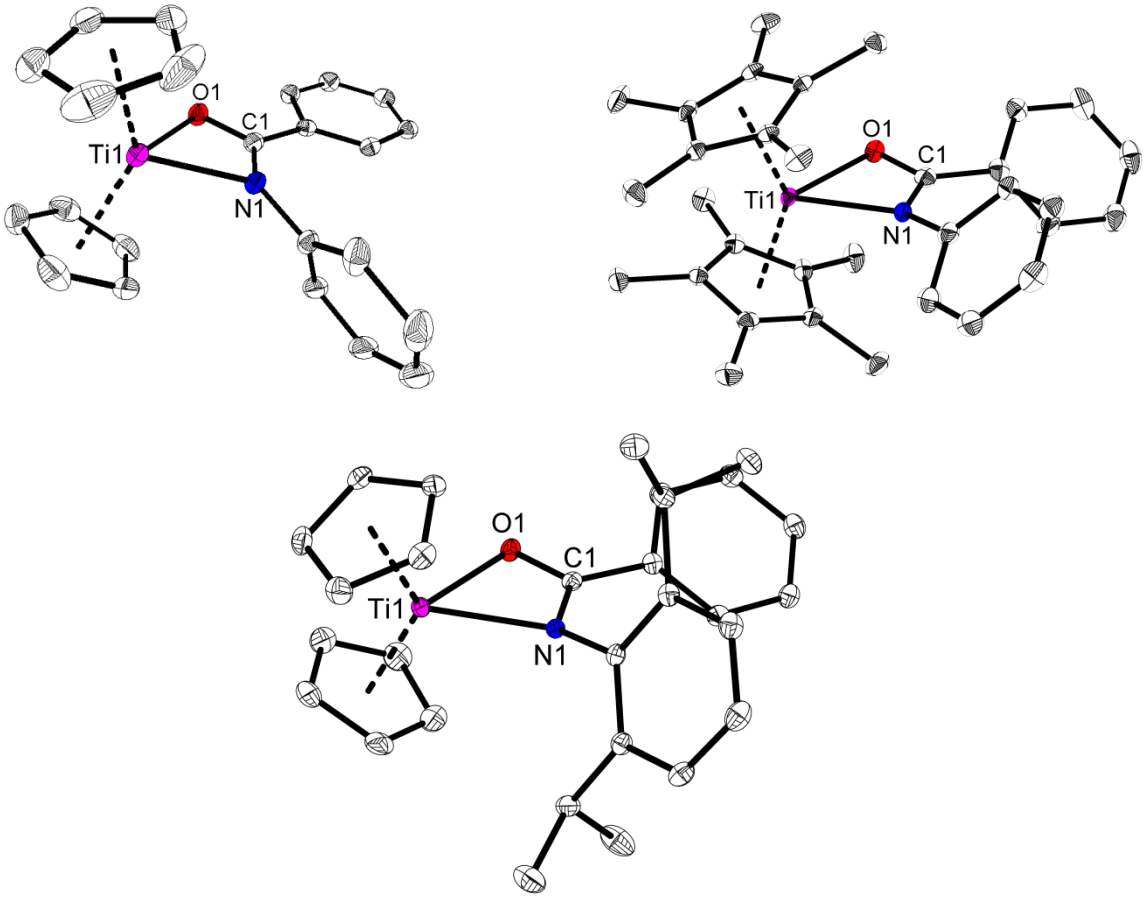

Figure 25. Molecular structures of 34 (top, left), 35 (top, right) and 36 (bottom) in the solid state. Hydrogen atoms are omitted for clarity. The thermal ellipsoids correspond to 30 % probability.

Table 2. Important structural data of amidato complexes 34 , 35 and 36.

	34	**35**	**36**
Ti – N [Å]	2.1703(15)	2.204(2)	2.2427(10)
Ti – O [Å]	2.1456(13)	2.162(2)	2.1146(9)
C – N [Å]	1.320(3)	1.301(3)	1.3158(14)
C – O [Å]	1.289(2)	1.294(3)	1.2896(13)
N – Ti1 – O [°]	60.80(5)	59.79(7)	60.52(3)
N – C – O [°]	113.7(2)	114.0(2)	115.1(1)
O1-Ti1-N1-C1	1.67(16)	4.6(2)	1.57(6)

The N-Ti-O angles of all three complexes are about 60°, leading to a highly distorted tetrahedral geometry. C-N bond distances are similar for complexes **34**, **35** and **36** while C-O bond lengths are even equal. They are longer than an amide C(sp^2)=O (and C(sp^2)=N, respectively) double bond, but shorter than a C(sp^2)-O (and C(sp^2)-N) single bond, corresponding to a bond order between 1 and 2.[22] The central metallacyclic unit is almost planar as seen in various Ti amidato complexes before.[120]

In order to get a detailed understanding of the bonding situation in solution, EPR experiments of **34** and **35** were performed. Their EPR spectra as well as the simulations are shown in Figure 26. Both complexes **34** and **35** exhibit an isotropic signal from a single electron, located at the Ti(III) centers (S = ½).[121] For **34**, a slightly higher g-value (1.9816) was observed than for **35** (1.9794). Therefore, the deviation from the isotropic g value of free electrons (Landé factor g_e = 2.0023) is smaller for **34**, pointing to a weaker spin-orbit coupling of the single electron than in **35**. This small deviation (and the resulting weak spin orbit coupling) could be an indication for strong delocalization of the spin density of the single electron at the Ti^{III} center towards the amidato ligand. Such delocalization can be observed in both complexes **34** and **35**, evidenced by triplet superhyperfine structure (shfs) splitting of the EPR signal due to coupling of the Ti^{III} electron with the nuclear spin (I = 1) of the ^{14}N nucleus (Table 3). For complex **35**, this fact is exemplified by the 2nd derivative of the EPR absorbance spectrum (Figure 26). Both coupling constants a(N) are in the same range as found for other cyclic Ti–N compounds.[122] However, based on spectrum simulations the a(N) value of complex **34** is larger compared to **35**, demonstrating a stronger spin density delocalization towards N. This fact is supported by a shorter Ti–N distance in the solid state structure of **34** as a result of the less sterically demanding Cp ligand, compared to the bigger Cp* ligand of **35**.

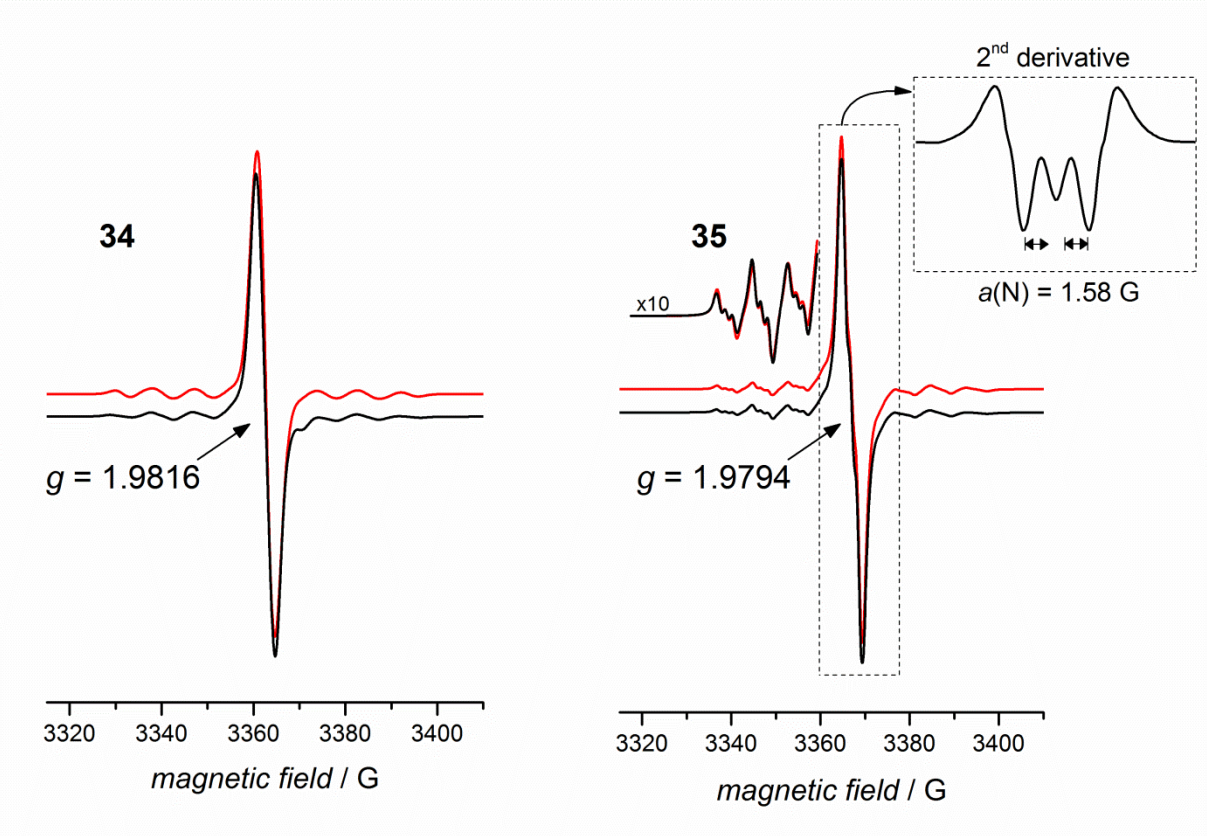

Figure 26. EPR spectra of complexes 34 (left) and 35 (right) in toluene at room temperature (black) and simulated spectra (red).

Moreover, the spectra clearly show the presence of hyperfine structure (hfs) splitting, resulting from the coupling of the Ti^{III} electron with the nuclear spin of the isotopes ^{47}Ti (I = 5/2, natural abundance: 7.40%) and ^{49}Ti (I = 7/2, natural abundance: 5.40%). In the hfs subsignals of these isotopes, the shfs is well resolved for complex **35** (Figure 26, tenfold enlarged cut-out), whereas the broader line width in the spectrum of complex **34** causes an unresolved shfs, which is only clarified by spectrum simulation (Table 3).

Table 3. Simulation parameters of complexes 34 and 35, corresponding to Figure 26 (red lines).

complex	**34**	**35**
g_{iso}	1.9816	1.9794
line width / G	3.78	1.86
shfs a(N) / G	2.95	1.58
hfs a(Ti) / G	9.08	7.98

2.6.3. Unusual Amide N-H Bond Activation Reactions

In contrast to the previously described reactions of titanocene complexes, the zirconocene complex $Cp_2Zr(py)(\eta^2\text{-}Me_3SiC_2SiMe_3)$ (**2**) shows a completely different behavior. Here, the N-H bond activation of amides occurs in a special manner, resulting in formation of zirconocene hydrido amidato complexes via formal oxidative addition. Reaction of alkyl substituted *N*-(*i*-propyl)*t*-butylamid with **2** at elevated temperatures resulted in formation of colourless crystals of **37** upon recrystallization from toluene solution. Using the sterically more demanding *N*-(2,6-diisopropylphenyl)benzamide, reaction occurs already at room temperature to yield colourless crystals of **38** in excellent yields according to Scheme 49.

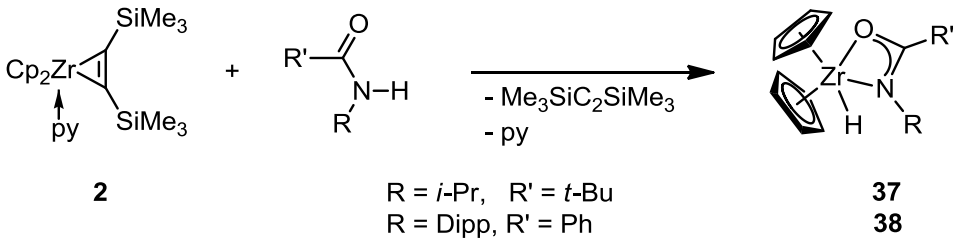

Scheme 49. Synthesis of complexes 37 and 38.

In ^{1}H NMR spectra, the resonances of the metal hydrido signals appear at 5.01 (**37**) and 5.72 ppm (**38**), respectively. Noteworthy, the resonances of the methine signals in **38** appear as equivalent resonances at 3.45 ppm. Using ^{13}C NMR spectroscopy the resonances of C1 appear at 185.8 ppm (**37**) and 176.9 ppm (**38**), which are characteristic for the κ^2-metallacyclic binding mode of the amidato ligand.[113,123] Additionally, complexes **37** and **38** were structurally characterized by X-ray analysis. Their molecular structures are shown in Figure 29. Noteworthy, the hydrido ligands were found from the difference Fourier map and refined freely.

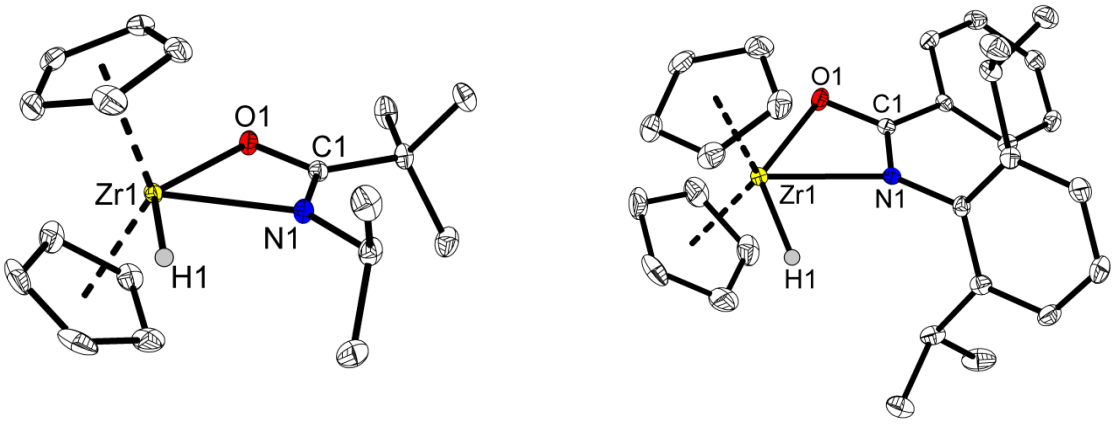

Figure 27. Molecular structures of 37 and 38 in the solid state. Hydrogen atoms except for H1 are omitted for clarity. The thermal ellipsoids correspond to 30 % probability.

The amidato ligands are bound in a chelating κ^2-fashion, forming a four-membered heterometallacycle. As previously described, the M-N distances are strongly influenced by the steric demand of the substituents at the N-atom. Therefore, the Zr1-N1 distance in **37** (2.2784(9) Å) is significantly shorter than in **38** (2.3155(15) Å). C1-O1 and C1-N1 bond lengths (Table 4) are consistent with partial multiple bond character,[22] as discussed in section 2.6.2.

Table 4. Important structural data of 37 and 38.

	37	**38**
Zr – N [Å]	2.2784(9)	2.3155(15)
Zr – O [Å]	2.2595(8)	2.2463(12)
Zr – H [Å]	1.77(2)	1.78(2)
C – N [Å]	1.3096(13)	1.314(2)
C – O [Å]	1.2984(12)	1.294(2)
N – Zr1 – O [°]	57.45(3)	57.41(5)
N – C – O [°]	113.51(9)	114.39(15)
O1-Zr1-N1-C1 [°]	0.79(6)	7.5(2)

In order to elucidate the reaction pathway for the formal oxidative addition, reaction of *N*-(*i*-propyl)*t*-butylamid with **2** was additionally monitored by NMR spectroscopy. Interestingly, at room temperature a different set of signals is observed. Resonances at 8.08 ppm in ^{1}H- and 234.5 as well as 113.8 ppm in ^{13}C NMR spectrum strongly indicate a σ-alkenyl unit as a result of hydrogen transfer from the amide to the

bis(trimethylsilyl)acetylene ligand. The downfield shift is characteristic for an agostic interaction of the transferred hydrogen atom with the Zr center. A similar behavior has been documented before for reactions of lactams (cyclic amides) with **2**.[115] Based on these observations, a possible reaction mechanism is depicted in Scheme 50. Most likely, the initial step is the substitution of the stabilizing pyridine ligand with coordinated amide, as suggested by similar reactions with *N*-alkylated lactams. The subsequent formation of intermediates takes place by a proton transfer from the Lewis acid activated amide to the bis(trimethylsilyl)acetylene ligand to give amidato supported σ-alkenyl complexes. Such metal vinyl species have been previously characterized as products of reactions of polar, protic E–H bonds of lactams, amines, water or acetylene with **2-L** (L = pyridine, THF).[115,124,125,126] In contrast to the previous results with lactams, β-hydride elimination occurs as final reaction step to liberate the bis(trimethylsilyl)acetylene and form the terminal hydrido species **37** (and **38**, respectively). However, for the reaction with the sterically demanding *N*-(2,6-diisopropylphenyl)benzamide, no intermediate could be spectroscopically characterized.

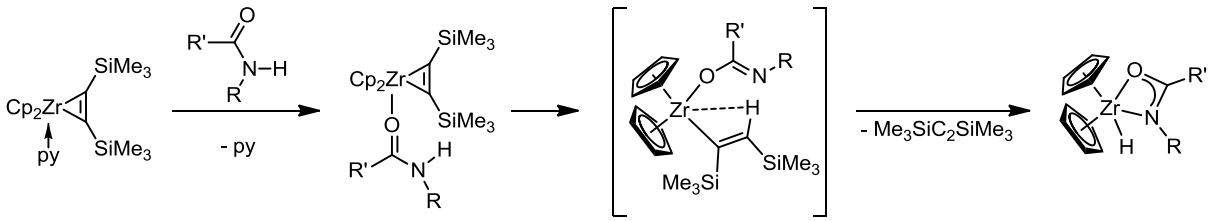

Scheme 50. Possible reaction mechanism for the formation of 37 and 38.

Depending on the bonding concept in **2** (Chapter 1) and regarding the products, this reaction can be described as a bis(trimethylsilyl)acetylene mediated oxidative addition. The oxidative addition of Si–H and C–H bonds to reduced zirconocene derivatives has yielded selected monomolecular terminal hydride complexes.[127,128,129] In the case of more polar E-H bonds, such as N-H bonds, there are few reported examples with group 4 metals.[130] The only structurally characterized product involves the oxidative addition of an N-H bond of aminoborane to yield zirconocene amidoborane complexes.[131] While late-transition-metal complexes are known to promote N-H oxidative addition,[132,133] characterized examples of the oxidative addition of amides are restricted to Pt,[134]

Ru,[135] and Ir[133, 136] examples. Noteworthy, this is the first reported oxidative addition of N–H bonds of amides at early transition metals.

2.6.4. Reactivity of Zirconocene Hydrido Amidato Complexes with Alkenes

It has been well documented that zirconocene hydrido species such as Schwartz's reagent react with alkenes in a stoichiometric fashion. These hydrozirconations can yield in the corresponding organic insertion products after work-up. However, hydrozirconation with Schwartz's reagent typically provides excellent regioselectivity for the linear product. Efforts to access the branched product selectively with traditional zirconocene type complexes have been unsuccessful so far.[137] Surprisingly, exposing both **37** and **38** to 1-octene results in clean formation of 2-octene, as shown in Scheme 51.

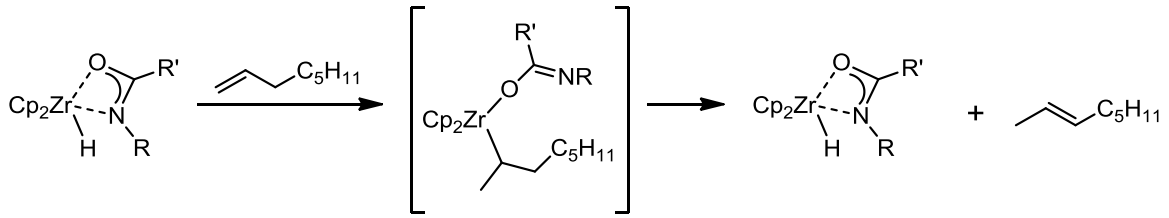

R = *i*-Pr, R' = *t*-Bu **37**
R = Dipp, R' = Ph **38**

Scheme 51. Isomerization of 1-octene to 2-octene selectively via 2,1-insertion.

Such isomerization reactions are well documented for Zr complexes,[138] however, the proposed hydrido intermediates were unobserved. Here, the hydrido complexes **37** and **38** act as catalysts their selves. The initial key step is presumably the formation of the branched insertion product, possible due to a switch of the chelating κ^2-amidato ligand to a monodentate κ^1-fashion, most likely bonded over the O-atom. Subsequent β-hydride elimination selectively results in formation of 2-octene. In contrast to Schwartz's reagent the insertion forms the branched species which is not accessible for the β-hydride elimination. However, the amidato ligand is potentially involved in the mechanism by either the C-O or the C-N function, acting as a Lewis Base able to abstract the H-atom showing distinguished properties for such reactions.

Considering these results, further insertion reactions with styrene were investigated, as styrene does not feature any allylic hydrogen atoms. Therefore, the undesired β-hydride

elimination could be prevented. Reaction of **37** with styrene was monitored by NMR spectroscopy. At room temperature, an equilibrium between both isomers of the branched insertion product **39a**/**39b** and **37** was observed (Scheme 52). Well resolved room temperature spectra showed that after 4 days a reaction equilibrium had been reached: 42:58 ratio of free styrene:**39**. The ^{13}C NMR spectrum is consistent with a κ^1-bound amidato ligand for **39a** (δ = 166.4 ppm). However, at 70 °C this equilibrium is shifted and only **37** and free styrene are observed. Therefore, complex **39** could not be purified and isolated for complete characterization.

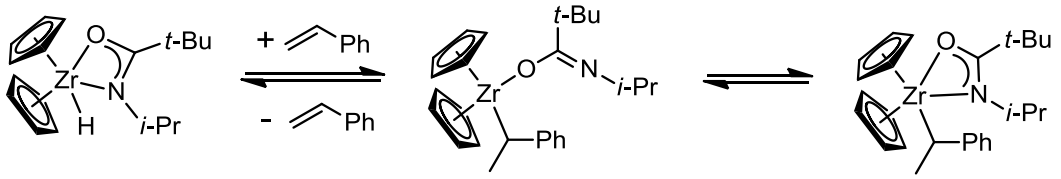

37 **39a** **39b**

Scheme 52. Equilibrium between 39 and 37/styrene.

Remarkably, reaction of **38** with styrene yielded the branched insertion product in good yields according to Scheme 53. Here, by increasing the reaction temperature to 70 °C, completion of the product regioselective reaction can be achieved within 4 h.

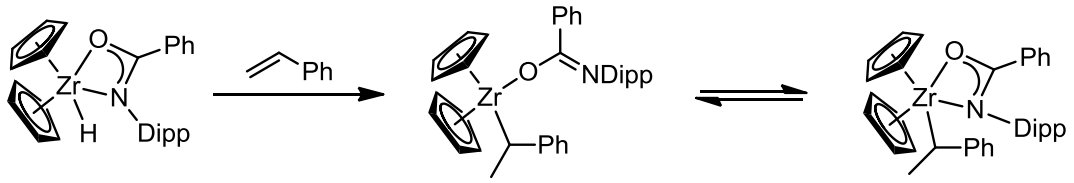

38 **40a** **40b**

Scheme 53. Insertion reaction of styrene with 38 to give 40, observed as an equilibrium between 40a and 40b.

In the ^1H NMR spectrum, the resonances of **40** appear broad at room temperature, due to an equilibrium between the κ^1- and the κ^2-amidato isomers (**40a**/**40b**) (Scheme 53). Therefore, low temperature NMR studies were performed. At -35 °C, sharp resonances of the κ^1-*O* bound isomer (**40a**) could be observed. In the ^1H NMR spectrum, the methine signals of the *i*-Pr groups of the ligand appear as independent septets at 3.07 and 3.00 ppm. Most importantly, the diagnostic doublet of the methyl group appears at

1.55 ppm (^3J = 7.0 Hz), due to coupling with the methine proton of the branched insertion product (δ = 3.17 ppm). In the ^{13}C NMR spectrum, the resonance of the central carbon atom of the amidato ligand appears at 156.1 ppm, upfield shifted compared to the corresponding resonance of **38** and consistent with a κ^1-*O* bound amidato ligand. These low temperature solution phase data match the molecular structure in the solid state, which is depicted in Figure 28. In the solid state, only the κ^1-*O* bound isomer **40a** was observed. Yellow crystals, suitable for X-ray analysis could be obtained from a saturated solution in hexanes. Complex **40** is a rare example of a 2,1-insertion product with zirconocene complexes.

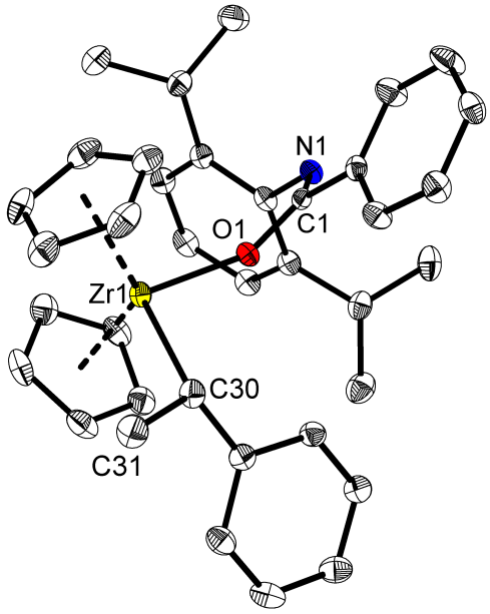

Figure 28. Molecular structure of 40a in the solid state. Hydrogen atoms are omitted for clarity. The thermal ellipsoids correspond to 30 % probability.

The Zr center is surrounded by two Cp ligands, the branched insertion product and the amidato ligand in a distorted tetrahedral geometry. Noteworthy, no agostic interaction of one of the hydrogen atoms of the methyl group with the Zr center could be detected. **40a** is the first structurally characterized example of a 2,1-insertion product in hydrozirconation with an alkene. Chirik and co-workers described the zirconocene complex Cp_2Zr(*cyclo*-C_5H_9)(Cl) via hydrozirconation of cyclopentene with Schwartz's reagent as the only structurally characterized example of a 1,2-insertion product.[139]

2.6.5. Zirconium and Hafnium Complexes with Amidato Ligands

In addition to the series of Ti^{III} amidato complexes (Section 2.6.2), selected zirconocene and hafnocene amidato chloride complexes have been synthesized as possible precursors for M^{III} amidato compounds. As shown in Chapter 2.3, a similar zirconocene chlorido complex could be easily reduced to the corresponding paramagnetic four-membered metallacycle.

Deprotonation of *N*-(2,6-diisopropylphenyl)benzamide with NaHMDS in toluene, followed by subsequent salt metathesis reaction with Cp_2ZrCl_2 (**6-Zr**) resulted in the formation of the four-membered heterometallacycle **41** according to Scheme 54. In contrast to other salt metathesis reactions, complex **41** is selectively formed; no evidence for the bis(amidato) complex was observed. **42** is synthesized according to an identical procedure by using benzanilide and Cp_2HfCl_2.

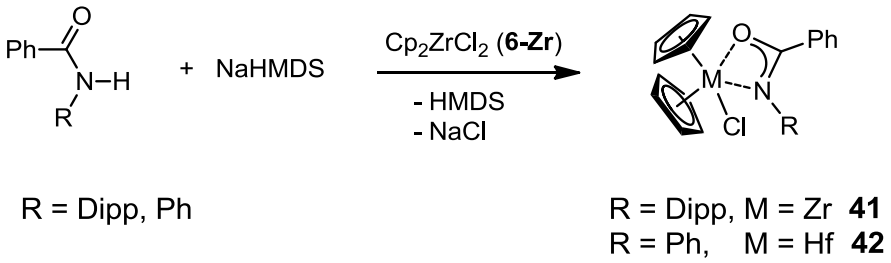

Scheme 54. Synthesis of 41 and 42 via salt metathesis reaction.

Surprisingly, protonolysis reaction of amides with Schwartz's reagent (**8**) already occurs at room temperature, also resulting in the formation of the zirconocene amidato chlorido complex **41** (Scheme 55), together with H_2 (monitored by ^1H NMR spectroscopy; δ = 4.47 ppm). This synthetic pathway was used for the bulky *N*-(2,6-di-isopropylphenyl)benzamide proligand, yielding complex **41** in excellent yields.

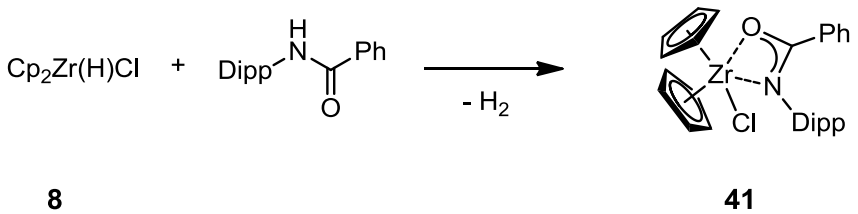

Scheme 55. Synthesis of 41 via protonolysis reaction

As only H_2 arises as byproduct from the reaction, this alternative route is a useful and straight forward pathway for the synthesis of zirconocene amidato chlorido complexes, especially by avoiding solid byproducts like NaCl. **41** and **42** are diamagnetic compounds, displaying singlets for equivalent Cp rings in both ^{1}H and ^{13}C NMR spectra. The resonances of the central carbon atoms of the amidato ligands appear between 170 and 180 ppm, indicating a chelating κ^2-*N*,*O*-binding mode of the amidate in solution. Single crystals of **41** and **42**, suitable for X-ray analysis, were obtained from toluene solution. The molecular structures of these very similar complexes are shown in Figure 29.

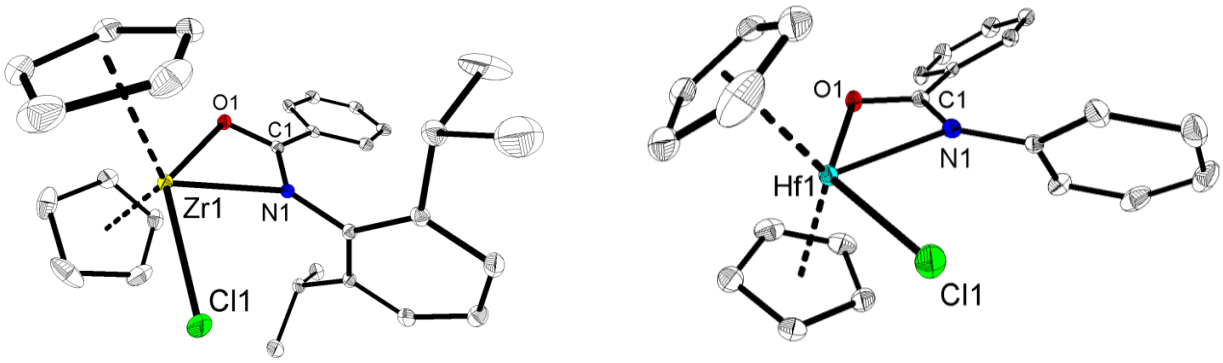

Figure 29. Molecular structure of 41 and 42 in the solid state. Hydrogen atoms are omitted for clarity. The thermal ellipsoids correspond to 30 % probability.

The metal is surrounded by two Cp units, the chlorido ligand and the chelating amidate. In contrast to the Zr^{IV} and Hf^{IV} complexes discussed in Chapter 2.4, the central metallacyclic unit is nearly planar with the chlorido ligand being almost located in this plane (0.09 Å above in **41** and 0.04 Å below in **42**, respectively).

Performing salt metathesis reaction of the deprotonated proligand *N*-(2,6-di-isopropylphenyl)benzamide with Cp_2ZrCl_2 (**6-Zr**) in a 2:1 stoichiometry yields the zirconocene bis(amidato) complex **43** in excellent yields. Not surprisingly, reaction of **41** with deprotonated *N*-(2,6-diisopropylphenyl)benzamide also resulted in quantitative formation of **43**. Moreover, **43** is formed as well in the reaction of **2** with two equivalents of amide. Noteworthy, the evolution of H_2 gas was observed by ^{1}H NMR spectroscopy (δ = 4.47) along with free bis(trimethylsilyl)acetylene (δ = 0.16). Notably, during this reaction, there was no evidence for bis(trimethylsilyl)ethylene

($Me_3SiCH=CHSiMe_3$) reduction product. This suggests that the formation of the zirconocene hydrido complex **38** is an intermediate en route to the bis(amidato) complex **43**. Indeed, the reaction of **38** with one equivalent of amide cleanly affords complex **43** together with H_2 gas. All four pathways are summarized in Scheme 56.

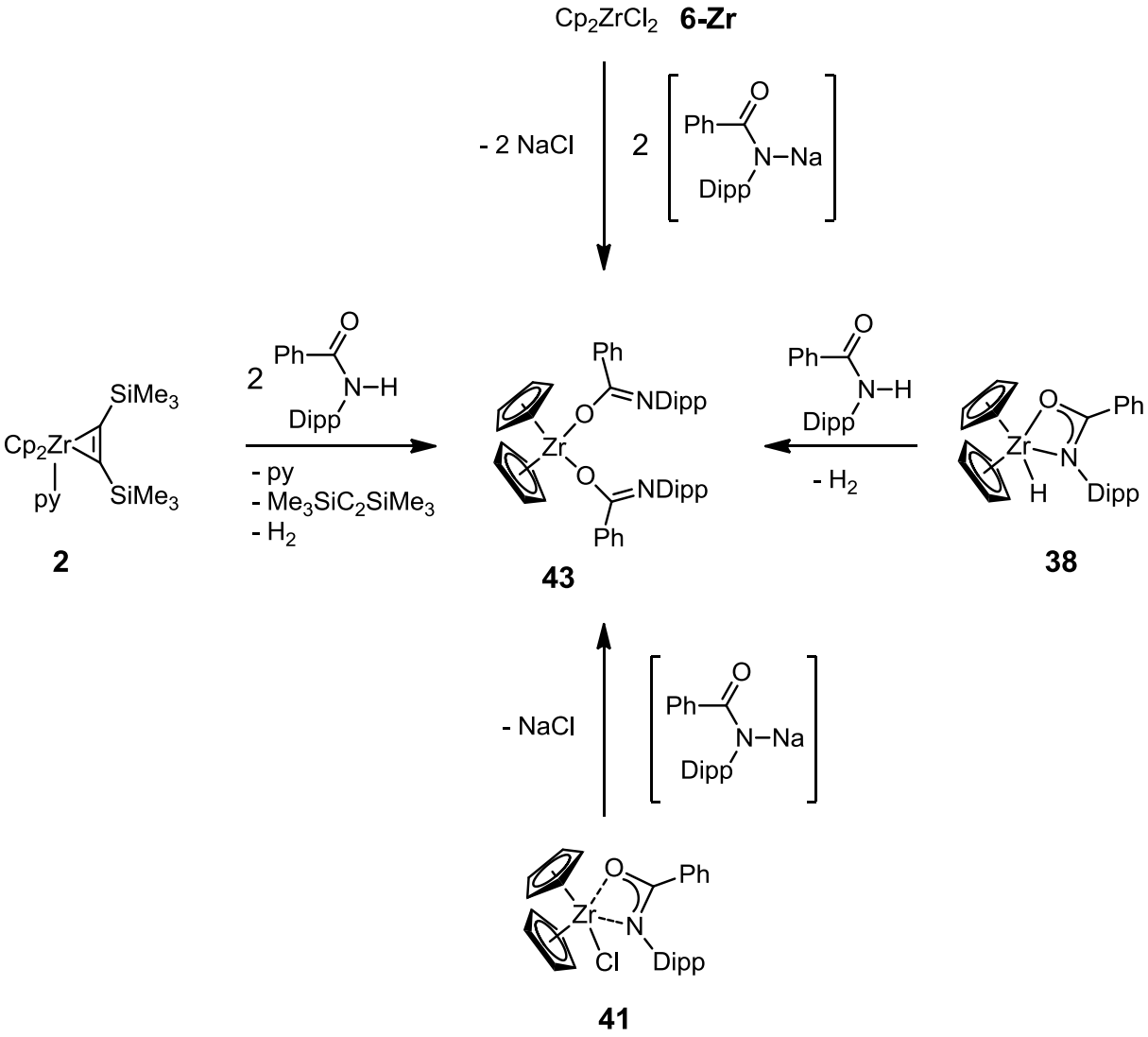

Scheme 56. Different synthetic routes to yield 43.

The molecular structure of complex **43** is depicted in Figure 30. The Zr center is surrounded by two Cp ligands and here two κ^1-*O* bound amidato ligands in a distorted tetrahedral geometry. Presumably, the sterically demanding amidato ligand precludes the isolation of the chelating κ^2-bonding motif. In the κ^1-*O* amidato binding mode the C-O bond lengths (av. 1.336 Å) correspond more closely to a single bond while the C-N bond lengths (av. 1.276 Å) are in the range of a C=N double bond.[22]

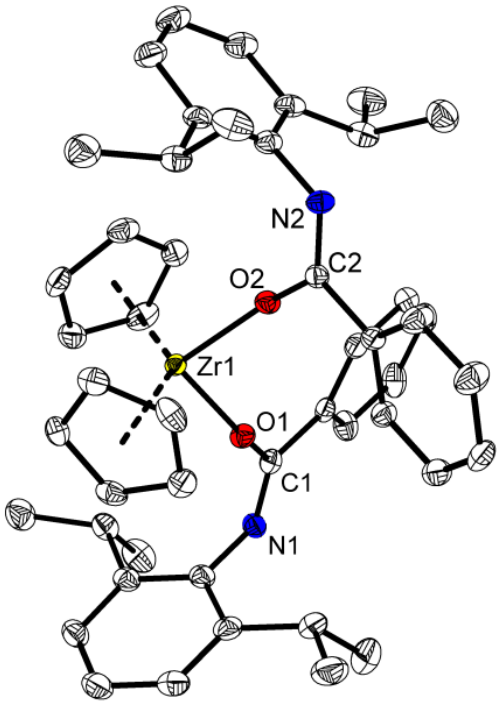

Figure 30. Molecular structure of 43 in the solid state. Hydrogen atoms and the second independent molecule of the asymmetric unit are omitted for clarity. The thermal ellipsoids correspond to 30 % probability.

However, in the room temperature ^{1}H NMR spectrum of complex **43**, all resonances appear broad, most likely due to an equilibrium between a four-membered κ^2-metallacycle of one of the amidato ligands and a κ^1-*O* bound amidato isomer in solution (Scheme 57).

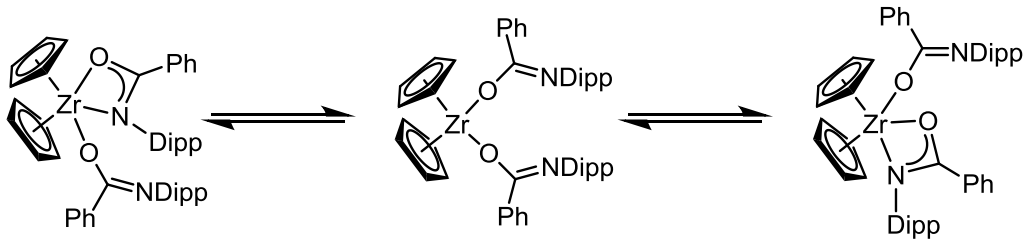

Scheme 57. Possible isomers of complex 43 in solution.

Low temperature NMR studies (-75 °C) confirmed such fluxionality and resonances for the κ^1-*O* bound and κ^2-*N*,*O* bound ligand could be observed. This is most clearly seen in the ^{13}C NMR spectrum, in which the resonance for the central carbon atom C1 of the metallacyclic amidato ligand (δ = 172.1) differs significantly from the resonance of the κ^1-*O* bound amidato ligand (δ = 163.3 ppm). Also, in the ^{1}H NMR spectrum two distinct

ligand environments are observed whereby the chemical shifts of the methine signals of the *i*-Pr groups of one ligand appear as one septet at 3.27 ppm, as seen for κ²-*N,O* coordination in complex **38.** The other ligand displays two independent septets at 3.63 and 3.54 ppm, known from the κ¹-*O* coordination in complex **40**.

Schafer and co-workers described the structures of zirconium bis(amidato) complexes, in which the κ¹-*O* amidato ligands are connected over a C_4 unit, displaying similar bond lengths and angles.[119] Zirconocene complexes, in which both κ¹-*O* bound amidato ligands are connected to the Cp framework over the substituents at the N-atom were investigated by the group of Erker.[140,141]

Complex **41** was tested as precursor for a Zr^{III} amidato complex in a reaction with Mg. Interestingly, instead of formation of the desired $Cp_2Zr\{\kappa^2\text{-}N,O\text{-}(Dipp)N\text{-}C(Ph)O\}$, a two electron reduction took place, yielding **44** by addition of pyridine. The resulting $[Cp_2Zr]$ fragment could not be found in the product mixture; its existence remains uncertain.

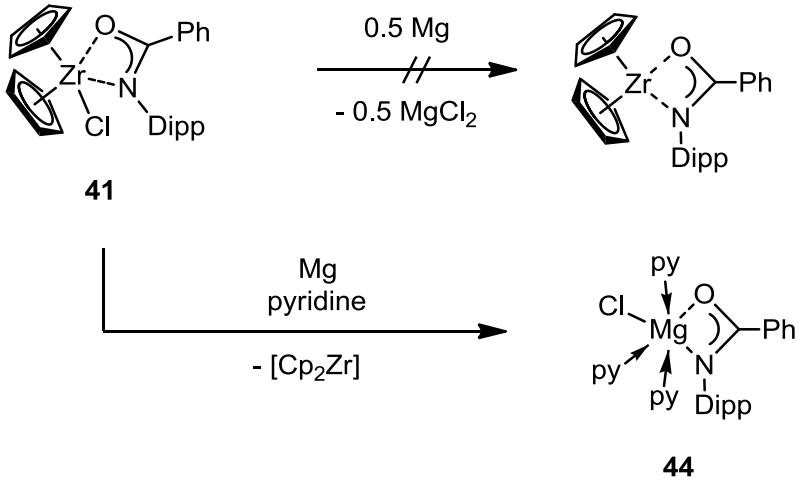

Scheme 58. Reduction of 41 with Mg to form 44.

In the ^{1}H NMR spectrum of **44**, four pyridine molecules were found to be coordinated to the Mg center. The molecular structure of **44** is depicted in Figure 31. The central Mg atom is surrounded by only three pyridine units, one chlorido ligand and the chelating κ²-*N,O* amidate in a distorted octahedral geometry. Two pyridine molecules occupy the axial positions while the third pyridine is located *trans* to the N-atom of the amidate. Subsequently, the chlorido ligand is located *trans* to its O-atom. Noteworthy, the Mg1-N3

distance (2.205(2) Å) is significantly shortened compared to that of Mg1-N2 and Mg1-N4 (2.2620(16) Å and 2.2547(16) Å, respectively). This shortening can be probably attributed to the weak *trans*-influence [142] of the amidato ligand, acting only as a two electron donor and, therefore, reducing the Mg1-N1 bond order to ½. *Trans*-influence on main group metals has been described before, i.e. for Al[143] and Sn.[144] The C1-N1 (1.310(2) Å) and C1-O1 (1.288(2) Å) distances are similar to those of the already discussed Ti and Zr complexes, also displaying a bond order between 1 and 2.[22]

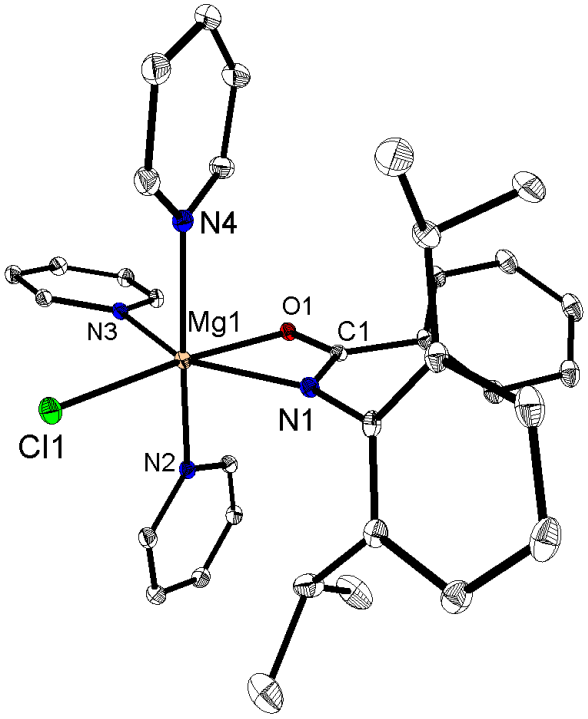

Figure 31. Molecular structure of 44 in the solid state. Hydrogen atoms are omitted for clarity. The thermal ellipsoids correspond to 30 % probability.

3. Summary

The work contained in this thesis is mainly focused on four-membered metallacycles of group 4 metallocenes, revealing the differences between "all-C"- and various heterometallacycles, which strongly depend on the elements used in the corresponding ligand. The described investigations elucidate the unusual binding situation that is present in such highly strained metallacycles and the resulting reactivity.

1. Propargylic systems such as 1-phenylbut-1-yne are able to rearrange to allenic units upon lithiation with *n*-butyllithium. Moreover, a second lithiation can be conducted. Subsequent salt metathesis with Cp_2TiCl_2 (**6-Ti**) yielded the titanacyclobuta-2,3-diene **9**. Complex **9** is very unstable and decomposes within hours at room temperature by liberating CpH.

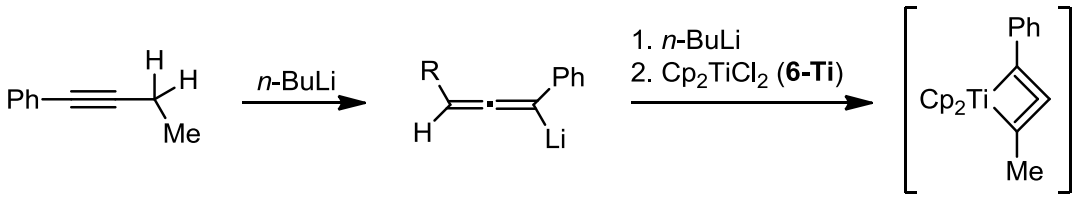

9

2. Differently substituted carbodiimides react with titanocene fragments [Cp'$_2$Ti] (Cp' = Cp, Cp*) to form highly strained four-membered metallacycles. These highly strained structures exhibit biradicaloid character, which leads to different stabilization modes, depending on both steric demand and electronic influence of the substituents of the carbodiimides. Using [Cp*$_2$Ti] and the sterically demanding Mes and Dipp substituted substrates, C-N cleavage occurs to result in the structurally characterized complexes **13** and **14b**. With the very bulky Dipp substituent, C-N cleavage also occurs with the smaller [Cp_2Ti] fragment, yielding complex **14a**.

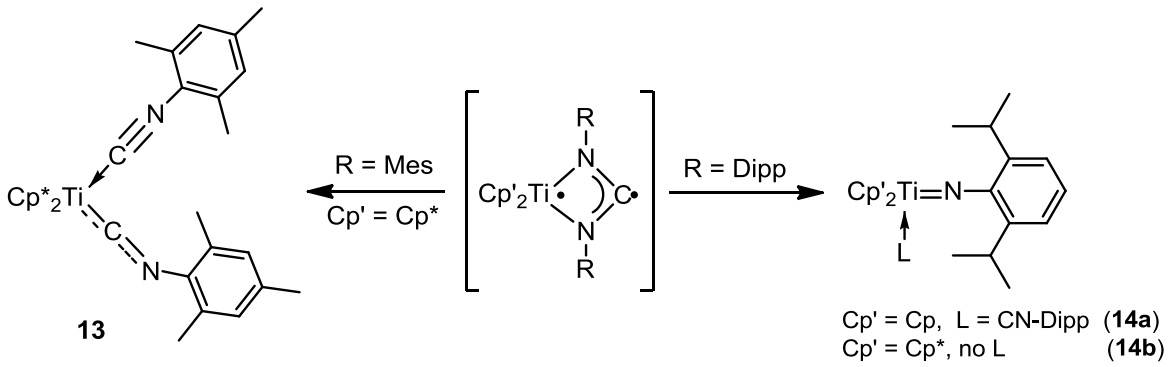

Reaction of mesityl substituted carbodiimide with the [Cp_2Ti] fragment resulted in partial C-N bond cleavage of the four membered metallacycle and C-H bond activation of one of the Cp ligands, leading to the structurally characterized complexes **11**and **12**, respectively.

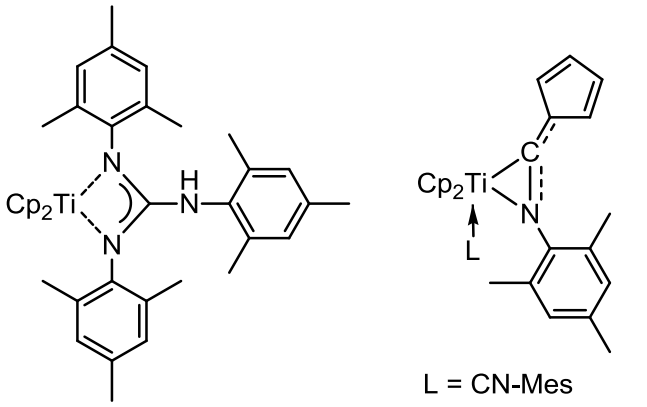

3. γ-Methylene-nitriles, isolobal to the propargylic systems mentioned above, also rearrange upon lithiation to form keteniminato species. Salt metathesis reaction with $Cp^*_2TiCl_2$ (**7**) resulted in the formation of the titanocene chlorido keteniminato complex **15**. Complex **15** was tested as a precursor for a novel titanacycloazabutadi-2,3-ene complex. However, all attempts to isolate the desired species failed.

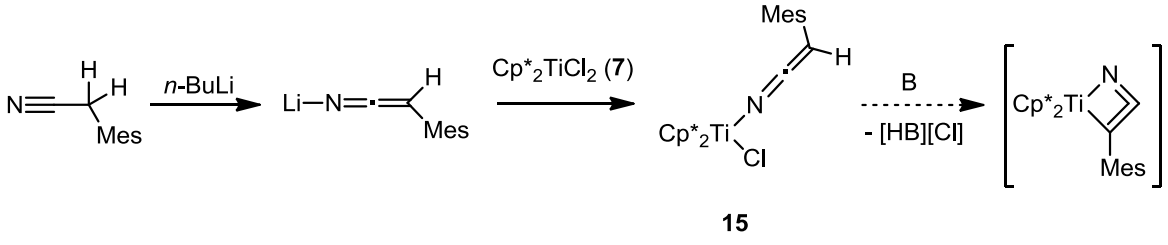

4. The influence of the steric demand of both metallocene fragment and ligand on the formation of four-membered metallacycles was investigated by using differently substituted 7-azaindoles. As a result, it can be stated that the influence of the Cp' units is much bigger than the substitution of the 7-azaindole. While the use of Cp* ligands does not result in the formation of a metallacycle, application of the Cp ligand tolerates even sterically demanding *t*-Bu groups at the 7-azaindole ligand, forming a four-membered metallacycle.

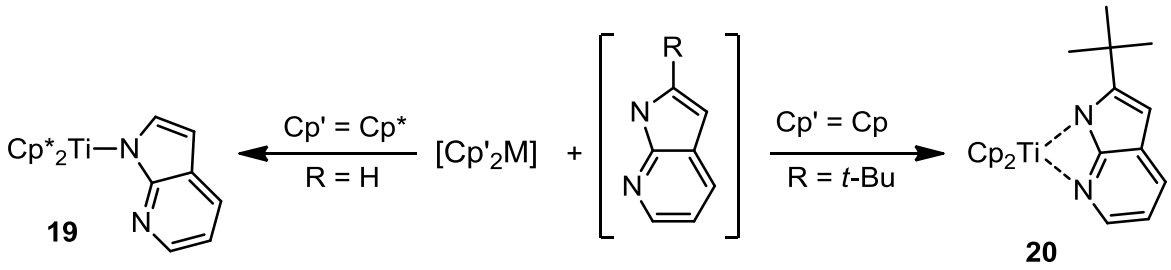

5. Bis(diphenylphosphino)amides are able to stabilize reduced metallocene fragments by forming planar a four-membered metallacycle with a [PNP] ligand. Thereby, the very rare zirconocene^{III} complex **23-Zr** was isolated and structurally characterized. Contrarily, the corresponding metallocene^{IV} fragments are stabilized via three-membered metallacycles in complexes **21-Zr** and **21-Hf**.

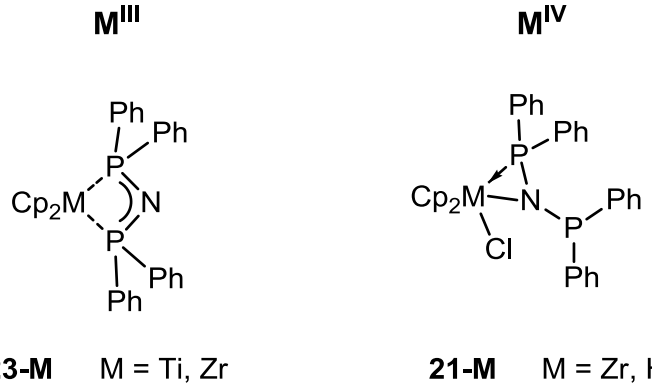

23-M M = Ti, Zr **21-M** M = Zr, Hf

6. Titanocene and zirconocene complexes of bis(diphenylphosphino)methanides form stable four-membered metallacycles in oxidation states +III and +IV, although these ligands are isolobal to the described bis(diphenylphosphino)amides. Depending on the oxidation state, the metallacycle is either planar (+III, Ti) or folded (+IV, Zr, Hf). The planarity can be explained by "in-plane"-aromaticity in these cycles as shown by

theoretical investigations. EPR experiments confirm the interaction of the single electron at the Ti center with the cyclic unit. Moreover, the possibility to stabilize mononuclear metallocene hydrido species by four-membered metallacycles was demonstrated for the zirconocene complex **26**.

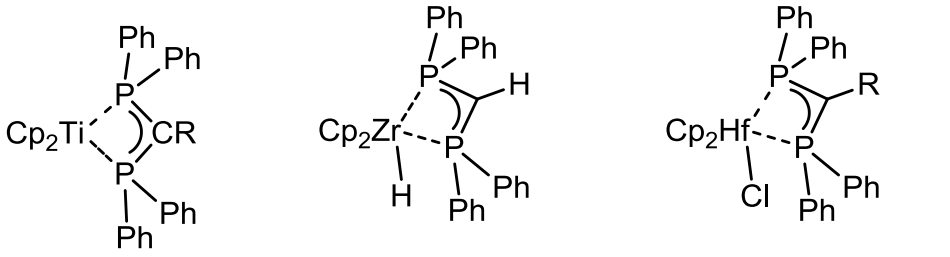

R = H (**25a**)
SiMe$_3$ (**25b**)

26

R = H (**27a**)
SiMe$_3$ (**27b**)

7. Reactions of bis(diphenylphosphino)acetylene with [Cp*$_2$Ti] and [(ebthi)M] (M = Ti, Zr) resulted in the formation of three-membered "all-C" metallacycles. No coordination of the phosphorus atoms of the ligand was observed in these complexes.

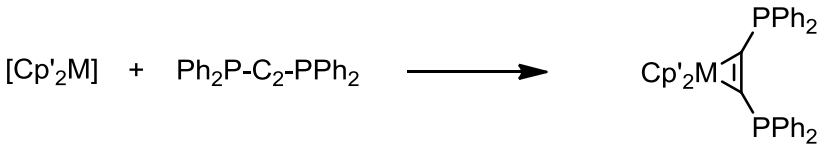

M = Ti; Cp'$_2$ = Cp*$_2$ (**3-Ti**)
(ebthi) (**4-Ti**)
M = Zr, Cp'$_2$ = (ebthi) (**4-Zr**)

M = Ti; Cp'$_2$ = Cp*$_2$ (**28-Ti**)
(ebthi) (**29-Ti**)
M = Zr, Cp'$_2$ = (ebthi) (**29-Zr**)

8. In the reaction of the [Cp$_2$Zr] fragment with bis(diphenylphosphino)acetylene, two different products were obtained. The three-membered "all-C" metallacycle **30a** gets stabilized intermolecularly by additional coordination of one of the phosphorus atoms of a second three-membered "all-C" metallacycle of **30a**. However, in solution also the four-membered metallacyclobuta-2,3-diene complex **30b** is present as a result of intramolecular stabilization. The equilibrium between both isomers of complex **30** in solution was investigated by VT NMR spectroscopy. A possible dynamic *flip-flop* interaction of both phosphorus atoms in complex **30b** was corroborated by ^{31}P NMR NOESY spectroscopy, thus leading to a significantly increased stability of the four-membered metallacycle.

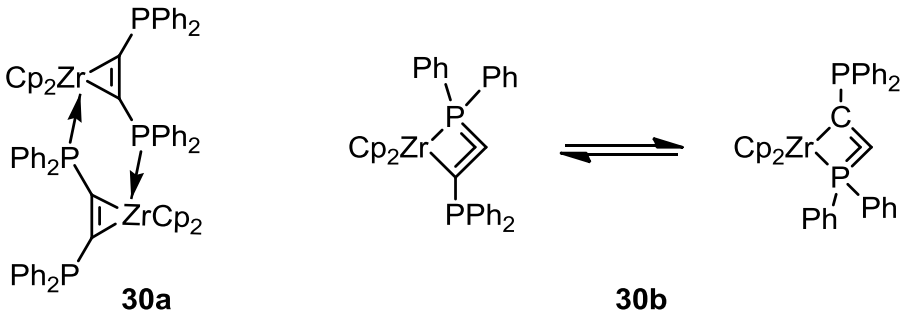

9. Upon exposure of (ebthi)Zr(η^2-$Ph_2PC_2PPh_2$) (**29-Zr**) to elevated temperatures, formation of the dinuclear complex **32** takes place by liberation of one ligand fragment. NMR analysis revealed the existence of the α-isomer, in which both, three-membered "all-C" metallacycle and the five-membered metallacycle involving coordination over both phosphorus atoms are present. This complex can also be generated from the reaction of **4-Zr** with bis(diphenylphosphino)acetylene at elevated temperatures.

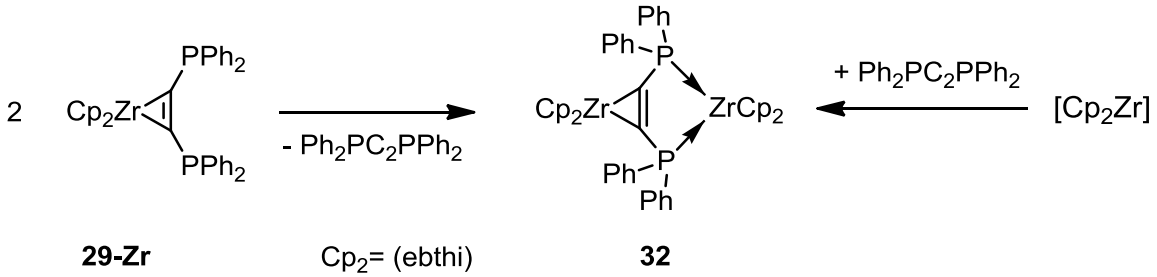

10. Amidinato ligands stabilize reduced titanocene^{III} species. Detailed EPR spectroscopic studies elucidate the interaction of the single electron at the Ti center with the cyclic system of the ligand. Molecular hydrogen could be detected as a byproduct.

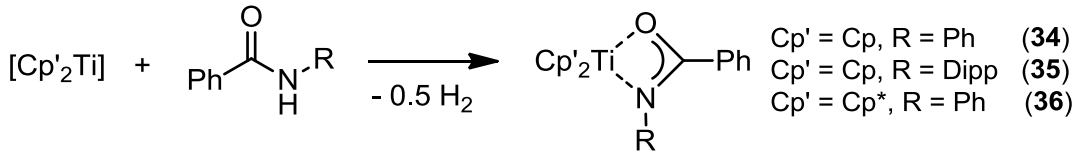

11. Reaction of $Cp_2Zr(py)(\eta^2$-$Me_3SiC_2SiMe_3)$ (**2**) with amides resulted in formal oxidative addition of the amide N-H bond to give zirconocene hydrido amidato complexes. The two complexes **37** and **38** could be structurally characterized.

Noteworthy, a σ-alkenyl complex could be observed as an intermediate, involving the spectator ligand $Me_3SiC{\equiv}CSiMe_3$.

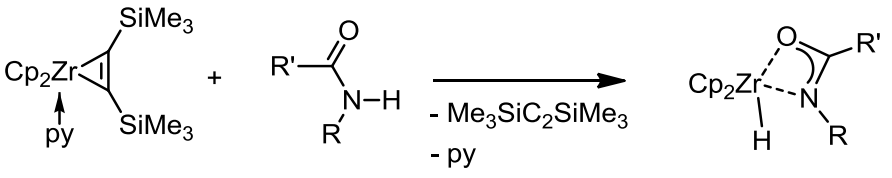

R = *i*-Pr, R' = *t*-Bu (**37**)
R = Dipp, R' = Ph (**38**)

12. In contrast to the structurally similar Schwartz' reagent, complexes **37** and **38** are able to form branched insertion products upon reaction with alkenes. While the use of 1-octene resulted in the formation of 2-octene via insertion and subsequent β-hydride elimination, the lack of allylic hydrogen atoms in styrene yielded the branched insertion products. As a product of styrene insertion into the Zr-H bond of **38**, complex **40** could be isolated and structurally characterized.

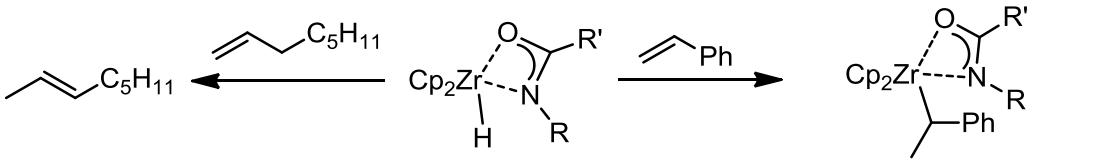

R = *i*-Pr, R' = *t*-Bu (**37**)
R = Dipp, R' = Ph (**38**)

R = *i*-Pr, R' = *t*-Bu (**39**)
R = Dipp, R' = Ph (**40**)

13. Zirconocene and hafnocene chlorido amidato complexes are easily prepared by salt metathesis reaction of sodium amidates with Cp_2MCl_2 (**6-M**). Moreover, the zirconocene complexes can also be obtained by protonolysis of the amide with Schwartz' reagent $Cp_2Zr(H)Cl$ (**8**).

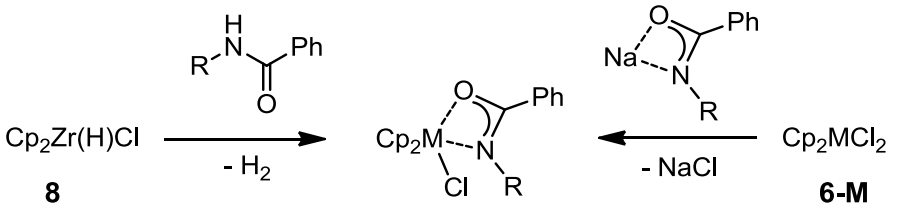

M = Zr, R = Dipp (**41**)
M = Hf, R = Ph (**42**)

M = Zr, Hf

Reduction of the zirconocene chlorido amidato complex **41** with Mg did not result in the formation of the desired zirconocene^{III} amidato complex but in two electron reduction to yield the Mg chlorido amidate complex **44**, which is the first monometallic and structurally characterized Mg amidato complex.

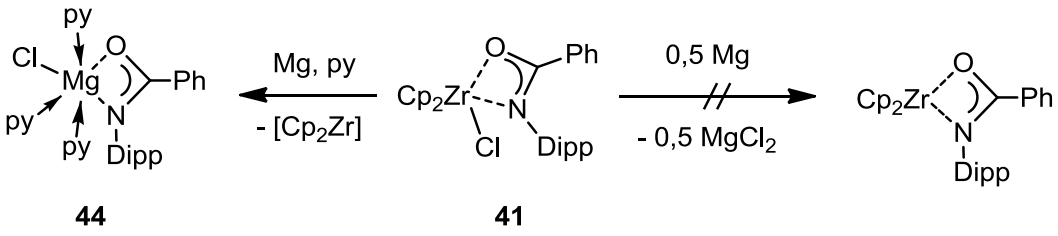

44 **41**

4. References

[1] G. P. Chiusoli, P. M. Maitlis, *Metal-catalysis in Industrial Organic Processes*, The Royal Society of Chemistry, Cambridge, **2006**.

[2] *Organization for Economic Co-operation and Development Environmental Outlook for the Chemicals Industry*; **2001**.

[3] A. Fürstner, *Angew. Chem. Int. Ed.* **2013**, *52*, 2794-2819.

[4] J. H. Wengrovius, J. Sancho, R. R. Schrock, *J. Am. Chem. Soc.* **1981**, *103*, 3932-3934.

[5] J. Heppekausen, R. Stade, A. Kondoh, G. Seidel, R. Goddard, A. Fürstner, *Chem. Eur. J.* **2012**, *18*, 10281-10299.

[6] I. Marek, *Titanium and Zirconium in Organic Synthesis*, Wiley-VCH, Weinheim, **2002**.

[7] L. L. Böhm, *Angew. Chem. Int. Ed.* **2003**, *42*, 5010-5030.

[8] T. E. Müller, K. C. Hultzsch, M. Yus, F. Foubelo, M. Tada, *Chem. Rev.* **2008**, *108*, 3795-3892.

[9] F. Pohlki, S. Doye *Chem. Soc. Rev.* **2003**, *32*, 104-114.

[10] U. Rosenthal, V. V. Burlakov, P. Arndt, W. Baumann, A. Spannenberg, *Organometallics* **2003**, *22*, 884- 900.

[11] E. D. Jemmis, S. Roy, V. V. Burlakov, H. Jiao, M. Klahn, S. Hansen, U. Rosenthal, *Organometallics* **2010**, *29*, 76-81.

[12] a) J. Ugolotti, G. Dierker, G. Kehr, R. Fröhlich, S. Grimme, G. Erker, *Angew. Chem. Int. Ed.* **2008**, *47*, 2622-2625; b) N. Suzuki, D. Hashizume, H. Koshino, T. Chihara, *Angew. Chem. Int. Ed.* **2008**, *47*, 5198-5202; c) J. Ugolotti, G. Kehr, R. Fröhlich, S. Grimme, G. Erker, *J. Am. Chem. Soc.* **2009**, *131*, 1996-2007.

[13] L. G. McCullough, M. L. Listemann, R. R. Schrock, M. R. Churchill, J. W. Ziller, *J. Am. Chem. Soc.* **1983**, *105*, 6729-6730.

[14] L. G. McCullough, R. R. Schrock, J. C. Dewan, J. C. Murdzek, *J. Am. Chem. Soc.* **1985**, *107*, 5987-5998.

[15] a) F. Basuli, B. C. Bailey, J. Tomaszewski, J. C. Huffman, D. J. Mindiola, *J. Am. Chem. Soc.* **2003**, *125*, 6052-6053; b) B. C. Bailey, H. Fan, E. W. Baum, J. C. Huffman, M.-H. Baik, D. J. Mindiola, *J. Am. Chem. Soc.* **2005**, *127*, 16016-16017; c) F. Basuli, B. C. Bailey, J. C. Huffman, D. J. Mindiola, *Organometallics* **2005**, *24*, 3321-3334.

[16] K. Kaleta, *Doctoral Thesis* **2012**.

[17] D. Seyferth, P. Langer, M. Doering, *Organometallics* **1995**, *14*, 4457-4459.

[18] a) J. Y. Becker, *J. Organomet. Chem.* **1977**, *127*, 1-5; b) S. Ma, Q. He, *Angew. Chem. Int. Ed.* **2004**, *43*, 988-990.

[19] J. Y. Becker, J. Klein, *J. Organomet. Chem.* **1978**, *157*, 1-6.

[20] S. Roy, E. D. Jemmis, A. Schulz, T. Beweries, U. Rosenthal, *Angew. Chem. Int. Ed.* **2012,** *51*, 5347-5350.

[21] R. L. Zuckerman, S. W. Krska, R. G. Bergman, *J. Am. Chem. Soc.* **2000**, *122*, 751-761.

[22] F. H. Allen, O. Kennard, D. G. Watson, L. Brammer, A. G. Orpen, R. Taylor, *J. Chem. Soc. Perkin Trans.* **1987**, *2*, S1-S19.

[23] S. A. Blum, V. A. Rivera, R. T. Ruck, F. E. Michael, R. G. Bergman, *Organometallics* **2005**, *24*, 1647-1659.

[24] R. Beckhaus, M. Wagner, R. Wang, *Eur. J. Inorg. Chem.* **1998**, 253-256.

[25] S. Gambarotta, S. Strologo, C. Floriani, A. Chiesi-Villa, C. Guastini, *J. Am. Chem. Soc.* **1985**, *107*, 6278-6282.

[26] Y. A. Wasslen, E. Tois, S. Haukka, K. A. Kreisel, G. P. A. Yap, M. D. Halls, S. N. T. Barry, *Inorg. Chem.* **2010**, *49*, 1976-1982.

[27] a) G. A. Vaughan, G. L. Hillhouse, A. L. Rheingold, *J. Am. Chem. Soc.* **1990**, *112*, 7994-8001; b) H. Wang, H.-S. Chan, Z. Xie, *Organometallics* **2005**, *24*, 3772-3779; c) N. Vujkovic, J. L. Fillol, B. D. Ward, H. Wadepohl, P. Mountford, L. H. Gade, *Organometallics* **2008**, *27*, 2518-2528; d) A. D. Schofield, A. Nova, J. D. Selby, C. D. Manley, A. D. Schwarz, E. Clot, P. Mountford, *J. Am. Chem. Soc.* **2010**, *132*, 10484-10497.

[28] a) M. Pasquali, C. Floriani, A. Chiesi-Villa, C. Guastini, *J. Am. Chem. Soc.* **1979**, *101*, 4740-4742; b) M. Pasquali, C. Floriani, A. Chiesi-Villa, C. Guastini, *Inorg. Chem.* **1981**, *20*, 349-355.

[29] a) R. L. Zuckerman, R. G. Bergman, *Organometallics* **2000**, *19*, 4795-4809; b) R. L. Zuckerman, R. G. Bergman, *Organometallics* **2001**, *20*, 1792-1807.

[30] K. Kaleta, M. Ruhmann, O. Theilmann, T. Beweries, S. Roy, P. Arndt, A. Villinger, E. D. Jemmis, A. Schulz, U. Rosenthal, *J. Am. Chem. Soc.* **2011**, *133*, 5463-5473.

[31] O. Theilmann, M. Ruhmann, A. Villinger, A. Schulz, W. W. Seidel, K. Kaleta, T. Beweries, P. Arndt, U. Rosenthal, *Angew. Chem. Int. Ed.* **2010**, *49*, 9282-9285.

[32] W. C. Schneider, *J. Am. Chem. Soc.* **1950**, *72*, 761-763.

[33] M. Findlater, N. J. Hill, A. H. Cowley, *Dalton Trans.* **2008**, 4419-4423.

[34] P. Pyykkö, M. Atsumi, *Chem. Eur. J.* **2009**, *15*, 12770-12779.

[35] F. M. Alías, T. R. Belderraín, M. Paneque, M. L. Poveda, E. Carmona, P. Valerga, *Organometallics* **1998**, *17*, 5620-5629.

[36] K. Kunz, G. Erker, G. Kehr, R. Fröhlich, *Organometallics* **2001**, *20*, 392-400.

[37] P. P. Fontaine, B. L. Yonke, P. Y. Zavalij, L. R. Sita, *J. Am. Chem. Soc.* **2010**, *132*, 12273-12285.

[38] T. Cuenca, R. Gómez, P. Gomez-Sal, P. Royo, *J. Organomet. Chem.* **1993**, *454*, 105-111.

[39] A. C. Filippou, A. R. Dias, A. M. Martins, C. C. Romão, *J. Organomet. Chem.* **1993**, *455*, 129-135.

[40] M. A. Bach, T. Beweries, V. V. Burlakov, P. Arndt, W. Baumann, A. Spannenberg, U. Rosenthal, *Organometallics* **2007**, *26*, 4592-4597.

[41] a) T. E. Hanna, I. Keresztes, E. Lobkovsky, W. H. Bernskoetter, P. J. Chirik, *Organometallics* **2004**, *23*, 3448-3458.

[42] F. Basuli, J. C. Huffman, D. J. Mindiola, *Inorg. Chem.* **2003**, *42*, 8003-8010.

[43] C. Lorber, R. Choukroun, L. Vendier, *Organometallics* **2008**, *27*, 5017-5024.

[44] L. Becker, V. V. Burlakov, P. Arndt, A. Spannenberg, W. Baumann, H. Jiao, U. Rosenthal, *Chem. Eur. J.* **2013**, *19*, 4230-4237

[45] J. Corset, M. Castellà-Ventura, F. Froment, T. Strzalko, L. Wartski, *J. Org. Chem.* **2003**, *68*, 3902-3911.

[46] J. Zhao, S. Zhang, W.-X. Zhang, Z. Xi, *Organometallics* **2011**, *30*, 3464-3467.

[47] I. L. Fedushkin, A. G. Morozov, O. V. Rassadin, G. K. Fukin, *Chem. Eur. J.* **2005**, *11*, 5749-5757.

[48] a) G. B. Deacon, E. E. Delbridge, B. W. Skelton, A. H. White, *Eur. J. Inorg. Chem.* **1999**, 751-761; b) G. B. Deacon, E. E. Delbridge, G. D. Fallon, C. Jones, D. E. Hibbs, M. B. Hursthouse, B. W. Skelton, A. H. White, *Organometallics* **2000**, *19*, 1713-1721.

[49] K. Kaleta, M. Ruhmann, O. Theilmann, S. Roy, T. Beweries, P. Arndt, A. Villinger, E. D. Jemmis, A. Schulz, U. Rosenthal, *Eur. J. Inorg. Chem.* **2012**, 611-617.

[50] J. Ellermann, W. Bauer, M. Schütz, F. W. Heinemann, M. Moll, *Monatsh. Chem.* **1998**, *129*, 547-566.

[51] J. Ellermann, M. Schütz, F. W. Heinmann, M. Moll, W. Bauer, *Chem. Ber.* **1997**, *130*, 141-144.

[52] M. T. Gamer, P. W. Roesky, *Inorg. Chem.* **2004**, *43*, 4903-4906.

[53] M. T. Gamer, G. Canseco-Melchor, P. W. Roesky, *Z. Anorg. Allg. Chem.* **2003**, *629*, 2113-2116.

[54] P. W. Roesky, *Inorg. Chem.* **2005**, *45*, 798-802.

[55] T. K. Panda, M. T. Gamer, P. W. Roesky, *Inorg. Chim. Acta* **2006**, *359*, 4765-4768.

[56] S. Datta, M. T. Gamer, P. W. Roesky, *Dalton Trans.* **2008**, 2839-2843.

[57] J. Ellermann, M. Schütz, F. W. Heinemann, M. Moll, *Z. Anorg. Allg. Chem.* **1998**, *624*, 257-262.

[58] M. T. Gamer, M. Rastätter, P. W. Roesky, *Z. Anorg. Allg. Chem.* **2002**, *628*, 2269-2272.

[59] J. Ellermann, W. Wend, *Z. Anorg. Allg. Chem.* **1986**, *543*, 169-185.

[60] J. Ellermann, P. Gabold, C. Schelle, F. A. Knoch, M. Moll, W. Bauer, *Z. Anorg. Allg. Chem.* **1995**, *621*, 1832-1843.

[61] V. V. Sushev, A. N. Kornev, Y. V. Fedotova, Y. A. Kursky, T. G. Mushtina, G. A. Abakumov, L. N. Zakharov, A. L. Rheingold, *J. Organomet. Chem.* **2003**, *676*, 89-93.

[62] M. Gomez, G. Muller, J. Sales, X. Solans, *J. Chem. Soc., Dalton Trans.* **1993**, 221-225.

[63] T. Beweries, V. V. Burlakov, M. A. Bach, P. Arndt, W. Baumann, A. Spannenberg, U. Rosenthal, *Organometallics* **2007**, *26*, 247-249.

[64] L. B. Kool, M. D. Rausch, H. G. Alt, M. Herberhold, B. Wolf, U. Thewalt, *J. Organomet. Chem.* **1985**, *297*, 159-169.

[65] R. Payne, J. Hachgenei, G. Fritz, D. Fenske, *Z. Naturforsch., B: Chem.Sci.* **1986**, *41*, 1535-1540.

[66] G. R. Desiraju, T. Steiner, in *The Weak Hydrogen Bond*, Oxford Unniversity Press, Oxford **1999**.

[67] P. C. Wailes, H. Weigold, *J. Organomet. Chem.* **1971**, *28*, 91-95.

[68] P. v. R. Schleyer, C. Maerker, A. Dransfeld, H. Jiao, N. J. R. v. E. Hommes, *J. Am. Chem. Soc.*, **1996**, *118*, 6317-6318.

[69] G. L. Casty, C. G. Lugmair, N. S. Radu, T. D. Tilley, J. F. Walzer, D. Zargarian, *Organometallics* **1997**, *16*, 8-12.

[70] W. H. Bernskoetter, A. V. Olmos, E. Lobkovsky, P. J. Chirik, *Organometallics* **2005**, *25*, 1021-1027.

[71] T. Beweries, U. Jäger-Fiedler, M. A. Bach, V. V. Burlakov, P. Arndt, W. Baumann, A. Spannenberg, U. Rosenthal, *Organometallics* **2007**, *26*, 3000-3004.

[72] a) F. A. Cotton, W. J. Roth, *Inorg. Chem.* **1983**, *22*, 3654-3656; b) B. Bechlars, I. Issac, R. Feuerhake, R. Clérac, O. Fuhr, D. Fenske, *Eur. J. Inorg. Chem.* **2008**, 1632-1644.

[73] M. Filby, A. J. Deeming, G. Hogarth, M.-Y. Lee, *Can. J. Chem.* **2006**, *84*, 319-329.

[74] J. C. Dewan, T. E. Wood, R. A. Walton, S. J. Lippard, *Inorg. Chem.* **1982**, *21*, 1854-1859.

[75] Y. Gao, D. G. Holah, A. N. Hughes, G. J. Spivak, M. D. Havighurst, V. R. Magnuson, *Polyhedron* **1999**, *17*, 3881-3888.

[76] M. I. Bruce, B. G. Ellis, P. J. Low, B. W. Skelton, A. H. White, *Organometallics* **2003**, *22*, 3184-3198.

[77] C. Krüger, Y.-H. Tsay, *Acta Crystallogr. Sect. B* **1972**, *28*, 1941-1946.

[78] Z. Mao, H.-Y. Chao, Z. Hui, C.-M. Che, W.-F. Fu, K.-K. Cheung, N. Zhu, *Chem. Eur. J.* **2003**, *9*, 2885-2894.

[79] R. Uson, A. Laguna, M. Laguna, E. Fernandez, M. D. Villacampa, P. G. Jones, G. M. Sheldrick, *J. Chem. Soc., Dalton Trans.* **1983**, 1679-1685.

[80] H. H. Karsch, G. Grauvogl, B. Deubelly, G. Mueller, *Organometallics* **1992**, *11*, 4238-4245.

[81] H. H. Karsch, D. Neugebauer, *Angew. Chem.* **1982**, *Angew. Chem. Int. Ed. Engl.* **1982**, *21*, 312-313.

[82] J. J. H. Edema, A. Meetsma, F. Van Bolhuis, S. Gambarotta, *Inorg. Chem.* **1991**, *30*, 2056-2061.

[83] H. H. Karsch, B. Deubelly, G. Grauvogl, J. Lachmann, G. Mueller, *Organometallics* **1992**, *11*, 4245-4249.

[84] H. H. Karsch, G. Grauvogl, M. Kawecki, P. Bissinger, O. Kumberger, A. Schier, G. Mueller, *Organometallics* **1994**, *13*, 610-618.

[85] H. H. Karsch, B. Deubelly, G. Grauvogl, G. Müller, *J. Organomet. Chem.* **1993**, *459*, 95-105.

[86] K. Izod, W. McFarlane, B. V. Tyson, W. Clegg, R. W. Harrington, *Dalton Trans.* **2004**, 4074-4078.

[87] a) H. H. Karsch, G. Grauvogl, P. Mikulcik, P. Bissinger, G. Müller, *J. Organomet. Chem.* **1994**, *465*, 65-71; b) R. Appel, K. Geisler, H.-F. Schöler, *Chem. Ber.* **1979**, *112*, 648-653.

[88] D. G. Dick, D. W. Stephan, *Organometallics* **1991**, *10*, 2811-2816.

[89] M. Tamm, unpublished results, *private communication*.

[90] K. Altenburger, P. Arndt, A. Spannenberg, W. Baumann, U. Rosenthal, *Eur. J. Inorg. Chem.* **2013**, 3200-3205.

[91] D. Rodewald, C. Schulzke, D. Rehder, *J. Organomet. Chem.* **1995**, *498*, 29-35.

[92] A. K. Powell, M. J. Went, *J. Chem. Soc., Dalton Trans.* **1992**, 439-445.

[93] F.-E. Hong, C. P. Chang-Chang, R.-E. Chang, S.-C. Chen, B.-T. Ko, *Organometallics* **2002**, *21*, 961-967.

[94] A. D. Miller, S. A. Johnson, K. A. Tupper, J. L. McBee, T. D. Tilley, *Organometallics* **2009**, *28*, 1252-1262.

[95] V. V. Burlakov, A. V. Polyakov, A. I. Yanovsky, Y. T. Struchkov, V. B. Shur, M. E. Vol'pin, U. Rosenthal, H. Görls, *J. Organomet. Chem.* **1994**, *476*, 197-206.

[96] C. Lefeber, W. Baumann, A. Tillack, R. Kempe, H. Görls, U. Rosenthal, *Organometallics* **1996**, *15*, 3486-3490.

[97] R. B. King, A. Efraty, *Inorg. Chim. Acta* **1970**, *4*, 319-323.

[98] C. Janiak, *J. Chem. Soc., Dalton Trans.* **2000**, 3885-3896.

[99] P. Delhaes, *Graphite and Precursors,* CRC Press, Boca Raton, **2001**.

[100] P. W. Blosser, J. C. Gallucci, A. Wojcicki, *J. Am. Chem. Soc.* **1993**, *115*, 2994-2995.

[101] A. Ohff, P. Kosse, W. Baumann, A. Tillack, R. Kempe, H. Goerls, V. V. Burlakov, U. Rosenthal, *J. Am. Chem. Soc.* **1995**, *117*, 10399-10400.

[102] R. T. Baker, J. F. Whitney, S. S. Wreford, *Organometallics* **1983**, *2*, 1049-1051.

[103] M. Hapke, N. Weding, A. Spannenberg, *Organometallics* **2010**, *29*, 4298-4304.

[104] G. Wilke, G. Herrmann, *Angew. Chem. Int Ed. Engl.* **1962**, *1*, 549-550.

[105] C. E. Kriley, C. J. Woolley, M. K. Krepps, E. M. Popa, P. E. Fanwick, I. P. Rothwell, *Inorg. Chem. Acta* **2000**, *300-302*, 200-205.

[106] C. Müller, C. N. Iverson, R. J. Lachicotte, W. D. Jones, *J. Am. Chem. Soc.* **2001**, *123*, 9718-9719.

[107] C. Müller, R. J. Lachicotte, W. D. Jones, *Organometallics* **2002**, *21*, 1190-1196.

[108] P. Arndt, W. Baumann, A. Spannenberg, U. Rosenthal, V. V. Burlakov, V. B. Shur, *Angew. Chem. Int. Ed.* **2003**, *42*, 1414-1418.

[109] T. Beweries, V. V. Burlakov, M. A. Bach, S. Peitz, P. Arndt, W. Baumann, A. Spannenberg, U. Rosenthal, B. Pathak, E. D. Jemmis, *Angew. Chem. Int. Ed.* **2007**, *46*, 6907-6910.

[110] V. Varga, K. Mach, J. Hiller, U. Thewalt, P. Sedmera, M. Polasek, *Organometallics* **1995**, *14*, 1410-1416.

[111] K. Altenburger, J. Semmler, P. Arndt, A. Spannenberg, M. J. Meel, A. Villinger, W. W. Seidel, U. Rosenthal, *Eur. J. Inorg. Chem.* **2013**, 4258-4267.

[112] Y. Dang, *Coord. Chem. Rev.* **1994**, *135-136*, 93-128.

[113] A. V. Lee, L. L. Schafer, *Eur. J. Inorg. Chem.* **2007**, 2245-2255.

[114] R. K. Thomson, F. E. Zahariev, Z. Zhang, B. O. Patrick, Y. A. Wang, L. L. Schafer, *Inorg. Chem.* **2009**, *44*, 8680-8689.

[115] P. Arndt, C. Lefeber, R. Kempe, A. Tillack, U. Rosenthal, *Chem. Ber.* **1996**, *129*, 1281-1285.

[116] S. Gambarotta, S. Strologo, C. Floriani, A. Chiesi-Villa, C. Guastini, *Inorg. Chem.* **1985**, *24*, 654-660.

[117] M. Oberhoff, G. Erker, R. Fröhlich, *Chem. Eur. J.* **1997**, *3*, 1521-1525.

[118] Y. Liu, B. Yan, *Organometallics* **2005**, *25*, 544-547.

[119] R. O. Ayinla, T. Gibson, L. L. Schafer, *J. Organomet. Chem.* **2011**, *696*, 50-60.

[120] a) R. K. Thomson, F. E. Zahariev, Z. Zhang, B. O. Patrick, Y. A. Wang, L. L. Schafer, *Inorg. Chem.* **2009**, *44*, 8680-8689; b) R. K. Thomson, L. L. Schafer, *Organometallics* **2010**, *29*, 3546-3555.

[121] M. Kessler, S. Schüler, D. Hollmann, M. Klahn, T. Beweries, A. Spannenberg, A. Brückner, U. Rosenthal, *Angew. Chem. Int. Ed.* **2012**, *51*, 6272-6275; J. W. Pattiasina,

H. J. Heeres, F. van Bolhuis, A. Meetsma, J. H. Teuben, *Organometallics* **1987**, *6*, 1004-1010.

[122] B. F. Fieselmann, D. N. Hendrickson, G. D. Stucky, *Inorg. Chem.* **1978**, *17*, 2078-2084.

[123] R. K. Thomson, F. E. Zahariev, Z. Zhang, B. O. Patrick, Y. A. Wang, L. L. Schafer, *Inorg. Chem.* **2009**, *44*, 8680-8689.

[124] P. Arndt, V. V. Burlakov, U. Jäger-Fiedler, M. Klahn, A. Spannenberg, W. Baumann, U. Rosenthal, *Coll. Czech. Chem. Comm.*, **2007**, *72*, 475-491.

[125] U. Rosenthal, A. Ohff, M. Michalik, H. Goerls, V. V. Burlakov, V. B. Shur, *Organometallics* **1993**, *12*, 5016-5019.

[126] D. Thomas, N. Peulecke, V. V. Burlakov, B. Heller, W. Baumann, A. Spannenberg, R. Kempe, U. Rosenthal, R. Beckhaus, *Z. Anorg. Allg. Chem.* **1998**, *624*, 919-924.

[127] C. A. Bradley, E. Lobkovsky, P. J. Chirik, *J. Am. Chem. Soc.* **2003**, *125*, 8110-8111

[128] D. P. Kruťko, R. S. Kirsanov, S. A. Belov, M. V. Borzov, A. V. Churakov, J. A. K. Howard, *Polyhedron* **2007**, *26*, 2864-2870.

[129] T. Takahashi, M. Hasegawa, N. Suzuki, M. Saburi, C. J. Rousset, P. E. Fanwick, E. Negishi, *J. Am. Chem. Soc.* **1991,** *113*, 8564-8566.

[130] T. E. Hanna, E. Lobkovsky, P. J. Chirik, *Eur. J. Inorg. Chem.* **2007**, 2677-2685.

[131] T. D. Forster, H. M. Tuononen, M. Parvez, R. Roesler, *J. Am. Chem. Soc.* **2009**, *131*, 6689-6691.

[132] For reviews of oxidative addition of N-H bonds to late-metal centers: a) T. Braun, *Angew. Chem. Int. Ed.* **2005**, *44*, 5012-5014. For recent examples: b) C. GuhaRoy, R. J. Butcher, S. Bhattacharya, *J. Organomet. Chem.* **2008**, *693*, 3923-3931; c) I. Mena, M. A. Casado, P. García-Orduña, V. Polo, F. J. Lahoz, A. Fazal, L. A. Oro, *Angew. Chem. Int. Ed.* **2011**, *50*, 11735-11738; d) A.-K. Jungton, C. Herwig, T. Braun, C. Limberg, *Chem. Eur. J.* **2012**, *18*, 10009-10013.

[133] M. G. Crestani, A. Steffen, A. M. Kenwright, A. S. Batsanov, J. A. K. Howard, T. B. Marder, *Organometallics* **2009**, *28*, 2904-2914.

[134] D. R. Schaad, C. R. Landis, *Organometallics* **1992**, *11*, 2024-2029.

[135] a) S. Nag, R. J. Butcher, S. Bhattacharya, *Eur. J. Inorg. Chem.* **2007**, 1251-1260; b) M. Arndt, K. S. M. Salih, A. Fromm, L. J. Goossen, F. Menges, G. Niedner-Schatteburg, *J. Am. Chem. Soc.* **2011**, *133*, 7428-7449.

[136] a) A. C. Sykes, P. White, M. Brookhart, *Organometallics* **2006**, *25*, 1664-1675; b) M. Dasgupta, H. Tadesse, A. J. Blake, S. Bhattacharya, *J. Organomet. Chem.* **2008**, *693*, 3281-3288; c) C. S. Sevov, J. Zhou, J. F. Hartwig, *J. Am. Chem. Soc.* **2012**, *134*, 11960-11963

[137] P. Perrotin, I. El-Zoghbi, P. O. Oguadinma, F. Schaper, *Organometallics* **2009**, *28*, 4912-4922.

[138] C. Averbuj, M. S. Eisen, *J. Am. Chem. Soc.* **1999**, *121*, 8755-8759.

[139] P. J. Chirik, M. W. Day, J. A. Labinger, J. E. Bercaw, *J. Am. Chem. Soc.* **1999**, *121*, 10308-10317.

[140] L. Duda, G. Erker, R. Fröhlich, F. Zippel, *Eur. J. Inorg. Chem.* **1998**, 1153-1162.

[141] D. Kunz, G. Erker, R. Fröhlich, G. Kehr, *Eur. J. Inorg. Chem.* **2000**, 409-416.

[142] K. M. Anderson, A. G. Orpen, *Chem. Comm.* **2001**, 2682-2683.

[143] J. T. Leman, A. R. Barron, *Organometallics* **1989**, *8*, 1828-1829.

[144] K. A. Paseshnitchenko, L. A. Aslanov, A. V. Jatsenko, S. V. Medvedev, *J. Organomet. Chem.* **1985**, *287*, 187-194.

Appendices

5. Experimental Section

5.1. General Procedures

As most of the described transition metal complexes are moisture- and air sensitive, all preparative scale reactions were conducted in oxygen- and moisture free glassware with magnetic stirring using Schlenk-line techniques or a glove box under an atmosphere of dry dinitrogen or argon. Experiments on NMR tube scale were carried out in Teflon cap sealed NMR tubes (5 mm). Solvents were dried according to common procedures using sodium/benzophenone and freshly distilled from sodium tetraethylaluminate prior to use. Benzene-d_6, toluene-d_8 and tetrahydrofuran-d_8 were dried over sodium and freshly distilled from sodium tetraethylaluminate prior to use.

Reagents for syntheses were used as received from Aldrich, Acros Organics or ABCR-chemicals and used without further purification. Metallocene dichlorides were received from either Aldrich (Cp_2TiCl_2, Cp_2ZrCl_2) or MCAT (Metallocene Catalysts & Life Science Technologies).

5.2. Analytical Methods

5.2.1. Elemental Analysis

Samples for elemental analysis were prepared in the glove box and measured using a Leco CHNS-932 elemental or a Carlo Erba Elemental EA 1108 analyzer. Dedicated samples were augmented with V_2O_5 to ensure complete incineration.

5.2.2. IR Spectroscopy

IR spectra were recorded under steady argon flow at a Bruker Alpha FT-IR spectrometer with a smart endurance attenuated total reflection (ATR). No IR-spectra of compounds synthesized in the cooperation with the Schafer group (Vancouver, Canada) were recorded.

5.2.3. Mass Spectrometry

Samples for mass spectrometry were prepared in the glove box and measured on a Finnigan MAT 95-XP (Thermo Electron) or Kratos MS-50 spectrometer. Measurements were carried out in either EI- (70 eV) or CI-mode (*i*-butane). Fragment signals are given in mass per charge number (*m/z*).

5.2.4. NMR Spectroscopy

NMR spectra were recorded on Bruker Avance 300 (^{1}H: 300, ^{13}C: 75, ^{31}P: 121), Bruker Avance 400 (^{1}H: 400, ^{13}C: 100, ^{31}P: 161) or Bruker Avance 600 (^{1}H: 600 ^{13}C: 150) instruments operating at the denoted spectrometer frequency given in Megahertz (MHz) for the specified nucleus. The samples were measured as solutions in the stated solvent at ambient temperature in non-spinning mode if not mentioned otherwise. Shifts δ are reported in parts per million (ppm) relative to tetramethylsilane (TMS) as an external standard for ^{1}H- and ^{13}C NMR spectra and calibrated against the solvent residual peak.[145] Coupling constants *J* are given in Hertz (Hz).

5.2.5. X-Ray Analysis

Single crystals were prepared under argon and measured on a STOE IPDS II or a Bruker Kappa Apex II DUO using graphite-monochromated $Mo_{K\alpha}$ (λ = 0.71073 Å) or $Cu_{K\alpha}$ radiation (λ = 1.54178 Å) under a continuous flow of nitrogen. The structures were solved by direct methods (SHELXS-97) and refined by Full-matrix Least-squares procedures on F^2 (SHELXL-97).[146] For compounds **11** and **29-Zr**, contributions of disordered solvent molecules were removed from the diffraction data with PLATON/ SQUEEZE.[147]

5.2.6. Melting Point Analysis

Determination of uncorrected melting or decomposition points was carried out in sealed capillaries under argon at Büchi 535 or MP 70 apparatus. No melting or decomposition points of compounds synthesized in the cooperation with the Schafer group (Vancouver, Canada) were measured.

5.2.7. EPR Spectroscopy

EPR spectra were recorded as solutions in toluene on Bruker EMX micro spectrometer with an ER 4119HS-WI high-sensitivity optical resonator and the following settings: 3.34

mW microwave power, 9.446 GHz microwave frequency (X-band), 100 kHz modulation frequency and 0.3 G modulation amplitude.

5.3. Syntheses

5.3.1. Reaction of $Cp_2Ti(\eta^2\text{-}Me_3SiC_2SiMe_3)$ (1) with 1,3-*N*,*N*′-Bis-(mesityl)carbodiimide (10-Mes-Mes) to 11 and 12:

The alkyne complex $Cp_2Ti(\eta^2\text{-}Me_3SiC_2SiMe_3)$ (**1**) (451 mg, 1.29 mmol) was dissolved in 15 mL of *n*-hexane and a solution of the carbodiimide **10-Mes-Mes** (381 mg, 1.36 mmol) in 15 mL of *n*-hexane was added dropwise at room temperature. The colour of the solution changed to dark red and the mixture was stirred at room temperature for 10 h. The volatiles were removed in vacuum and the residue was suspended in 20 mL of *n*-hexane, followed by filtration and storing of the solution at -40 °C. After 3 days a fine precipitate formed, which was isolated by filtration and re-crystallized from a mixture of THF (5 mL) and pentane (3 mL) at room temperature. After two weeks turquoise crystals of **11** formed, which were isolated, washed with cold pentane and dried in vacuum. Light brown crystalline material of complex **12** was obtained from the concentrated mother liquor of the *n*-hexane extraction at -40 °C (vide supra).

$Cp_2Ti[\eta^2\text{-}(Mes)NCN(Mes)_2NH(Mes)]$ (11):

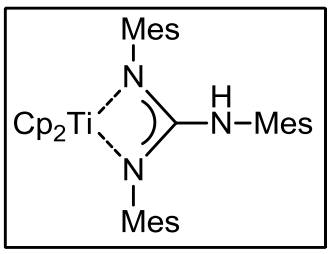

Yield: 254 mg (33%).

Mp.: 167 °C (dec.).

EA: Anal. calcd. for $C_{38}H_{44}N_3Ti$: C, 77.27; H, 7.51; N, 7,11. Found: C, 77.26; H, 7.56; N, 7.01.

IR: (16 scans): 3377 (vw), 2914 (w), 1643 (w), 1602 (w), 1518 (m), 1475 (m), 1440 (m), 1362 (w), 1311 (m), 1254 (w), 1222 (m), 1204 (w), 1145 (w), 1068 (w), 1016 (m), 882 (w), 847 (m), 793 (s), 780 (vs), 699 (s), 568 (s), 545 (s), 510 (m), 467 (s).

MS: (EI) 590 $[M]^+$, 525 $[M-Cp]^+$, 413 $[M-Cp_2Ti]^+$, 278 [Mes-NCN-Mes]$^+$, 134 $[HNMes]^+$.

$Cp_2Ti(\eta^1\text{-}C{=}N{-}Mes)[\eta^2\text{-}(C_5H_4{-}C{=}N{-}Mes)]$ (12):

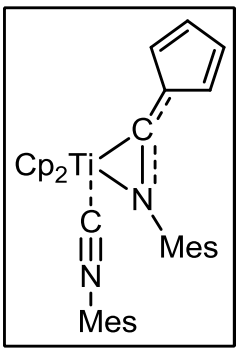

Yield: 51 mg (7%).

Unfortunately, due to the low yield, neither melting point nor elemental analysis could be performed.

NMR: ^{1}H (300 MHz, benzene-d_6): δ = 7.22 (ddd, ^3J = 3.9 Hz, ^4J = 2.0 Hz, ^4J = 1.7 Hz, 1H), 7.20 (ddd, ^3J = 4.3 Hz, ^3J = 2.7 Hz, ^4J = 1.7 Hz, 1H), 6.92 (ddd, ^3J = 4.4 Hz, ^3J = 2.6 Hz, ^4J = 1.8 Hz, 1H), 6.60 (ddd, ^3J = 4.0 Hz, ^4J = 2.0 Hz, ^4J = 1.7 Hz, 1H), 6.58 (m, 2H), 6.33 (m, 2H), 5.51 (s, 10H), 2.09 (s, 3H), 2.04 (s, 6H), 1.83 (s, 3H), 1.70 (s, 6H). ^{13}C NMR (100 MHz, benzene-d_6): δ = 187.8, 180.7, 153.9, 145.3, 140.0, 134.6, 132.7, 130.0, 128.8, 120.9, 117.9, 117.1, 115.4, 112.4, 105.4, 20.9, 20.6, 20.0, 17.7.

IR: (16 scans): 2916 (vw), 2164 (vw), 1638 (w), 1561 (w), 1478 (m), 1438 (w), 1261 (w), 1223 (w), 1095 (m), 1016 (m), 850 (s), 796 (vs), 731 (s), 660 (s), 545 (s), 466 (s), 426 (m).

MS: (CI) 533 $[M+H]^+$, 468 $[M-Cp]^+$, 388 $[M\text{-}CNMes+H]^+$, 323 $[Cp_2TiCNMes]^+$.

5.3.2. Synthesis of $Cp^*_2Ti(\eta^1\text{-}CN{-}Mes)_2$ (13):

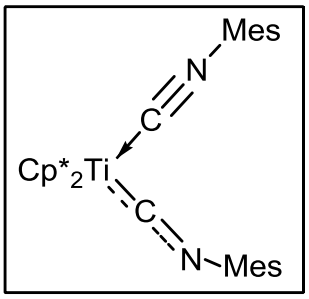

The alkyne complex $Cp^*_2Ti(\eta^2\text{-}Me_3SiC_2SiMe_3)$ (**3-Ti**) (472 mg, 0.97 mmol) was dissolved in 15 mL of *n*-hexane and a solution of the carbodiimide **10-Mes-Mes** (0.282 g, 1.01 mmol) in 15 mL of *n*-hexane was added at room temperature. The mixture was heated at 50 °C for three days, during this time the colour of the solution changed to deep red. After cooling to room temperature all volatiles were removed in vacuum and the black residue was dissolved in 5 mL of *n*-hexane. Upon standing at -78 °C for several weeks, black crystals had formed which were isolated by filtration, washed with 0.2 mL of cold *n*-hexane and dried in vacuum.

Yield: 235 mg (41%).

Mp.: 150 °C (dec.).

EA: Anal. calcd For $C_{47}H_{60}N_2Ti$: C, 78.92; H, 8.61; N, 4.60. Found: C, 76.42; H, 8.11; N, 4.48.

NMR: ^{1}H (300 MHz, benzene-d_6): δ = 6.68 (s, 4H), 2.46 (s, 12H), 2.08 (s, 6H), 1.92 (s, 30H). ^{13}C (100 MHz, benzene-d_6): δ = 251.7, 134.9, 132.2, 130.6, 129.2, 105.1, 20.9, 20.5, 12.1.

IR (16 scans): 2961 (w), 2908 (m), 2854 (w), 2112 (s), 1801 (w), 1605 (w), 1558 (w), 1541 (w), 1507 (w), 1473 (m), 1437 (s), 1374 (s), 1260 (w), 1199 (w), 1065 (m), 1021 (m), 954 (w), 851 (s), 790 (s), 712 (s), 569 (vs), 465 (vs), 420 (s), 397 (vs), 385 (vs)

MS (EI) 609 $[M+H]^+$, 608 $[M]^+$, 463 $[Cp^*_2Ti(CNMes)]^+$, 318 $[Cp^*_2Ti]^+$, 156 $[CNMes+H]^+$.

5.3.3. Synthesis of $Cp_2Ti(\eta^1$-C=N−Dipp)(=N−Dipp) (14a):

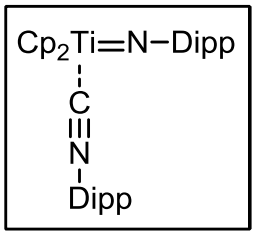

The alkyne complex $Cp_2Ti(\eta^2$-$Me_3SiC_2SiMe_3)$ (**1**) (386 mg, 1.06 mmol) was dissolved in 15 mL of *n*-hexane and a solution of the carbodiimide **10-Dipp-Dipp** (389 mg, 1.07 mmol) in 15 mL of *n*-hexane was added dropwise at room temperature. Immediately upon addition the colour of the solution changed to dark red. The mixture was stirred at room temperature for 6 h, followed by removal of all volatiles in vacuum. The residue was suspended in 20 mL of *n*-hexane and the solution was filtered. The filtrate was concentrated to dryness in vacuum, the product was washed with cold *n*-hexane and dried in vacuum.

Yield: 425 mg (74%).

Mp.: 105 °C.

EA: Anal. calcd For $C_{35}H_{44}N_2Ti$: C, 77.76; H, 8.20; N, 5.18. Found: C, 77.57; H, 8.30; N, 5.09.

NMR: ^{1}H (300 MHz, benzene-d_6): δ = 7.07 (d, ^3J = 7.5 Hz, 2H), 6.98 (t, ^3J = 6.9 Hz, 1H), 6.66 (d, ^3J = 7.8 Hz, 2H), 6.76 (t, ^3J = 7.5 Hz, 1H), 5.99 (s, 10H),

3.86 (p, ^3J = 6.0 Hz, 1H), 3.53 (p, ^3J = 6.0 Hz, 1H), 1.26 (d, ^3J = 6.0 Hz, 12H); 1.15 (d, ^3J = 6.0 Hz, 12H). ^{13}C: (100 MHz, benzene-d_6): δ = 158.4, 145.5, 133.9, 130.8, 123.9, 122.4, 117.2, 107.8, 30.1, 27.6, 24.6, 22.9.

IR: (16 scans): 3062 (vw), 2957 (m), 2925 (w), 2864 (w), 2160 (m), 2028 (vw), 1926 (w), 1619 (vw), 1582 (w), 1458 (w), 1435 (w), 1412 (m), 1384 (w), 1343 (m), 1284 (w), 1258 (w), 1181 (w), 1138 (vw), 1096 (w), 1058 (w), 1016 (w), 935 (w), 780 (vs), 746 (s), 734 (s), 621 (s), 538 (s), 464 (m), 436 (m).

MS: (CI) 540 $[M]^+$.

5.3.4. Synthesis of Cp*$_2$Ti=N−Dipp (14b):

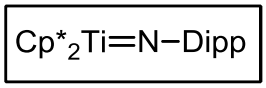

The alkyne complex Cp*$_2$Ti(η^2-Me$_3$SiC$_2$SiMe$_3$) (**3-Ti**) (276 mg, 0.57 mmol) was dissolved in 15 mL of toluene and a solution of the carbodiimide **10-Dipp-Dipp** (205 mg, 1.57 mmol) in 15 mL of toluene was added dropwise at room temperature. The mixture was stirred at room temperature for 2 h, followed by warming to 100 °C for 24 h. During this time the colour changed to bright red. The volatiles were removed in vacuum and the residue was dissolved in 8 mL of hot toluene. Red crystals of complex **14b** were obtained at room temperature.

Yield: 252 mg (66%).

Mp.: 126 °C (dec.).

EA: Anal. calcd for $C_{32}H_{47}NTi$: C, 77.87; H, 9.60; N, 2.84. Found: C, 74.16; H, 9.39; N, 3.32.

NMR: ^{1}H (300 MHz, benzene-d_6): δ = 7.05 (m, 3H), 3.65 (p, ^3J = 6.0 Hz, 1H), 1.86 (s, 10H), 1.33 (d, ^3J = 6.0 Hz, 12H). ^{13}C (100 MHz, benzene-d_6): δ = 143.0, 125.5, 124.1, 123.7, 114.1, 29.5, 23.4, 12.2.

IR: (16 scans): 2960 (m), 2907 (m), 2867 (w), 2164 (vs), 1629 (vw), 1584 (w), 1435 (s), 1409 (w), 1378 (m), 1362 (w), 1323 (m), 1255 (m), 1181 (m), 1096 (m), 1059 (w), 1021 (w), 934 (m), 791 (s), 745 (vs), 596 (m), 552 (m), 519 (m), 396 (s).

MS: (EI) 493 $[M]^+$, 178 $[Cp_2Ti]^+$.

5.3.5. Synthesis of $Cp^*_2Ti(Cl)N=C=C(H)(Mes)$ (15):

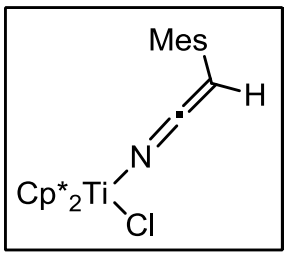

Into a solution of mesitylacetonitrile (271 mg, 1.70 mmol) in 10 mL of THF was dropped a solution of *n*-butyllithium in *n*-hexane (1.12 mL, 1.6 M) and the reaction mixture stirred for 4 h at room temperature. After cooling to -78 °C, the reaction mixture was slowly dropped into a cooled (-78 °C) suspension of $Cp^*_2TiCl_2$ (**7**) (663 mg, 1.70 mmol) in 10 mL of THF and stirred for additional 2 hours at -78 C. While warming up to room temperature, the colour turned to dark blue. Subsequent removing of all volatiles in vacuum resulted in a dark blue residue, which was suspended in 20 mL of toluene and filtered. After concentration to 10 mL, the suspension is filtered again and the resulting dark blue solution is concentrated to dryness, washed with cold *n*-hexane and dried in vacuum. Crystals, suitable for X-ray analysis were obtained from a saturated solution of *n*-hexane at -78 °C.

Yield: 563 mg (65 %).

Mp.: 163 °C (dec.).

EA: Anal. calcd. for $C_{31}H_{42}ClNTi$: C, 72.72; H, 8.27; N, 2.74. Found: C, 72.57; H, 8.16; N, 2.81.

NMR: ^1H (300 MHz, benzene-d_6): δ = 6.92 (s, 2H, Mes), 3.81 (s, 1H, CH), 2.55 (s, 6H, Mes), 2.23 (s, 3H, Mes), 1.76 (s, 30H, Cp*). ^{13}C (75 MHz, benzene-d_6): δ = 171.9 (N*C*C), 135.4, 133.0, 132.9, 129.0 (Mes), 123.5 (Cp*), 43.2 (CH), 22.0 (Mes), 21.1 (Mes), 12.2 (Cp*).

IR: (16 scans): 2962 (vw), 2905 (vw), 2857 (vw), 2044 (vs), 1473 (m), 1458 (w), 1431 (w), 1419 (vw), 1374 (m), 1362 (w), 1116 (m), 1017 (m), 848 (m), 787 (w), 724 (w), 633 (w), 598 (m), 541 (m), 493 (vs), 458 (s), 426 (s), 419 (s), 408 (s).

MS: (CI) 512 $[M+H]^+$, 477 $[M-Cl]^+$, 318 $[Cp^*_2Ti]^+$.

5.3.6. Reaction of 15 with *n*-Butyllithium:

15 (55 mg, 0.11 mmol) was dissolved in 4 mL of toluene and cooled to -78 °C. Under stirring, a solution of *n*-butyllithium in *n*-hexane (74 µL, 1.6 M) was slowly dropped into

the reaction mixture. After additional stirring at -78 °C for 4 hours, the reaction mixture was warmed to room temperature, changing the colour from dark blue to brown. After filtration, the solution was concentrated to 2 mL and stored at -78 °C. The resulting paramagnetic brown precipitate was investigated by EPR spectroscopy, showing a variety of different products. No desired product could be isolated.

5.3.7. Synthesis of [$Cp_2Zr(\kappa^1$-*N*,*N*'-N=C=C(Mes)-C(CH_2Mes)=N-]$_2$ (16):

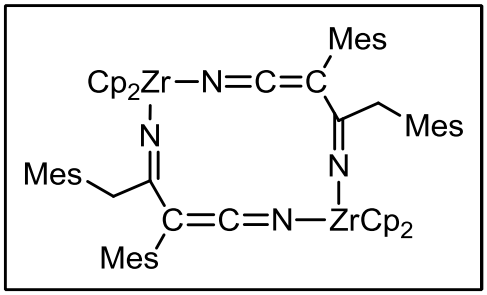

Into a solution of mesitylacetonitrile (324 mg, 2.03 mmol) in 15 mL of THF was dropped a solution of *n*-butyllithium in *n*-hexane (1.40 mL, 1.6 M) and the reaction mixture stirred for 4 h at room temperature. After cooling to -78 °C, the reaction mixture was slowly dropped into a cooled (-78 °C) suspension of Cp_2ZrCl_2 (**6-Zr**) (397 mg, 1.02 mmol) in 10 mL of THF and stirred for additional 2 hours at -78 C. While warming up to room temperature, the colour turned from slight yellow to dark red. Subsequent removing of all volatiles in vacuum resulted in a dark red residue, which was suspended in 20 mL of toluene and filtered. After concentration to 10 mL, the resulting dark red solution is stored at +8 °C for several months, yielding yellow crystals, suitable for X-ray analysis, which were filtered and dried in vacuum.

Yield: 489 mg (45 %).

Mp.: 180 °C (dec.).

Unfortunately, due to decomposition in the solid state, no suitable elemental analysis could be performed.

NMR: ^{1}H (300 MHz, benzene-d_6): δ = 6.96 (s, 4H, Mes), 6.79 (s, 4H, Mes), 5.77 (s, 20H, Cp), 3.20 (s, 4H, CH_2), 2.61 (s, 12H, Mes), 2.30 (s, 12H, Mes), 2.20 (s, 6H, Mes), 2.18 (s, 6H, Mes). ^{13}C (75 MHz, benzene-d_6): δ = 175.9, 147.8, 139.5, 137.2, 136.5, 135.2, 133.9, 133.4, 129.1, 128.8, 109.8 (Cp), 63.7, 37.1, 21.3, 21.1 21.0.

IR: (16 scans): 3466 (w), 3318 (w), 3101 (w), 2961 (w), 2913 (w), 2855 (w), 2132 (m), 1437 (m), 1260 (m), 1092 (m), 1012 (vs), 849 (m), 792 (vs), 740 (s), 710 (s), 607 (w).

MS: (CI) 1072 $[M]^+$, 939 $[M\text{-}CH_2Mes]^+$.

5.3.8. Synthesis of $Cp^*_2Ti(\kappa^1$-*N*-pyrrolato[2,3-b]pyridine)) (19):

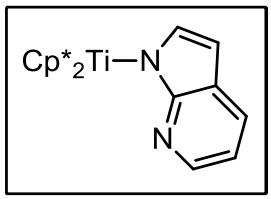

To a stirred solution of $Cp^*_2Ti(\eta^2\text{-}Me_3SiC_2SiMe_3)$ (**3-Ti**) (1,00 g, 2.05 mmol) in 10 mL of toluene was added a solution of 7-azaindole (247 mg, 2.09 mmol) in 10 ml of toluene. After stirring the reaction mixture for 8 hours at room temperature, the colour turned from light brown to dark red. All volatiles were removed in vacuum and the resulting dark red residue was suspended in 30 mL of a *n*-hexane and filtered. The dark red solution was stored at -40 °C for 3 days to give dark red crystals which were filtered, washed with 3 mL of cold *n*-hexane and dried in vacuum.

Yield: 754 mg (85 %).

Mp.: 156 °C (dec.).

EA: Anal. calcd. for $C_{27}H_{35}N_2Ti$: C, 74.47; H, 8.10; N, 6.43. Found: C, 74.37; H, 8.17; N, 6.28.

IR: (16 scans): 3030 (vw), 2856 (vw), 2719 (vw), 1729 (vw), 1584 (w), 1552 (vw), 1454 (w), 1288 (w), 1260 (vw), 1197 (vw), 1151 (w), 1111 (vw), 1061 (w), 1024 (w), 951 (vw), 928 (w), 899 (w), 873 (vw), 794 (w), 774 (s), 719 (s), 636 (m), 595 (w), 561 (w), 546 (vw), 457 (s), 435 (vs), 407 (s), 391 (s).

MS: (EI) 435 $[M]^+$, 300 $[M\text{-}Cp]^+$, 155 $[M\text{-}Cp\text{-}L]^+$, 118 $[L]^+$.

5.3.9. Synthesis of $Cp_2Ti(\kappa^2$-*N*,*N*-2-(*t*-Bu)-pyrrolato[2,3-b]pyridine) (20):

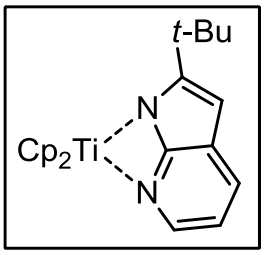

Into a stirred solution of 2-*t*-Bu-1H-pyrrrolo[2,3-B]pyridine (505 mg, 2.90 mmol) in 20 mL of THF was dropped a solution of *n*-butylethylmagnesium in THF (1.7 mL, 0.9 M). After stirring for 16 hours at room temperature, the reaction mixture was added to a slurry of $(Cp_2TiCl)_2$ (**5**) in 15 mL of THF. Additional stirring for 3 hours and subsequent removal of all volatiles in vacuum resulted in a dark green precipitate which was suspended in 30 mL of toluene and filtered. The dark green solution was concentrated in vacuum to 4 mL and stored at -78 °C for 5 days, yielding the dark green product, which was filtered and dried in vacuum. Crystals, suitable for X-ray analysis, were obtained from a saturated solution of *n*-hexane at -40 °C after 14 days.

Yield: 898 mg (88 %).

Mp.: 117 °C (dec.).

EA: Anal. calcd. for $C_{21}H_{23}N_2Ti$: C, 71.89; H, 6.60; N, 7.97. Found: C, 71.92; H, 6.50; N, 7.61.

IR: (16 scans): 3209 (w), 3128 (w), 2960 (m), 2909 (w), 2862 (w), 1601 (vw), 1583 (w), 1540 (vw), 1491 (w), 1438 (m), 1353 (w), 1326 (vw), 1293 (m), 1276 (s), 1222 (w), 1209 (w), 1194 (m), 1124 (vw), 1113 (w), 1064 (vw), 1011 (m), 976 (vw), 901 (vw), 787 (vs), 766 (vs), 752 (vs), 701 (s), 665 (m), 628 (s), 563 (m), 419 (w).

MS: (EI) 351 $[M]^+$, 286 $[M\text{-}Cp]^+$, 178 $[Cp_2Ti]^+$.

5.3.10. Synthesis of $Cp_2Hf(Cl)[\kappa^2$-*N*,*P*-$N(PPh_2)_2]$ (21-Hf):

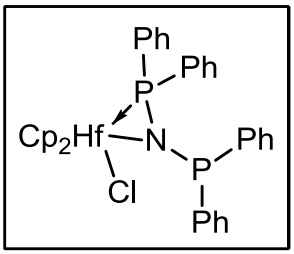

To a stirred solution of *N*,*N*-bis(diphenylphosphino)amine (410 mg, 1.06 mmol) in 20 mL of THF was added a 2.5 M solution of *n*-butyllithium in hexane (0.47 mL, 1.17 mmol) at room temperature. After stirring the reaction mixture for 2 hours, the colour turned to light yellow. The mixture was dropped slowly into a solution of Cp_2HfCl_2 (**6-Hf**) (404 mg,

1.06 mmol) in 15 mL of THF. After stirring for 3 days, all volatiles were removed in vacuum and the yellow residue was suspended in 40 mL of toluene, filtered and concentrated to a volume of 4 mL in vacuum. The precipitated product was dissolved at 80 °C. Slow cooling to room temperature yields colourless crystals, suitable for X-ray analysis, which were filtered, washed with cold toluene and dried in vacuum. The mother liquor was cooled to -78 °C to complete crystallization.

Overall yield: 695 mg (90%).

Mp.: 153 °C (dec.).

EA: Anal. calcd. for $C_{34}H_{30}ClHfNP_2$: C, 56.06; H, 4.12; N, 1.92. Found: C, 56.08; H, 4.15; N, 2.06.

NMR: ^{1}H (300 MHz, benzene-d_6): δ = 7.92 (t, ^{3}J = 7.5 Hz, 8H, Ph), 7.07 (m, 12H, Ph), 5.78 (t, ^{3}J = 8.4 Hz, 10H, Cp). ^{13}C (75 MHz, benzene-d_6): δ = 133.16 – 128.79 (Ph), 110.62 (s, Cp). $^{31}P\{^{1}H\}$ (121 MHz, benzene-d_6): δ = 60.26, -4.72.

IR: (16 scans): 3052 (vw), 3015 (vw), 2998 (vw), 1582 (vw), 1478 (vw), 1432 (w), 1309 (vw), 1181 (vw), 1092 (w), 1067 (vw), 1026 (vw), 1014 (w), 999 (w), 964 (m), 820 (m), 743 (m), 715 (s), 694 (vs), 672 (s), 616 (w), 522 (m), 493 (m), 466 (m), 431 (w).

MS: (CI) 730 $[M+H]^+$.

5.3.11. Synthesis of $Cp_2Ti(Cl)(\eta^1\text{-}Ph_2P\text{-}N(H)\text{-}PPh_2)$ (22):

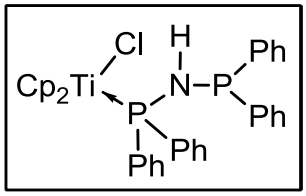

To a stirred solution of $(Cp_2TiCl)_2$ (**5**) (269 mg, 0.63 mmol) in 10 mL of THF was added a solution of *N*,*N*-bis(diphenylphosphino)amine (520 mg, 1.35 mmol) in 15 ml of THF. While the reaction mixture was stirred at 50 °C for 16 hours, its colour turned to dark green. After cooling to room temperature, the solvent was removed in vacuum. The dark green residue was dried in vacuum. Crystals suitable for X-ray analysis were grown from a saturated toluene solution at 8 °C.

Yield: 720 mg (95%).

Mp.: 139 °C (dec.).

EA: Anal. calcd. for $C_{34}H_{31}ClNP_2Ti$: C, 68.19; H, 5.22; N, 2.34. Found: C, 68.22, H, 5.31; N, 2.49.

IR: (16 scans): 3246 (vw), 3047 (w), 2983 (vw), 1480 (vw), 1433 (m), 1260 (w), 1182 (w), 1123 (vw), 1093 (w), 1066 (w), 1019 (w), 1009 (w), 883 (m), 814 (m), 799 (s), 745 (s), 732 (s), 690 (vs), 591 (m), 550 (s), 530 (s), 510 (vs), 492 (s), 467 (s), 434 (m), 397 (s).

MS: (CI) 599 $[M]^+$, 563 $[M\text{-}Cl]^+$.

5.3.12. Synthesis of $Cp_2Ti(\kappa^2\text{-}P,P\text{-}Ph_2P\text{-}N\text{-}PPh_2)$ (23-Ti):

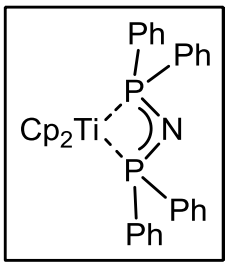

From $Cp_2Ti(\eta^2\text{-}Me_3SiC_2SiMe_3)$ (1):

To a stirred solution of $Cp_2Ti(\eta^2\text{-}Me_3SiC_2SiMe_3)$ (**1**) (542 mg, 1.56 mmol) in 10 mL of toluene was added a solution of *N*,*N*-bis(diphenylphosphino)amine (628 mg, 1.63 mmol) in 10 ml of toluene. After stirring the reaction mixture for 3 days at 85 °C, the colour turned from light brown to dark brown. The mixture was cooled to room temperature and all volatiles were removed in vacuum. The dark brown residue was dissolved in 20 mL of a mixture of THF/*n*-hexane (3:1) and stored at -30 °C for 3 days to give dark green crystals which were filtered, washed with 3 mL of cold *n*-hexane and dried in vacuum. Crystals suitable for X-ray analysis were obtained from a saturated solution of THF at 8 °C.

Yield: 746 mg (85%).

From $(Cp_2TiCl)_2$ (5):

To a stirred solution of $(Cp_2TiCl)_2$ (**5**) (245 mg, 0.574 mmol) in 10 mL of THF was added a solution of $(thf)_3Li[N(PPh_2)_2]$ (442 mg, 1.15 mmol) in 10 mL of THF. The reaction mixture was stirred at 50 °C for 8 hours. After cooling to room temperature, the solvent was removed in vacuum. The dark green residue was suspended in 20 mL of toluene and filtered. All volatiles were removed in vacuum and the green precipitate was dried in vacuum.

Yield: 716 mg, (95%).

From $Cp_2Ti(Cl)(\eta^1\text{-}Ph_2P\text{-}N(H)\text{-}PPh_2)$ (22):

To a stirred solution of **22** (152 mg, 0.254 mmol) in 10 mL of THF was added a 1.6 M solution of *n*-butyllithium in hexane (0.24 mL, 0.38 mmol). The light green solution turned dark green immediately. The solvent was removed in vacuum and the dark green residue was suspended in 20 ml of toluene and filtered. All volatiles were removed in vacuum and the dark green precipitate was dried in vacuum.

Yield: 122 mg (85%).

Mp.: 111 °C (dec.).

EA: Anal. calcd. for $C_{34}H_{30}NP_2Ti \cdot THF$: C, 71.93; H, 6.04; N, 2.21. Found: C, 72.03; H, 6.04; N, 2.27.

IR: (16 scans): 2921 (vs), 1789 (m), 1585 (s), 1464 (vs), 1377 (vs), 1303 (s), 1179 (m), 1154 (m), 1092 (s), 1073 (s), 1010 (s), 967 (vs), 806 (vs), 754 (s), 737 (s), 694 (vs), 542 (s), 525 (s), 484 (s), 450 (w), 415 (w), 379 (s).

MS: (EI) 562 $[M]^+$, 385 $[M\text{-}Cp_2Ti]^+$, 377 $[M\text{-}PPh_2]^+$, 178 $[Cp_2Ti]^+$.

5.3.13. Synthesis of $Cp_2Zr(\kappa^2\text{-}P,P\text{-}Ph_2P\text{-}N\text{-}PPh_2)$ (23-Zr):

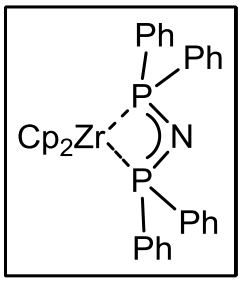

Complex **21-Zr** (126 mg, 0.197 mmol) and magnesium (5 mg, 0.206 mmol) were suspended in 10 mL of THF and heated to 50 °C for 3.5 hours. The colour slowly changed from pale yellow to orange and later to dark brown. After cooling to room temperature, all volatiles were removed in vacuum and the dark brown precipitate was suspended in 20 mL of toluene and filtered. The solution was concentrated to 10 mL and stored at -78 °C to give dark orange crystals of **23-Zr**, suitable for X-ray analysis, which were filtered, washed with cold toluene and dried in vacuum.

Yield: 65 mg (55 %).

Mp.: 146 °C (dec.).

EA: Anal. calcd. for $C_{34}H_{30}NP_2Zr$: C, 67.41; H, 4.99; N, 2.31. Found: C, 66.18; H, 5.28; N, 2.17.

IR: (16 scans): 3393 (w), 3049 (vw), 1631 (vw), 1573 (w), 1476 (vw), 1432 (w), 1303 (vw), 1179 (vw), 1094 (w), 1067 (vw), 1013 (w), 967 (m), 882 (w), 793 (s), 735 (s), 693 (vs), 539 (s), 520 (s), 502 (s), 479 (s).

MS (EI) 604 $[M]^+$, 385 $[M\text{-}Cp_2Ti]^+$, 262 $[M\text{-}NPPh_2]^+$.

5.3.14. Reaction of $Cp_2Hf(Cl)[\kappa^2\text{-}N,P\text{-}N(PPh_2)_2]$ (21-Hf) with Mg to $Cp_2Hf(H)[\kappa^2\text{-}N,P\text{-}N(PPh_2)_2]$ (24):

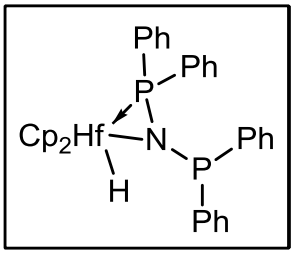

Complex **21-Hf** (448 mg, 0.615 mmol) and magnesium (15 mg, 0.615 mmol) were suspended in 10 mL of THF and stirred for 3 days. The colour slowly changed from pale yellow to dark purple. After removing all volatiles in vacuum, the dark purple precipitate was suspended in 20 mL of toluene and filtered. The solution was concentrated to 10 mL and stored at -78 °C for 3 days. The resulting purple precipitate was filtered and re-dissolved in a mixture of 5 mL of THF and 15 mL *n*-hexane and stored at -40 °C for another 5 days do give a pale yellow precipitate which was filtered again and dissolved in 2 mL of toluene. Storage for one week at -78 °C yielded few colourless crystals of **24**, suitable for X-ray analysis, which were filtered, washed with cold toluene and dried in vacuum.

Yield: 13 mg (3 %).

Unfortunately, due to the low yield, no melting point, elemental analysis or IR spectroscopy could be performed.

NMR: ^1H (300 MHz, benzene-d_6): δ = 8.31 (d, ^2J = 7.1 Hz, 1H), 7.90 (t, ^3J = 7.0 Hz, 2H), 7.75 (t, ^3J = 7.0 Hz, 2H), 7.38-7.30 (m, 4H), 7.25-7.16 (m, 4H), 7.07-6.99 (m, 8H), 5.51 (d, ^2J = 0.9 Hz, 10H). $^{31}P\{^1H\}$ (121 MHz, benzene-d_6): δ = -40.29. Due to the low concentration of the sample, no ^{13}C spectrum could be obtained.

MS: (CI) 386 $[M\text{-}Cp_2Hf]^+$, 245 $[CpHf]^+$.

5.3.15. Synthesis of $Cp_2Ti(\kappa^2$-*P*,*P*-Ph_2P-C(H)-$PPh_2)$ (25a)

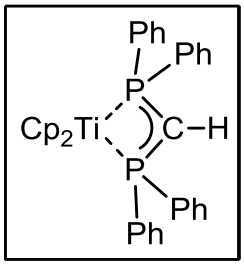

To a stirred solution of Ph_2P-CH_2-PPh_2 (720 mg, 1.87 mmol) in 15 mL of THF, a solution of *n*-butyllithium in *n*-hexane (1.6 M, 1.40 mL, 2.25 mmol) was added dropwise at -78 °C. While stirring for one hour, the reaction mixture slowly turned to light yellow. After warming up the solution to room temperature, the mixture was dropped slowly into a solution of $[(Cp_2TiCl)_2]$ (**5**) (400 mg, 0.94 mmol) in 20 mL of THF. After stirring overnight, all volatiles were removed in vacuum and the dark blue residue was suspended in 30 mL of toluene, filtered and concentrated to 10 mL in vacuum. The already precipitated product was dissolved at 80 °C. Slowly cooling to room temperature gave dark blue crystals, suitable for X-ray diffraction analysis, which were filtered, washed with cold toluene and dried in vacuum. The mother liquor was cooled to -78 °C and stored for 3 days to complete crystallization.

Overall Yield: 957 mg (91%).

Mp.: 249 °C (dec.).

EA: Anal. calcd. for $C_{35}H_{31}P_2Ti$: C, 74.87; H, 5.87. Found: C, 74.55; H, 5.57.

IR: (16 scans): 3066 (vw), 3045 (vw), 2998 (vw), 1583 (vw), 1476 (w), 1432 (m), 1304 (vw), 1184 (vw), 1122 (m), 1091 (w), 1014 (w), 895 (m), 863 (w), 795 (s), 750 (m), 734 (s), 692 (vs), 558 (s), 531 (vs), 515 (vs), 470 (m), 443 (m), 412 (m).

MS: (CI) 562 $[M+H]^+$, 561 $[M]^+$.

5.3.16. Synthesis of $Cp_2Ti(\kappa^2$-*P*,*P*-Ph_2P-C($SiMe_3$)-$PPh_2)$ (25b)

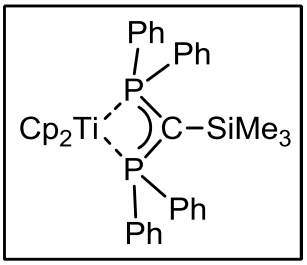

From $Cp_2Ti(\eta^2$-$Me_3SiC_2SiMe_3)$ (1):

To a stirred solution of $Cp_2Ti(\eta^2$-$Me_3SiC_2CSiMe_3)$ (**1**) (500 mg, 1.43 mmol) in 10 mL of *n*-hexane was added a slurry of Ph_2P-$CH(SiMe_3)$-PPh_2 (655 mg, 1.43 mmol) in 15 mL of *n*-hexane. While stirring the reaction mixture for 3 days at 65 °C, the colour turned from light brown to dark green. After cooling to RT, the mixture was

filtered and then all volatiles were removed in vacuum resulting in a dark green precipitate of **25b** which was dried in vacuum.

Yield: 817 mg (90 %).

From $(Cp_2TiCl)_2$ (5):

To a stirred solution of Ph_2P-CH($SiMe_3$)-PPh_2 (702 mg, 1.54 mmol) in 15 mL of THF, a solution *n*-butyllithium in hexane (1.6 M, 1.06 mL, 1.69 mmol) was added dropwise at -78 °C. While stirring for one hour, the reaction mixture slowly turned to light yellow. After warming up the solution to room temperature, the mixture was dropped slowly into a solution of $(Cp_2TiCl)_2$ (**5**) (328 mg, 0.77 mmol) in 15 mL of THF. After stirring overnight, all volatiles were removed in vacuum and the dark green residue was suspended in 35 mL of *n*-hexane, filtered and concentrated to 5 mL in vacuum. The mixture was filtered again and the dark green precipitate was washed with cold *n*-hexane and dried in vacuum.

Yield: 725 mg (74 %).

Mp.: 205 °C (dec.).

EA: Anal. calcd. for $C_{38}H_{39}P_2SiTi$: C, 72.03; H, 6.20. Found: C, 71.91; H, 6.26.

IR: (16 scans): 3052 (vw), 2947 (vw), 2894 (vw), 1584 (vw), 1478 (vw), 1434 (w), 1244 (w), 1182 (w), 1113 (w), 1015 (w), 895 (m), 921 (m), 837 (m), 791 (s), 737 (s), 691 (vs), 500 (vs), 473 (vs).

MS: (EI) 633 $[M]^+$, 178 $[Cp_2Ti]^+$.

5.3.17. Synthesis of $Cp_2Zr(H)(\kappa^2$-*P*,*P*-Ph_2P-C(H)-$PPh_2)$ (26):

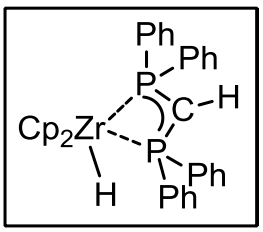

To a stirred solution of Ph_2P-CH_2-PPh_2 (384 mg, 1.00 mmol) in 10 mL of THF, a solution *n*-butyllithium in *n*-hexane (1.6 M, 0.75 mL, 1.20 mmol) was added dropwise at -78 °C. While stirring for one hour, the reaction mixture slowly turned to light yellow. After warming up to room temperature, the mixture was stirred for 16 h. Then, it was slowly dropped into a solution of $Cp_2Zr(H)Cl$ (**8**) (258 mg, 1.00 mmol) in 5 mL of THF at -40 °C. Stirring overnight and

warming up to room temperature again yielded a pale yellow solution. All volatiles were removed in vacuum and the yellow precipitate was suspended in 20 mL of toluene and filtered and concentrated to a volume of 7 mL. After 3 days at room temperature, pale yellow crystals precipitated which were filtered, washed with cold toluene and dried in vacuum. The mother liquor was cooled to -78 °C to complete crystallization.

Overall yield: 454 mg (75 %).

Mp.: 189 °C (dec.).

EA: Anal. calcd. for $C_{35}H_{32}P_2Zr$: C, 69.28; H, 5.48. Found: C, 69.30; H, 5.25.

NMR: ^{1}H (300 MHz, benzene-d_6): δ = 8.15 (t, ^3J = 8.5 Hz, 4H, Ph), 7.89 (t, ^3J = 8.3 Hz, 4H, Ph), 7.27-7.17 (m, 8H, Ph), 7.10-7.01 (m, 4H, Ph), 5.31 (d, ^3J(H-P) = 0.9 Hz, 10H, Cp), 3.15 (ddd, ^2J(H-P^1) = 73 Hz, ^2J(H-P^2) = 24 Hz, ^4J(H-H) = 2.3 Hz, 1H, ZrH), 2.68 (td, ^2J(H-P) = 4.7 Hz, ^4J(H-H) = 2.3 Hz), 1H, CH). ^{13}C (75 MHz, benzene-d_6): δ = 145.0, 144.8, 144.6, 144.4, 130.8 (dd, ^2J(C-P) = 22.5 Hz, ^2J(C-P) = 9,1 Hz), 120.6, 20.6 (dd, ^1J(C-P)=54 Hz, ^1J(C-P)=50 Hz). ^{31}P{^{1}H} (121 MHz, benzene-d_6): δ = -14.16 (d, ^2J = 144Hz), -16.46 (d, ^2J = 144Hz).

IR: (16 scans): 3067 (w), 3047 (m), 2982 (w), 1476 (m), 1432 (s), 1128 (m), 1087 (m), 1011 (m), 891 (s), 874 (m), 809 (vs), 749 (s), 735 (s), 691 (vs), 589 (vs), 529 (vs), 513 (vs), 468 (s), 455 (s), 439 (s).

MS: (EI) 603 $[M]^+$, 384 $[M\text{-}Cp_2Zr]^+$, 220 $[Cp_2Zr]$.

5.3.18. Synthesis of $Cp_2Hf(Cl)(\kappa^2\text{-}P,P\text{-}Ph_2P\text{-}C(H)\text{-}PPh_2)$ (27a):

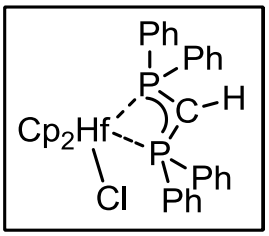

To a stirred solution of $Ph_2P\text{-}CH_2\text{-}PPh_2$ (393 mg, 1.02 mmol) in 20 mL of THF a solution of *n*-butyllithium in *n*-hexane (2.5 M, 0.45 mL, 1.12 mmol) was added dropwise at room temperature. After stirring for 1 h, the reaction mixture turned yellow. It was then dropped slowly into a solution of Cp_2HfCl_2 (**6-Hf**) (388 mg, 1.02 mmol) in 15 mL of THF. After stirring for 3 days, all volatiles were removed in vacuum. The bright yellow residue was twice suspended in 15 mL of toluene and filtered. The combined solutions were concentrated to a volume of

10 mL, the yellow precipitate dissolved at elevated temperature (80°C). After cooling the reaction mixture slowly to room temperature, yellow crystals, suitable for X-ray analysis were obtained. These were filtered, washed with cold toluene and dried in vacuum. The mother liquor was stored at -78 °C to complete crystallization.

Overall yield: 503 mg (68 %).

Mp.: 170 °C (dec.).

EA: Anal. calcd. for $C_{35}H_{31}P_2ClZr$: C, 57.70; H, 4.43. Found: C, 57.70; H, 4.35.

NMR: ^{1}H (300 MHz, benzene-d_6): δ = 8.25 (t, ^3J=8.0 Hz, 4H, Ph), 7.78 (t, ^3J=7.5 Hz, 4H, Ph), 7.47-7.42 (m, 2H, Ph), 7.25 (t, ^3J=7.3 Hz, 4H, Ph), 7.11-7.02 (m, 8H, Ph), 5.68 (t, ^3J(H-P) = 1.2 Hz, 10H, Cp), 2.58 (t, ^2J(H-P) = 4.2 Hz, 1H, CH). ^{13}C (75 MHz, benzene-d_6): δ = 144.2, 133.3, 128.7, 128.6, 128.2, 127.8, 111.1 (Cp), 44.3 (CH). ^{31}P{^{1}H} (121 MHz, benzene-d_6): δ = -4.55 (d, ^2J = 235 Hz), -10.57 (d, ^2J = 235 Hz).

IR: (16 scans): 3131 (vw), 3059 (vw), 3045 (vw), 2961 (vw), 1582 (vw), 1478 (w), 1432 (m), 1365 (vw), 1306 (vw), 1261 (w), 1184 (vw), 1132 (w), 1090 (m), 1024 (m), 1009 (m), 908 (m), 815 (vs), 750 (s), 737 (vs), 693 (vs), 619 (w), 597 (vs), 531 (s), 509 (s), 471 (m), 459 (m), 443 (m).

MS: (EI) 603 $[M]^+$, 384 $[M\text{-}Cp_2Zr]^+$, 220 $[Cp_2Zr]$.

5.3.19. Synthesis of $Cp_2Hf(Cl)(\kappa^2\text{-}P,P\text{-}Ph_2P\text{-}C(SiMe_3)\text{-}PPh_2)$ (27b):

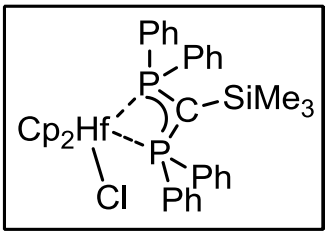

To a stirred solution of $Ph_2P\text{-}CH(SiMe_3)\text{-}PPh_2$ (434 mg, 0.95 mmol) in 15 mL of THF, a solution *n*-butyllithium in hexane (2.5 M, 0.42 mL, 1.05 mmol) was added dropwise at RT. While stirring for two hours, the reaction mixture slowly turned to pale yellow. Then, the reaction mixture was dropped slowly into a solution of Cp_2HfCl_2 (**6-Hf**) (361 mg, 0.95 mmol) in 15 mL of THF. After stirring for three days, all volatiles were removed in vacuum and the pale yellow residue was suspended in 35 mL of hexane, filtered and concentrated to 5 mL in vacuum. The product is filtered from the solution, washed with cold toluene and dried in vacuum.

Yield: 546 mg (72 %).

Mp.: 278 °C (dec.).

EA: Anal. calcd. for $C_{38}H_{39}ClP_2SiHf$: C, 57.07; H, 4.92. Found: C, 57.10; H, 5.04.

NMR: ^{1}H (300 MHz, benzene-d_6): δ = 8.17 (t, ^3J=8.3 Hz, 4H, Ph), 7.95 (t, ^3J=7.8 Hz, 4H, Ph), 7.31-7.20 (m, 8H, Ph), 7.12-7.10 (m, 2H, Ph), 5.58 (dd, ^3J(H-P^1) = 1.5 Hz, ^3J(H-P^2) = 0.7 Hz, 10H, Cp), 0.13 (s, 9H, $SiMe_3$). ^{13}C (75 MHz, benzene-d_6): δ = 141.3, 134.2, 132.4, 129.3, 128.9, 128.5, 128.2, 127.9, 127.8, 125.6, 125.3, 111.0 (Cp), 3.9 ($SiMe_3$). The P*C*P signal was not found. ^{31}P{^{1}H} (121 MHz, benzene-d_6): δ = 10.41 (d, ^2J = 219 Hz), 7.88 (d, ^2J = 219 Hz).

IR: (16 scans): 3050 (w), 3002 (w), 2895 (vw), 2961 (vw), 1435 (w), 1430 (m), 1250 (w), 1240 (m), 1091 (w), 1069 (vw), 1023 (w), 1017 (w), 1003 (s), 944 (vs), 842 (m), 826 (s), 815 (vs), 806 (vs), 749 (s), 740 (vs), 732 (s), 694 (vs), 637 (w), 532 (w), 512 (m), 493 (s), 478 (m), 465 (s).

MS: (CI) 800 $[M]^+$.

5.3.20. Reaction of $Cp_2Hf(Cl)(\kappa^2$-*P*,*P*-Ph_2P-C(H)-PPh_2) (27a) with *t*-Butyllithium:

To a stirred solution of **27a** (200 mg, 0.275 mmol) in 10 mL of THF was added a solution of *t*-butyllithium (2.5 M, 0.18 mL, 0.300 mmol) in THF at -78 °C. After stirring for 1 h, the mixture was slowly warmed to room temperature while the colour turned from yellow to orange. After removing of all volatiles in vacuum, the orange residue was collected. NMR analysis did not reveal a desirable product.

5.3.21. Synthesis of $Cp^*_2Ti(\eta^2$-$Ph_2PC_2PPh_2$) (28):

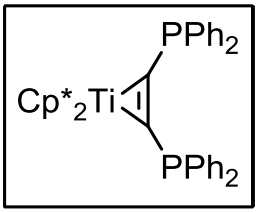

To a stirred solution of $Cp^*_2Ti(\eta^2$-$Me_3SiC_2SiMe_3$) (**3-Ti**) (662 mg, 1.35 mmol) in 10 ml of toluene was added a solution of

$Ph_2PC{\equiv}CPPh_2$ (534 mg, 1.35 mmol) in 10 ml of toluene. After stirring the reaction mixture for 24 h at 65 °C, the colour turned from light brown to dark green. The mixture was cooled to room temperature and all volatiles were removed in vacuum. The dark green residue was dissolved in 10 ml of *n*-hexane and stored at -78 °C for 3 days. The emerald green precipitate was filtered, washed with cold *n*-hexane and dried in vacuum. Crystals suitable for X-ray analysis were obtained from a saturated solution of *n*-hexane at room temperature.

Yield: 761 mg (79 %).

Mp.: 159 °C (dec.).

EA: Anal. calcd. for $C_{46}H_{40}P_2Ti$: C, 77.52; H, 7.07. Found: C, 77.34; H, 7.02.

NMR: ^1H (300 MHz, benzene-d_6): δ = 7.05 – 6.97(m, 20H), 1.83 (s, 30H, Me). ^{13}C (75 MHz, benzene-d_6): δ = 213.39 (d, ^1J = 77.5 Hz), 140.37 (m), 133.93 (m), 129.28 (s), 127.83 (t, ^4J = 3.1 Hz); 124.98 (s,(Cp*), 13.29 (s, Me). $^{31}P\{^1H\}$ (121 MHz, benzene-d_6): δ = 7.14.

IR: (16 scans): 3048 (vw), 2980 (w), 2895 (w), 2721 (vw), 1582 (w), 1559 (vw), 1508 (vw), 1476 (w), 1430 (m), 1376 (w), 1270 (vw), 1153 (vw), 1088 (w), 1064 (w), 1023 (w), 797 (vw), 734 (s), 692 (vs), 655 (m), 597 (w), 558 (vs), 507 (m), 491 (s), 415 (s), 398 (m), 387 (m).

MS: (CI) 712 $[M]^+$, 527 $[M\text{-}PPh_2]^+$, 318 $[Cp^*_2Ti]^+$.

5.3.22. Synthesis of (ebthi)Ti(η²-$Ph_2PC_2PPh_2$) (29-Ti):

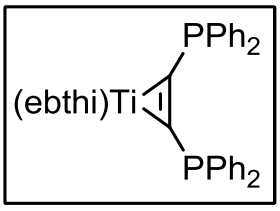

To a stirred solution of (ebthi)Ti(η²-$Me_3SiC_2SiMe_3$) (**4-Ti**) (210 mg, 0.44 mmol) in 10 ml of toluene was added a solution of $Ph_2PC{\equiv}CPPh_2$ (172 mg, 0.44 mmol) in 10 ml of toluene at -40 °C. After stirring for 1 h at -40 °C, the solution was allowed to warm up to room temperature and then heated for 3 days at 60 °C, turning the colour of the reaction mixture from brown to dark brown. After cooling to room temperature, all volatiles were removed in vacuum und the resulting dark brown precipitate was slurred in 20 ml of *n*-hexane and 7 ml of THF, filtered and stored at -78 °C for 7 days. The dark brown

precipitate was filtered again and the solution was stored at room temperature over night to give dark green crystals of **29-Ti**, which were filtered and dried in vacuum.

Yield: 201 mg (65 %).

Mp.: 142 °C (dec.).

EA: Anal. calcd. for $C_{46}H_{44}P_2Ti$: C, 78.18; H, 6.28. Found: C, 77.91; H, 6.63.

NMR: ^{1}H (300 MHz, benzene-d_6): δ = 7.53 – 7.49 (m, 4H, *o*-Ph), 7.45 (d, ^2J = 3.2 Hz, 2H, Cp), 7.19 – 7.46 (m, 6H, *m*-Ph, *p*-Ph), 6.93 – 6.89 (m, 6H *m*-Ph, *p*-Ph), 6.48- 6.44 (m, 4H, *o*-Ph), 4.60 (d, ^2J = 3.2 Hz, 2H, Cp), 3.93 – 3.91 (m, 2H), 3.24 – 3.20 (m, 2H), 2.33 – 2.29 (m, 4H, CH_2), 1.79 – 1.75 (m, 4H, CH_2), 1.45 – 1.42 (m, 4H, CH_2), 1.22 – 1.19 (m, 4H, CH_2). ^{13}C (75 MHz, benzene-d_6): δ = 213.81 (d, ^1J = 76.8 Hz), 142.24 (t, ^1J = 4.7 Hz), 138.51 (t, ^1J = 7.4 Hz), 129.28 (s), 135.73 (t, ^2J = 12.0 Hz), 132.11 (t, ^2J = 8.2 Hz), 129.65, 128.57, 127.86, 127.46 (t, J = 2.6 Hz), 126.96, 126.58, 126.12, 117.60, 113.68, 26.79, 25.98, 25.94, 23.86, 23.72, 23.02. ^{31}P{^{1}H} (121 MHz, benzene-d_6): δ = 2.06.

IR: (16 scans): 3066 (vw), 3044 (vw), 2915 (w), 2857 (w), 1653 (vw), 1581 (vw), 1551 (vw), 1474 (w), 1432 (m), 1372 (vw), 1300 (vw), 1280 (w), 1236 (vw), 1180 (vw), 1093 (w), 1064 (w), 1026 (w), 1000 (vw), 904 (w), 645 (vw), 814 (vw), 790 (s), 734 (s), 692 (vs), 656 (m), 640 (m), 568 (s), 215 (m), 496 (s), 475 (m), 437 (m), 422 (m), 400 (m).

MS: (EI) 264 [ebthi]$^+$, 185 [PPh_2]$^+$.

5.3.23. Synthesis of (ebthi)Zr(η^2-$Ph_2PC_2PPh_2$) (29-Zr):

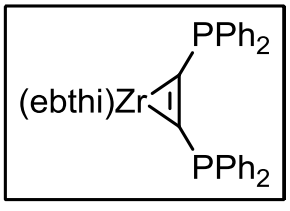

To a stirred solution of (ebthi)Zr(η^2-$Me_3SiC_2SiMe_3$) (**4-Zr**) (263 mg, 0.500 mmol) in 15 ml of toluene was added a solution of $Ph_2PC{\equiv}CPPh_2$ (197 mg, 0.500 mmol) in 10 ml of toluene at 25°C. After stirring for 6 h, the reaction mixture turned from grey to dark green. Additional 3 days of stirring lead to completion of the reaction. After removing of all volatiles in vacuum, the resulting dark green precipitate was dissolved in 10 ml of toluene and filtered. The dark green solution

was stored at -78 °C to yield a dark green precipitate after 3 days, which was filtered, washed with cold toluene and dried in vacuum. Crystals suitable for X-ray analysis were obtained from a saturated solution of toluene at room temperature.

Yield: 265 mg (71 %).

Mp.: 140 °C (dec.).

EA: Anal. calcd. for $C_{46}H_{44}P_2Zr$: C, 73.66; H, 5.91. Found: C, 73.61; H, 6.30.

NMR: ^{1}H (300 MHz, benzene-d_6): δ = 7.53 – 7.48 (m, 4H, *o*-Ph), 7.21 – 7.06 (m, 8H, Ph), 7.05 – 6.93 (m, 8H, Ph), 6.72 (d, ^2J = 6.0 Hz, 2H, Cp), 5.05 (d, ^2J = 6.0 Hz, 2H, Cp), 3.62 – 3.53 (m, 2H), 2.87 – 2.77 (m, 2H), 2.34 – 2.22 (m, 2H), 1.81 – 1.72 (m, 2H), 1.65 – 1.54 (m, 4H), 1.50 – 1.24 (m, 8H). ^{13}C (75 MHz, benzene-d_6): δ = 144.0, 135.3, 135.2, 132.6 (t, J = 8.1 Hz), 129.8, 128.9, 128.8, 126.7 (d, J = 4.2 Hz), 125.7, 125.3, 124.7, 111.9, 110.8, 27.1, 25.5, 24.0, 23.2. ^{31}P{^{1}H} (121 MHz, benzene-d_6): δ = 3.20.

IR: (16 scans): 3046 (w), 2915 (m), 2850 (w), 1582 (w), 1477 (w), 1430 (s), 1301 (w), 1274 (vw), 1178 (vw), 1090 (w), 1066 (w), 1025 (w), 999 (w), 905 (vw), 846 (vw), 817 (vw), 786 (s), 730 (s), 692 (vs), 662 (s), 578 (m), 531 (m), 505 (m), 486 (m), 462 (m).

MS: (EI) 749 $[M+H]^+$, 394 $[M\text{-}(ebthi)Zr]^+$, 264 $[(ebthi)]^+$.

5.3.24. Reaction of bis(diphenylphosphino)acetylene with $Cp_2Zr(py)(\eta^2\text{-}Me_3SiC_2SiMe_3)$ (2):

To a stirred solution of $Cp_2Zr(py)(\eta^2\text{-}Me_3SiC_2SiMe_3)$ (**2**) (350 mg, 0.743 mmol) in 15 ml of toluene was added a solution of $Ph_2PC{\equiv}CPPh_2$ (293 mg, 0.743 mmol) in 10 ml of toluene at -40 °C. While the reaction mixture was allowed to warm up to room temperature, the colour turned from grey to dark orange. After stirring for additional 18 h, all volatiles were removed in vacuum and the resulting dark orange precipitate was dissolved in 20 ml of toluene and filtered. The resulting solution was concentrated to ca. 10 ml and stored at -40°C to yield a dark yellow precipitate after 7 days, which was filtered, washed with cold toluene and dried in vacuum.

[$Cp_2Zr(\eta^2\text{-}Ph_2PC_2PPh_2)]_2$ (30a):

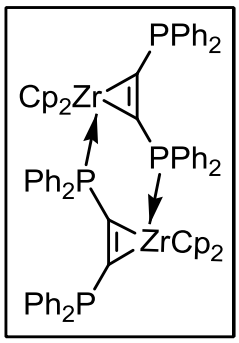

Crystals suitable for X-ray analysis were obtained from a saturated solution of toluene at room temperature.

Yield: 289 mg (63 %).

Mp.: 68 °C (dec.).

EA: Anal. calcd. for $C_{72}H_{60}P_4Zr_2 \cdot 2$ toluene: C, 72.95; H, 5.41. Found: C, 73.69; H, 5.09.

NMR: ^{1}H (300 MHz, benzene-d_6): δ = 7.69 – 7.64 (m, 8H), 7.58 – 7.50 (m, 4H), 7.11 – 6.89 (m, 8H), 5.52 (s, 10H, Cp). ^{13}C (75 MHz, benzene-d_6): δ = 135.4, 134.3, 133.4, 131.0, 129.8, 128.9, 125.6, 119.5, 105.8. ^{31}P{^{1}H} (121 MHz, benzene-d_6): δ = 15.35 (dd, J = 8.5 Hz, J = 3.6), 8.41 (dd, J = 8.5 Hz, J = 3.6 Hz).

IR: (16 scans): 3046 (w), 2998 (w), 2850 (w), 1581 (w), 1477 (w), 1431 (m), 1306 (vw), 1180 (vw), 1155 (vw), 1089 (w), 1015 (w), 913 (vw), 793 (s), 736 (s), 692 (vs), 616 (w), 579 (s), 535 (w), 503 (m), 464 (m), 442 (m), 428 (w).

MS: (EI) 429 $[(M/2)\text{-}PPh2]^+$, 394 $[(M/2)\text{-}Cp_2Zr]^+$, 185 $[PPh_2]^+$.

$Cp_2Zr(\kappa^2\text{-}C,P\text{-}Ph_2P\text{-}C{=}C{=}PPh_2)$ (30b):

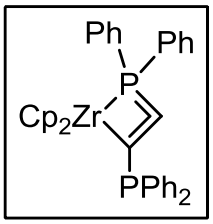

Complex **30b** was exclusively observed in solution. Therefore, only the NMR data is given.

NMR: ^{1}H (300 MHz, benzene-d_6): δ = 7.77 (t, ^3J = 7.1 Hz, 8H, Ph), 7.58 – 7.53 (m, 4H), 7.43 – 7.41 (m, 2H), 7.21 – 7.14 (m, 6H), 5.88 (s, 10H, Cp). ^{13}C: 111.8 (Cp). ^{13}C (75 MHz, benzene-d_6): δ = 111.8 (Cp). Other ^{13}C signals could not be certainly assigned to complex **30b**. ^{31}P{^{1}H} (121 MHz, benzene-d_6): δ = 12.04 (d, ^3J = 190.2 Hz), -15.72 (d, ^3J = 190.2 Hz).

5.3.25. Synthesis of (ebthi)Zr(μ_2-σ^2,η^2-$Ph_2PC_2PPh_2$-P,P')Zr(ebthi) (32):

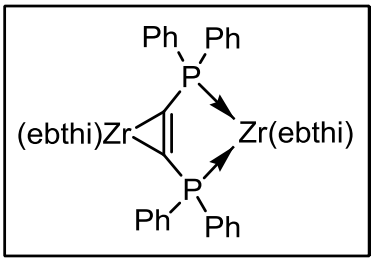

From (ebthi)Zr(η^2-$Ph_2PC_2PPh_2$) (29-Zr):

Complex **29-Zr** (265 mg, 0.353 mmol) was dissolved in 15 mL of toluene. While stirring at 100 °C for 3 hours, the reaction mixture turned from dark blue to purple. After cooling to room temperature, all volatiles were removed in vacuum and the resulting dark purple precipitate was suspended in 35 mL of *n*-hexane. After filtration from the insoluble $Ph_2PC{\equiv}CPPh_2$, the purple solution was stored at -78 °C to yield a dark purple solid, which was filtered, washed with cold *n*-hexane and dried in vacuum.

Yield: 109 mg (56 %).

From (ebthi)Zr(η^2-$Me_3SiC_2SiMe_3$) (4-Zr):

To a stirred solution of **4-Zr** (351 mg, 0.667 mmol) in 10 ml of toluene was added a solution of $Ph_2PC{\equiv}CPPh_2$ (132 mg, 0.334 mmol) in 10 ml of toluene at 25°C. While stirring for 16 h at 100 °C, the reaction mixture turned from green to intense purple. After cooling to room temperature, all volatiles were removed in vacuum and the resulting dark purple precipitate was suspended in 25 mL of *n*-hexane. After 3 days at -78 °C, a purple precipitate had formed which was filtered, washed with cold *n*-hexane and dried in vacuum.

Yield: 185 mg (25 %).

Mp.: 76 °C (dec.).

EA: Anal. calcd. for $C_{66}H_{68}P4Zr_2$: C, 71.70; H, 6.20%. Found: C, 71.05; H, 6.43.

NMR: ^{1}H (300 MHz, benzene-d_6): δ = 7.99 – 7.91 (m, 8H, Ph), 7.72 – 7.65 (m, 8H, Ph), 7.56 – 7.51 (m, 4H, Ph), 6.37 (d, ^2J = 3.0 Hz, 2H Cp), 5.99 (dd, J = 8.8 Hz, J = 3.0 Hz, 2H, Cp), 5.74 (d, J = 3.0 Hz, 2H, Cp), 5.39 (d, J = 3.0 Hz, 2H, Cp), 3.29 – 3.17 (m, 2H), 2.85 – 2.27 (m, 2H), 1.98 – 1.73 (m, 8H), 1.46 – 1.29 (m, 8H). ^{13}C (75 MHz, benzene-d_6): δ = 134.2, 133.4, 133.2, 133.0, 132.1, 130.3, 130.0, 128.8, 128.5, 128.1, 127.9, 127.1, 111.8,

103.9, 31.9, 28.8, 27.7, 24.9, 24.7, 23.0, 22.9, 16.1, 14.3. $^{31}P\{^{1}H\}$ (121 MHz, benzene-d_6): δ = 168.67.

Due to decomposition of the complex during the IR measurement, no valuable IR data could be obtained.

MS (EI) 1025 $[M\text{-}Ph]^+$, 948 $[M\text{-}2Ph]^+$, 264 $[(ebthi)]^+$.

5.3.26. Reaction of $Cp^*_2Ti(\eta^2\text{-}Ph_2PC_2PPh_2)$ (28) with $(Cy_3P)_2Ni(\eta^2\text{-}H_2C{=}CH_2)$ to 33:

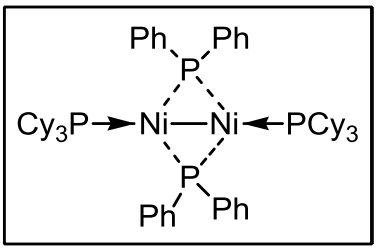

To a stirred solution of **28** (400 mg, 0.561 mmol) in 20 ml of THF was added a solution of $(Cy_3P)_2Ni(\eta^2\text{-}C_2H_4)$ (364 mg, 0.561 mmol) in 15 ml of THF at 25°C. After stirring for 16 h, the reaction mixture turned from green to dark brown. After removing of all volatiles in vacuum, the resulting dark brown precipitate was dissolved in a mixture of 15 mL of toluene and 15 mL THF and filtered. The dark brown solution was stored at +8 °C to yield dark brown crystals after 3 weeks, which were filtered, washed with cold toluene and dried in vacuum.

Yield: 29 mg (5 %).

Unfortunately, due to the low yield, no melting point or elemental analysis or could be performed.

NMR: ^{1}H (300 MHz, benzene-d_6): δ = 7.06 – 6.95 (m, Ph), 1.70 – 0.98 (m, Cy). Due to the low concentration of the sample, no ^{13}C spectrum could be obtained. $^{31}P\{^{1}H\}$ (121 MHz, benzene-d_6): δ = 45.88, 10.32.

IR: (16 scans): 3046 (vw), 2921 (m), 2844 (m), 1578 (w), 1474 (vw), 1445 (w), 1434 (m), 1170 (w), 1125 (m), 1064 (w), 1039 (w), 1022 (m), 998 (m), 913 (w), 886 (w), 847 (m), 817 (w), 734 (s), 693 (vs), 556 (s), 509 (vs), 482 (vs), 437 (s), 412 (s).

MS: (EI) 280 $[PCy_3]^+$, 185 $[PPh_2]^+$.

5.3.27. Synthesis of $Cp_2Ti[\kappa^2$-*N*,*O*-(Ph)N-C(Ph)-O] (34):

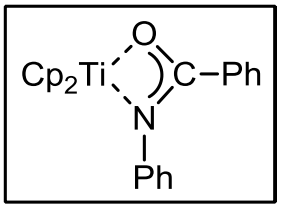

To a stirred solution of $Cp_2Ti(\eta^2$-$Me_3SiC_2SiMe_3)$ (**1**) (172 mg, 0.494 mmol) in 10 mL of toluene was added a solution of benzanilide (97 mg, 0.494 mmol) in 10 mL of toluene. After stirring the reaction mixture for 16 h at 85 °C, the colour turned from light brown to dark green. The mixture was cooled to room temperature and all volatiles were removed in vacuum. The dark green residue was dissolved in 15 mL of *n*-hexane and stored at -78 ° C for 3 days. The dark green precipitate was filtered, washed with cold toluene and dried in vacuum. Crystals suitable for X-ray analysis were obtained from a saturated solution of *n*-hexane at -78 °C.

Yield: 141 mg (76 %).

Mp.: 145 °C (dec.).

EA: Anal. calcd. for $C_{23}H_{20}NOTi$: C, 73.81; H, 5.39; N, 3.74. Found: C, 73.66; H, 5.57; N, 3.52%.

IR: (16scans): 2973 (w), 2904 (vw), 2859 (vw), 2722 (vw), 1719 (vw), 1509 (vw), 1473 (w), 1449 (w), 1376 (w), 1366 (w), 1340 (w), 1309 (m), 1236 (vs), 1138 (vs), 1021 (w), 978 (s), 868 (w), 853 (m), 806 (w), 745 (w), 704 (w), 661 (m), 647 (w), 578 (w).

MS: (CI) 374 $[M]^+$.

5.3.28. Synthesis of $Cp^*_2Ti[\kappa^2$-*N*,*O*-(Ph)N-C(Ph)-O] (35):

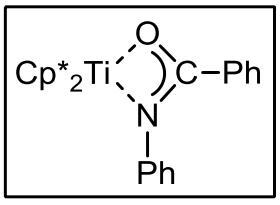

To a stirred solution of $Cp^*_2Ti(\eta^2$-$Me_3SiC_2SiMe_3)$ (**3-Ti**) (377 mg, 0.771 mmol) in 10 mL of toluene was added a solution of benzanilide (152 mg, 0.771 mmol) in 15 mL of toluene. After stirring the reaction mixture for 16 h at 85 °C, the colour turned from light brown to dark green. The mixture was cooled to room temperature and all volatiles were removed in vacuum. The dark green residue was dissolved in 20 mL of *n*-hexane and stored at -78 °C for 7 days. The dark green precipitate was filtered, washed with cold toluene and dried in vacuum.

Crystals suitable for X-ray analysis were obtained from a saturated solution of *n*-hexane at -30 °C.

Yield: 339 mg (85 %).

Mp.: 183 °C (dec.).

EA: Anal. calcd. for $C_{33}H_{40}NOTi$: C, 77.03; H, 7.84; N, 2.72. Found: C, 77.04; H, 7.97; N, 2.64.

IR: (16 scans): 3063 (vw), 2974 (vw), 2899 (w), 2853 (w), 2723 (vw), 1654 (vw), 1599 (w), 1580 (w), 1510 (s), 1481 (s), 1450 (m), 1440 (m), 1416 (s), 1377 (m), 1323 (w), 1260 (m), 1154 (w), 1122 (w), 1069 (m), 1027 (m), 925 (m), 920 (m), 795 (m), 763 (s), 735 (s), 705 (vs), 692 (vs), 672 (s), 636 (m), 609 (m), 513 (m), 436 (m), 425 (m).

MS: (CI) 514 $[M]^+$.

5.3.29. Synthesis of $Cp_2Ti[\kappa^2$-*N*,*O*-(Ph)N-C(Ph)-O] (36):

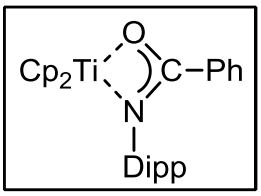

To a stirred solution of $Cp_2Ti(\eta^2$-$Me_3SiC_2SiMe_3)$ (**1**) (154 mg, 0.442 mmol) in 10 mL of toluene was added a slurry of *N*-(2,6-diisopropylphenyl)benzamide (124 mg, 0.442 mmol) in 7 mL of toluene. After stirring the reaction mixture for 16 h at 85 °C, the colour turned from light brown to dark green. The mixture was cooled to room temperature and all volatiles were removed in vacuum. The dark green residue was dissolved in 5 mL of toluene and filtered. The dark solution was concentrated to 2 mL and stored at -35 °C for 7 days to result a dark green precipitate which was filtered and dried in vacuum. Crystals suitable for X-ray analysis were obtained from a saturated solution of toluene at room temperature.

Yield: 185 mg (91 %).

EA: Anal. calcd. for $C_{29}H_{32}NOTi$: C, 75.98; H, 7.04; N, 3.06. Found: C, 75.99; H, 7.08; N, 3.09.

MS (EI) 458 $[M]^+$, 264 $[M\text{-}Cp_2Ti\text{-}Me]^+$, 178 $[Cp_2Ti]^+$.

5.3.30. Synthesis of $Cp_2Zr(H)[\kappa^2$-*N*,*O*-(*i*-Pr)N-C(*t*-Bu)-O] (37):

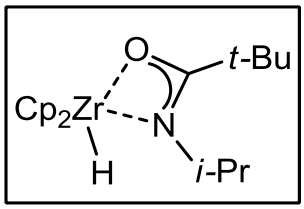

From $Cp_2Zr(py)(\eta^2$-$Me_3SiC_2SiMe_3)$ (2):

A solution of *N*-(*i*-propyl)*t*-butylamid (62 mg, 0.433 mmol) in 4 mL of toluene was added to a solution of $Cp_2Zr(py)(\eta^2$-$Me_3SiC_2SiMe_3)$ (**2**) (204 mg, 0.433 mmol) in 5 mL of toluene. Upon stirring the reaction mixture for 25 h at 65 °C, the reaction mixture turned from dark purple to dark teal. After cooling the mixture to room temperature, all volatiles were removed under vacuum and the resulting dark green precipitate was dissolved in hexanes, filtered and stored at -33 °C to give colourless crystals, which were filtered and dried under vacuum. The mother liquor was concentrated and stored at -33 °C to complete crystallization.

Overall yield: 123 mg (78 %).

From $Cp_2Zr(H)Cl$ (8):

A suspension of *N*-(*i*-propyl)*t*-butylamid (142 mg, 0.99 mmol) and NaHMDS (191 mg, 1.04 mmol) in 10 mL of toluene is stirred for 16 h at room temperature. After removing all volatiles in vacuum, the pale yellow residue is suspended in 10 mL of toluene and slowly dropped into a slurry of $Cp_2Zr(H)Cl$ (**8**) (256 mg, 0.99 mmol) in 5 mL of toluene. After stirring for additional 16 h at room temperature, the reaction mixture is filtered through celite. The resulting slight yellow solution is concentrated in vacuum to 3 mL and stored at -33 °C for three days to yield colourless prisms, suitable for X-ray analysis, which were filtered and dried in vacuum.

Yield: 306 mg (85 %).

EA: Anal. calcd. for $C_{18}H_{27}NOZr$: C, 59.29, H, 7.46, N, 3.84. Found: C, 58.69, H, 7.33, N, 3.79.

NMR: ^{1}H (400 MHz, benzene-d_6): δ = 5.81 (s, 10H, Cp), 5.01 (s, 1H, Zr-*H*), 3.70 (sept, ^3J = 6.4 Hz, 1H, C*H*), 1.08 (d, ^3J = 6.2 Hz, 6H, Me), 1.01 (s, 9H, *t*-Bu). ^{13}C (100 MHz, benzene-d_6): δ = 185.8 (*C*-*t*-Bu), 106.0 (Cp), 46.2 (*C*H), 39.0 (*C*Me_3), 27.4 (Me), 23.9 (Me).

MS: 363 $[M]^+$, 297 $[M\text{-}Cp]^+$,220 $[Cp_2Zr]^+$.

5.3.31. Synthesis of $Cp_2Zr(H)[\kappa^2$-*N*,*O*-(Dipp)N-C(Ph)-O] (38):

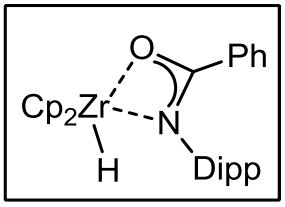

From $Cp_2Zr(py)(\eta^2$-$Me_3SiC_2SiMe_3)$ (2):

A slurry of *N*-(2,6-diisopropylphenyl)benzamide (176 mg, 0.626 mmol) in 4 mL of toluene was added to a solution of $Cp_2Zr(py)(\eta^2$-$Me_3SiC_2SiMe_3)$ (**2**) (295 mg, 0.626 mmol) in 7 mL of toluene. Upon stirring the reaction mixture for 16 h, the solution turned from dark purple to dark green. After removing all volatiles under vacuum, the resulting dark green precipitate was dissolved in hexanes, filtered and stored at -33 °C to give colourless crystals, which were filtered and dried under vacuum. The mother liquor was concentrated and stored at -33 °C to complete crystallization. Crystals suitable for X-ray diffraction analysis were grown from a saturated toluene solution.

Overall yield: 270 mg (86 %).

From $Cp_2Zr(H)Cl$ (8):

A Suspension of *N*-(2,6-diisopropylphenyl)benzamide (375 mg, 1.33 mmol) and NaHMDS (260 mg, 1.42 mmol) in 10 mL of toluene is stirred for 16 h at room temperature. After removing all volatiles in vacuum, the pale yellow residue is suspended in 10 mL of toluene and slowly dropped into a slurry of $Cp_2Zr(H)Cl$ (**8**) (344 mg, 1.33 mmol) in 7 mL of toluene. After stirring for additional 16 h at room temperature, the reaction mixture is filtered through celite. The resulting slight yellow solution is concentrated in vacuum to 5 mL and stored at -33 °C overnight to yield colourless prisms, which were filtered and dried in vacuum.

Yield: 513 mg (77 %).

EA: Anal. calcd. for $C_{29}H_{33}NOZr$: C 69.27, H 6.62, N 2.79. Found: C 69.16, H 6.41, N 2.87.

NMR: ^{1}H (600 MHz, benzene-d_6): δ = 7.44 (d, ^3J = 7.0 Hz, 2H), 7.13 – 7.06 (m, 3H), 6.87 (t, ^3J = 7.3 Hz, 1H), 6.82 (t, ^3J = 7.8 Hz, 2H), 5.99 (s, 10H, Cp), 5.72 (s, 1H, Zr-*H*), 3.45 (sept, ^3J = 6.9 Hz, 2H,C*H*), 1.37 (d, ^3J = 7.0 Hz, 6H, Me), 0.80 (d, ^3J = 6.9 Hz, 6H, Me). ^{13}C (150 MHz, benzene-d_6): δ = 176.9 (*C*-Ph), 143.3, 141.7, 131.1, 129.5, 128.3, 127.9, 125.4, 124.4, 107.0 (Cp), 27.8 (*C*H), 25.0 (Me), 23.9 (Me).

MS: (EI) 501 $[M]^+$, 435 $[M\text{-}Cp]^+$, 220 $[Cp_2Zr]^+$.

5.3.32. Reaction of $Cp_2Zr(H)[\kappa^2\text{-}N,O\text{-}(i\text{-}Pr)N\text{-}C(t\text{-}Bu)\text{-}O]$ (37) with 1-octene:

A J. Young NMR tube was filled with a solution of $Cp_2Zr(H)[\kappa^2\text{-}N,O\text{-}(i\text{-}Pr)N\text{-}C(t\text{-}Bu)\text{-}O]$ (**37**) (10 mg, 0.027 mmol) and 1-octene (7 µL, 0.045 mmol) in 0.8 mL of toluene-d_8. The reaction mixture was heated for 2 days at 65 °C and monitored by ^{1}H NMR spectroscopy. ^{1}H NMR spectrum showed complete consumption of 1-octene (characteristic ^{1}H peaks: 5.01 (m, 1H), 5.79 (m, 1H)) and formation of only 2-octene (characteristic 1H peaks: 5.43 (m, 2H)). The ^{13}C NMR analysis revealed the formation of only *trans*-2-octene (characteristic ^{13}C peaks: 132.0 (s) and 124.8 (s)).[148]

5.3.33. Reaction of $Cp_2Zr(H)[\kappa^2\text{-}N,O\text{-}(Dipp)N\text{-}C(Ph)\text{-}O]$ (38) with 1-octene:

A J. Young NMR tube was filled with a solution of $Cp_2Zr(H)[\kappa^2\text{-}N,O\text{-}(Dipp)N\text{-}C(Ph)\text{-}O]$ (**38**) (30 mg, 0.070 mmol) and 1-octene (25 µL, 0.160 mmol) in 0.8 mL of toluene-d_8. The reaction mixture was heated for 3 days to 70 °C and monitored by ^{1}H NMR spectroscopy. The ^{1}H NMR spectrum showed complete consumption of 1-octene (characteristic ^{1}H peaks: 5.01 (m, 1H), 5.79 (m, 1H)) and formation of only 2-octene was observed (characteristic 1H peaks: 5.43 (m, 2H)). The ^{13}C NMR analysis revealed the formation of only *trans*-2-octene (characteristic ^{13}C peaks: 132.0 (s) and 124.8 (s)).[148]

5.3.34. Reaction of $Cp_2Zr(H)[\kappa^2\text{-}N,O\text{-}(i\text{-}Pr)N\text{-}C(t\text{-}Bu)\text{-}O]$ (37) with styrene to $Cp_2Zr[CH(Me)(Ph)][\kappa^2\text{-}N,O\text{-}(i\text{-}Pr)N\text{-}C(t\text{-}Bu)\text{-}O]$ (39a/39b):

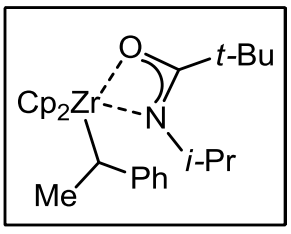

Into a J. Young NMR tube was filled a solution of $Cp_2Zr(H)[\kappa^2\text{-}N,O\text{-}(i\text{-}Pr)N\text{-}C(t\text{-}Bu)\text{-}O]$ (**37**) (21 mg, 0.058 mmol) and styrene (9 µL, 0.079 mmol) in 1 mL of toluene-d_8. The reaction was monitored by ^{1}H NMR spectroscopy for 8 days at room temperature. During that time, the resonances of **37** decreased slowly and a new set of resonances of

39 appeared. Heating the reaction mixture to 70 °C for 3 h resulted in the formation of only **37** and styrene.

NMR: ^{1}H (400 MHz, benzene-d_6): δ = 7.26 (t, ^{3}J = 8.0 Hz, 2H, *Ph*), 7.22-7.20 (m, 1H, *Ph*); 6.94 (t, ^{3}J = 8.0 Hz, 2H, *Ph*), 5.86 (s, 5H, Cp), 5.57 (s, 5H, Cp), 3.56 (sept, ^{3}J = 6.1 Hz, 1H, C*H*Me$_2$), 2.73 (quart, ^{3}J = 7.0 Hz, 1H, ZrC*H*), 1.80 (d, ^{3}J = 7.0 Hz, 3H, CH*Me*), 1.26 (d, ^{3}J = 6.1 Hz, 3H, *Me*), 1.05 (s, 9H, *t*-Bu), 0.92 (d, ^{3}J = 6.1 Hz, 3H, *Me*). ^{13}C (100 MHz, benzene-d_6): δ = 166.4 (O-*C*), 155.5 (CHMe-*Ph, ipso-C*), 128.7, 126.5, 126.3, 113.0 (Cp), 112.0 (Cp), 58.3 (Zr-*C*HMePh), 46.2 (*C*HMe$_2$), 39.0 (*C*-*t*-Bu), 28.7 (*t-Bu*), 27.6 (*Me*), 25.1 (*Me*), 22.6 (*Me*).

5.3.35. Synthesis of Cp$_2$Zr[CH(Me)(Ph)][κ^2-*N*,*O*-(Dipp)N-C(Ph)-O] (40a):

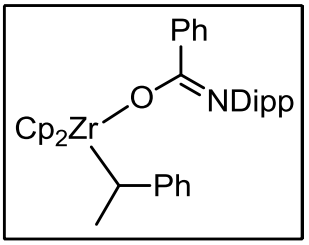

A J. Young NMR tube was filled a solution of Cp$_2$Zr(H)[κ^2-*N*,*O*-(Dipp)N-C(Ph)-O] (**38**) (33 mg, 0.077 mmol) and styrene (12 µL, 0.105 mmol) in 1 mL of benzene-d_6. The reaction was monitored by ^{1}H NMR spectroscopy for 7 days. During that time, the colour turned from colourless to intense yellow. The reaction mixture was then poured into a vial. Subsequently all volatiles were removed, and redissolved in hexanes. Upon cooling the solution to -33°C, yellow crystals suitable for X-ray analysis were afforded, which were filtered and dried under vacuum.

Yield: 25 mg (61 %).

EA: Anal. calcd. for C$_{18}$H$_{27}$NOZr: C 73.22, H 6.81, N 2.31. Found: C 72.66, H 7.12, N 3.12.

NMR: ^{1}H (400 MHz, 238 K, benzene-d_6): δ = 8.45 (d, ^{3}J = 7.3 Hz, 2H, O-C(Dipp)-*Ph*), 7.26 (t, ^{3}J = 7.3 Hz, 2H, O-C(Dipp)-*Ph*), 7.28 – 6.88 (m, 9H), 5.63 (s, 5H, Cp), 5.02 (s, 5H, Cp), 3.17 (quart, ^{3}J = 7.0 Hz, 1H, ZrC*H*), 3.07 (sept, ^{3}J = 6.8 Hz, 1H, C*H*), 3.00 (sept, ^{3}J = 6.8 Hz, 1H, C*H*), 1.55 (d, ^{3}J = 7.0 Hz, 3H, Me), 1.83 – 1.33 (m, 12H, *i*-Pr). ^{13}C (150 MHz, 238 K, benzene-d_6): δ = 156.1 (O-*C*), 154.6 (CHMe-*Ph, ipso-C*), 146.0 (Dipp, *ipso-C*), 137.6 (Dipp, *C*-*i*-Pr), 136.9 (Dipp, *C*-*i*-Pr), 136.4 (OC-*Ph*, *ipso*-C), 130.4, 129.2, 128.2,

125.8, 124.5, 123.2, 123.0, 122.3, 121.9 (all aromatic *C*H), 113.5 (Cp), 112.2 (Cp), 58.2 (Zr-*C*HMePh), 29.1 (*C*HMe$_2$), 29.0 (*C*HMe$_2$), 23.5 (*Me*, Dipp), 23.2 (*Me*, Dipp), 22.7 (*Me*, Dipp), 22.4 (CH*Me*Ph), 22.4 (Me, Dipp).

MS: (EI) 605 $[M]^+$, 501 $[M\text{-}PhCHMe]^+$, 281 $[L+H]^+$, 220 $[Cp_2Zr]^+$, 105 $[PhCHMe]^+$.

5.3.36. Synthesis of Cp$_2$Zr(Cl)[κ^2-*N*,*O*-(Dipp)N-C(Ph)-O] (41):

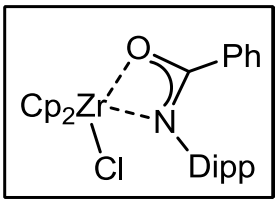

From Cp$_2$ZrCl$_2$ (6-Zr):

A suspension of *N*-(2,6-diisopropylphenyl)benzamide (375 mg, 1.33 mmol) and NaHMDS (260 mg, 1.42 mmol) in 10 mL of toluene is stirred for 16 h at room temperature. After removing all volatiles in vacuum, the pale yellow residue is suspended in 10 mL of toluene and slowly dropped into a slurry of Cp$_2$ZrCl$_2$ (**6-Zr**) (390 mg, 1.33 mmol) in 10 mL of toluene. After stirring for additional 16 h at room temperature, the reaction mixture is filtered through celite. The resulting slight yellow solution is concentrated in vacuum to 3 mL and stored at -33 °C overnight to yield colourless prisms, suitable for X-ray analysis, which were filtered and dried in vacuum.

Yield: 502 mg (70 %).

From Cp$_2$Zr(H)Cl) (8):

A J. Young NMR tube is filled with Schwartz' reagent (**8**) (20 mg, 0.078 mmol), *N*-(2,6-diisopropylphenyl)benzamide (22 mg, 0.78 mmol) and 1 mL of benzene-d_6 and sealed. Already after sealing, gas evolution was observed. After standing for 10 h at room temperature, all precipitate was dissolved. ^{1}H NMR analysis revealed molecular H_2 gas (δ = 4.47 ppm, singlet) as byproduct.

Yield: Quantitative according to ^{1}H NMR analysis.

EA: Anal. calcd. for $C_{29}H_{32}ClNOZr$: C, 64.83; H, 6.00; N, 2.61. Found: C, 64.66; H, 5.94; N, 2.64.

NMR: ^{1}H (300 MHz, benzene-d_6): δ = 7.44 (d, ^{3}J= 7.0 Hz, 2H), 7.16 – 7.07 (m, 3H), 6.94 – 6.82 (m, 3H), 6.17 (s, 10H, Cp), 3.53 (sept, ^{3}J = 6.8 Hz, 2H, C*H*), 1.41 (d, ^{3}J = 6.8 Hz, 6H, Me), 0.87 (d, ^{3}J = 6.8 Hz, 6H, Me). ^{13}C (100 MHz, benzene-d_6): δ = 173.5 (*C*-Ph), 142.7, 140.8, 131.4, 129.9, 127.5, 126.3, 125.6, 124.1, 114.1 (Cp), 28.1(*C*H), 25.0 (Me), 23.7 (Me).

MS: (EI) 535 $[M]^+$, 470 $[M\text{-}Cp]^+$, 264 $[L\text{-}Me]^+$.

5.3.37. Synthesis of $Cp_2Hf(Cl)[\kappa^2\text{-}N,O\text{-}(Ph)N\text{-}C(Ph)\text{-}O]$ (42):

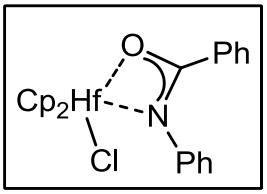

Into a suspension of benzanilide (265 mg, 1.34 mmol) in 10 mL of toluene was dropped a solution of NaHMDS in toluene (2.35 mL, 2.0 M) and the reaction mixture stirred for 4 h at room temperature. After removing all volatiles in vacuum, the pale yellow residue is suspended in 10 mL of toluene and slowly dropped into a slurry of Cp_2HfCl_2 (**6-Hf**) (510 mg, 1.34 mmol) in 10 mL of toluene. After stirring for additional 16 h at room temperature, the reaction mixture is filtered and the resulting slight yellow solution is concentrated in vacuum to 7 mL and stored at -30 °C overnight to yield colourless prisms, suitable for X-ray analysis, which were filtered and dried in vacuum.

Yield: 498 mg (69 %).

Mp.: 193 °C.

EA: Anal. calcd. for $C_{23}H_{20}ClNOHf$: C, 51.12; H, 3.73; N, 2.59. Found: C, 51.17; H, 3.96; N, 2.50.

NMR: ^{1}H (300 MHz, benzene-d_6): δ = 7.44 – 7.41 (m, 2H, Ph), 7.10 (d, ^{3}J = 7.7 Hz, 2H, Ph), 6.97 – 6.84 (m, 6H, Ph), 5.99 (s, 10H, Cp). ^{13}C (75 MHz, benzene-d_6): δ = 176.8 (*C*-Ph), 145.9, 132.5, 131.3, 129.8, 128.7, 128.2, 127.9, 126.6, 112.7 (Cp).

IR: (16 scans): 3094 (vw), 3051 (vw), 1655 (vw), 1600 (w), 1584 (w), 1530 (vs), 1487 (s), 1454 (s), 1421 (s), 1367 (w), 1317 (w), 1301 (w), 1264 (m), 1182 (w), 1128 (w), 1069 (w), 1021 (m), 1013 (s), 938 (m), 842

(m), 799 (vs), 782 (vs), 736 (s), 709 (vs), 696 (vs), 673 (s), 631 (m), 614 (m), 519 (w), 495 (m), 437 (s), 410(w).

MS: (EI) 541 $[M]^+$, 506 $[M\text{-}Cl]^+$.

5.3.38. Synthesis of $Cp_2Zr[\kappa^1\text{-}O\text{-}OC(Ph)N(Dipp)]_2$ (43):

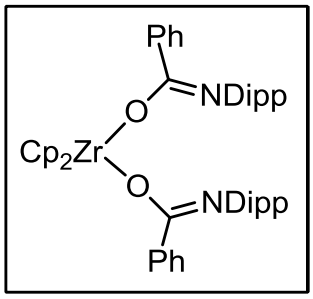

From Cp_2ZrCl_2 (6-Zr):

A Suspension of *N*-(2,6-diisopropylphenyl)benzamide (340 mg, 1.21 mmol) and NaHMDS (222 mg, 1.21 mmol) in 10 mL of toluene is stirred for 16 h at room temperature. After removing all volatiles in vacuum, the pale yellow residue is suspended in 10 mL of toluene and slowly dropped into a slurry of Cp_2ZrCl_2 (**6-Zr**) (177 mg, 0.60 mmol) in 10 mL of toluene. After stirring for additional 16 h at room temperature, the reaction mixture is filtered through celite. The resulting slight yellow solution is concentrated in vacuum to 7 mL and stored at -33 °C for 7 days to yield colourless prisms, which were filtered and dried in vacuum.

Yield: 721 mg (76 %).

From $Cp_2Zr(Cl)[\kappa^2\text{-}N,O\text{-}(Dipp)N\text{-}C(Ph)\text{-}O]$ (41):

A suspension of *N*-(2,6-diisopropylphenyl)benzamide (150 mg, 0.53 mmol) and NaHMDS (103 mg, 0.56 mmol) in 10 mL of toluene is stirred for 18 h at room temperature. After removing all volatiles in vacuum, the pale yellow residue is suspended in 10 mL of toluene and slowly dropped into a slurry of $Cp_2Zr(Cl)[\kappa^2\text{-}N,O\text{-}(Dipp)N\text{-}C(Ph)\text{-}O]$ (**41**) (286 mg, 0.53 mmol) in 5 mL of toluene. After stirring for additional 24 h at room temperature, the reaction mixture is filtered through celite. The resulting slight yellow solution is concentrated in vacuum to 5 mL and stored at -33 °C for 3 weeks to yield colourless crystals, which were filtered and dried in vacuum.

Yield: 332 mg (80 %).

From $Cp_2Zr(py)(\eta^2\text{-}Me_3SiC_2SiMe_3)$ (2):

An J. Young NMR tube was filled with a slurry of $Cp_2Zr(py)(\eta^2\text{-}Me_3SiC_2SiMe_3)$ (**2**) (35 mg, 0.074 mmol) and *N*-(2,6-diisopropylphenyl)benzamide (42 mg, 0.149 mmol) in 0.7 mL of benzene-d_6. The purple reaction mixture was allowed to stand over 3 days until all precipitate dissolved, resulting in a colourless clear solution. NMR analysis revealed formation of **43** together with $Me_3SiC_2SiMe_3$ (0.16 ppm) and H_2 (4.47 ppm).

Yield: Quantitative according to ^{1}H NMR analysis.

From $Cp_2Zr(H)[\kappa^2$-*N*,*O*-(Dipp)N-C(Ph)-O] (38):

38 (214 mg, 0.426 mmol) and *N*-(2,6-diisopropylphenyl)benzamide (120 mg; 0.426 mmol) were suspended into 7 mL of toluene. Upon stirring the reaction mixture for 2 days at room temperature, all precipitate dissolved. The colourless solution was then concentrated to ca. 3 mL and stored at -33 °C, yielding colourless crystals, suitable for X-ray analysis, which were filtered and dried in vacuum.

Yield: 241 mg (72 %).

EA: Anal. calcd. for $C_{48}H_{54}N_2O_2Zr$: C 73.71, H 6.96, N 3.58. Found: C 73.79, H 6.80, N 3.87.

NMR: ^{1}H (400 MHz, 198 K, benzene-d_6): δ = 8.63 (d, ^3J = 7.8 Hz, 2H, Ph), 7.55 (d, ^3J = 7.8 Hz, 1H, Dipp), 7.31 (t, ^3J = 7.8 Hz, 2H, Ph), 7.20 – 7.00 (m, 5H), 6.89 – 6.78 (m, 5H), 6.66 (t, ^3J = 7.5 Hz, 1H), 6.52 (s, 5H, Cp), 5.39 (s, 5H, Cp), 3.63 (sept, ^3J = 6.4 Hz, 1H, C*H*), 3.54 (sept, ^3J = 6.4 Hz, 1H, C*H*), 3.27 (sept, ^3J = 6.4 Hz, 2H, C*H*), 1.62 – 1.35 (m, 9H, Me), 1.15 – 1.00 (m, 6H, *Me*), 0.80 (d, ^3J = 6.4 Hz, 3H, Me). ^{13}C (100 MHz, 198 K, benzene-d_6): δ = 172.1 (κ^2-O-*C*(Dipp)Ph), 163.3 (κ^1-O-C(Dipp)Ph), 157.4, 146.4, 141.7, 136.2, 131.3, 129.7, 129.4, 129.1, 128.4, 127.8, 127.3, 122.9, 122.8 (aromatics), 114.6 (Cp), 113.7 (Cp), 29.2 (κ^2-*C*HMe_2), 28.5 (κ^1-*C*HMe_2), 27.8 (κ^1-*C*HMe_2), 24.5 (κ^1-CH*Me*Me), 23.8 (κ^1-CHMe*Me*), 23.6 (κ^2-CH*Me*$_2$), 23.5 (κ^1-CH*Me*Me), 23.0 (κ^1-CHMe*Me*), 21.3 (κ^2-CH*Me*$_2$).

MS: (EI) 780 $[M]^+$, 715 $[M\text{-}Cp]^+$, 220 $[Cp_2Zr]^+$.

5.4. References

[145] H. E. Gottlieb, V. Kotlyar, A. Nudelman, *J. Org. Chem.* **1997**, *62*, 7512-7515.

[146] G. M. Sheldrick, *Acta Crystallogr. Sect. A* **2008**, *64*, 112-122.

[147] A. L. Spek, *Acta Crystallogr. Sect. D* **2009**, *65*, 148-155.

[148] C. Tsay, J. C. Peters, *Chem. Sci.* **2012**, *3*, 1313-1318.

6. Additional Information

6.1. Table of Publications and Presentations

6.1.1. Publications

Contents of this work are published in the following journals.

1. Highly Strained Heterometallacycles of Group 4 Metallocenes with Bis(diphenylphosphino)amide Ligands; M. Haehnel, S. Hansen, A. Spannenberg, P. Arndt, T. Beweries, U. Rosenthal, *Chem. Eur. J.* **2012**, *18*, 10546-10553.
2. Di-μ-sulfido-bis-{[rac-1,2-bis-(η^5-4,5,6,7-tetra-hydro-inden-1-yl)ethane]-zirconium(IV)} toluene monosolvate; M. Haehnel, K. Altenburger, A. Spannenberg, P. Arndt, U. Rosenthal, *Acta Cryst. Sect. E* **2012**, *68*, m1425.
3. Reactions of Titanocene Bis(trimethylsilyl)acetylene Complexes with Carbodiimides: An Experimental and Theoretical Study of Complexation versus C–N Bond Activation; M. Haehnel, M. Ruhmann, O. Theilmann, S. Roy, T. Beweries, P. Arndt, A. Spannenberg, A. Villinger, E. D. Jemmis, A. Schulz, U. Rosenthal, *J. Am. Chem. Soc.* **2012**, *134*, 15979-15991.
4. Recent advances in the chemistry of heterometallacycles of group 4 metallocenes; T. Beweries, M. Haehnel, U. Rosenthal, *Catal. Sci. Tech.* **2013**, *3*, 18-28.
5. Highly Strained Heterometallacycles of Group 4 Metallocenes with Bis(diphenylphosphino)methanide Ligands; M. Haehnel, S. Hansen, J. B. Priebe, A. Spannenberg, P. Arndt, A. Brückner, U. Rosenthal, *Chem. Eur. J.* **2013**, *19*, 7568-7574.
6. {N,N-Bis[bis(2,2,2-trifluoroethoxy)phosphanyl]methylamine-κ^2-P,P'}bis(η^5-cyclopentadienyl)titanium(II); M. Haehnel, S. Hansen, A. Spannenberg, T. Beweries, *Acta Cryst. Sect. E* **2013**, *69*, m346.
7. Facile Access to Tuneable Schwartz´s Reagents – Oxidative Addition Products from the Reaction of Amide N-H-Bonds with Reduced Zirconocene Complexes; M. Haehnel, J. C.-H. Yim, L. L. Schafer, U. Rosenthal, *Angew. Chem. Int. Ed.* ***2013****, 52,* 11415-11419.

8. Synthesis, Characterization and Reactivity of Group 4 Metallocene Bis(diphenylphosphino)acetylene Complexes – A Reactivity and Bonding Study; Martin Haehnel, Sven Hansen, Kathleen Schubert, Perdita Arndt, Anke Spannenberg, Haijun Jiao, Uwe Rosenthal, J. Am. Chem. Soc. **2013**, *135*, 17556–17565.

9. (μ^3-Hydrido)[μ^3-2-(trimethylsilyl)ethylidyne-κ^3C^1:C^1:C^1]tetrakis[(η^5-cyclopentadienyl)cobalt(II)], M. Haehnel, A. Spannenberg, U. Rosenthal, *Acta Cryst. Sect. E* **2013**, *69*, m651.

10. Bis(μ_2-isopropylimido-κ^2N:N)bis[(η^5-cyclopentadienyl)(ethenolato-κO)titanium(IV)], M. Haehnel, A. Spannenberg, U. Rosenthal, *Acta Cryst. Sect. E* **2014**, 70, m16.

11. Synthesis and Characterization of Titanium 7-Azaindolato Complexes and their Lithium Precursors, M. Haehnel, P. Arndt, A. Spannenberg, U. Rosenthal, *ZAAC* **2014**, *accepted*.

12. Four-membered Heterometallacyclic d^0 and d^1 Complexes of Group IV Metallocenes with Amidato Ligands, M. Haehnel, J. B. Priebe, C.-H. Yim, A. Spannenberg, A. Brückner, L. L. Schafer, U. Rosenthal, *Chem. Eur. J.* **2014**, *submitted*.

6.1.2. Presentations

Stabilizing the Radical – Reactions of Carbodiimides with Group 4 Metallocenes.
M. Haehnel, M. Ruhmann, A. Spannenberg, P. Arndt, T. Beweries, A. Schulz, U. Rosenthal, *XXV International Conference on Organometallic Chemistry (ICOMC)*, September 2-7, 2012, Lisbon, Portugal (Flash Presentation with Poster).

Gespannte 4-gliedrige biradikalische Hetero-Titanacyclen und deren Stabilisationsmodi.
M. Haehnel, U. Rosenthal, 15th *Norddeutsches Doktorandenkolloquium (NDDK)*, September 24-25, 2012, Krelingen, Germany.

Stabilizing the Radical – Reactions of Carbodiimides with Titanocene Complexes.
M. Haehnel, M. Ruhmann, A. Spannenberg, P. Arndt, T. Beweries, A. Schulz, U. Rosenthal, *44. Symposium on Catalysis*, November 5-6, 2012, Prague, Czech Republic.

6.1.3. Posters

Highly strained 4-membered hetero-metallacycles of group 4 metallocenes with a PNP-ligand.
M. Haehnel, A. Spannenberg, P. Arndt, U. Rosenthal, *XIX European Conference on Organometallic Chemistry (EuCOMC)*, July 3-7, 2011, Toulouse, France.

Highly strained 4-membered hetero-metallacycles of group 4 metallocenes with a PNP-ligand.
M. Haehnel, A. Spannenberg, P. Arndt, U. Rosenthal, *14. JCF-Frühjahrs-Symposium*, 18.-21. March 18-21 2012, Rostock, Germany.

Stabilizing the Radical – Reactions of Carbodiimides with Group 4 Metallocenes.
M. Haehnel, M. Ruhmann, A. Spannenberg, P. Arndt, T. Beweries, A. Schulz, U. Rosenthal, *XXV International Conference on Organometallic Chemistry (ICOMC)*, September 2-7, 2012, Lisbon, *Portugal* (Poster with Flash Presentation).

6.2. X-Ray Crystallographic Appendix

	11	**12**	**13**
formula	$C_{38}H_{44}N_3Ti$	$C_{35}H_{36}N_2Ti$	$C_{47}H_{60}N_2Ti$
F_w [g · mol^{-1}]	590.66	532.56	700.87
colour	blue	light brown	brown
crystal system	triclinic	monoclinic	monoclinic
space group	$P\bar{1}$	$P2_1/c$	$P2_1/c$
lattice constants			
a, b, c [Å]	8.5462(4)	16.2024(6)	13.6940(3)
	11.2725(6)	10.7320(4)	30.0123(6)
	20.5189(10)	16.4713(6)	9.9271(2)
α, β, γ [°]	94.375(4)	90.00	90.00
	90.937(4)	95.448(3)	101.067(1)
	94.744(4)	90.00	90.00
cell volume [Å^3]	1963.7(2)	2851.2(2)	4004.05(14)
Z	2	4	4
density [g · cm^{-3}]	0.999	1.241	1.163
temperature [K]	150(2)	150(2)	150(2)
μ(Mo Kα) [mm^{-1}]	0.243	0.326	2.049
no. of collected rflns	28767	39698	31394
no. of unique rflns	7318	5601	6520
no. of observed rflns	3787	3034	5480
no. of parameters	392	329	468
GOF on F^2	0.657	0.767	1.025
R_1 (I > 2σ(I))	0.0368	0.0412	0.0444
wR_2 (all data)	0.0596	0.0872	0.1218

	14b	**15**	**16**
formula	$C_{32}H_{47}NTi$	$C_{31}H_{42}ClNTi$	$C_{64}H_{68}N_4Zr_2$
F_w [g · mol^{-1}]	493.61	512.01	1075.66
colour	red	green	yellow
crystal system	orthorhombic	orthorhombic	monoclinic
space group	$P2_12_12_1$	$Pna2_1$	$P2_1/c$
lattice constants			
a, b, c [Å]	10.7229(2)	18.9174(10)	16.2979(4)
	16.2730(3)	10.6618(6)	14.1050(3)
	16.3219(3)	13.5116(6)	23.6069(5)
α, β, γ [°]	90.00	90.00	90.00
	90.00	90.00	95.174(1)
	90.00	90.00	90.00
cell volume [Å^3]	2848.07(9)	2725.2(2)	5404.7(2)
Z	4	4	4
density [g · cm^{-3}]	1.151	1.248	1.322
temperature [K]	150(2)	150(2)	150(2)
μ(Mo Kα) [mm^{-1}]	0.320	3.688	0.429
no. of collected rflns	48630	17726	183635
no. of unique rflns	6792	3512	12411
no. of observed rflns	6360	3113	11160
no. of parameters	321	320	627
GOF on F^2	1.056	1.014	1.102
R_1 (I > 2σ(I))	0.0348	0.0341	0.0250
wR_2 (all data)	0.0955	0.0825	0.0711

	17	**18**	**19**
formula	$C_{26}H_{42}Li_2N_8$	$C_{17}H_{29}LiN_4$	$C_{27}H_{35}N_2Ti$
F_w [g · mol^{-1}]	480.56	296.38	435.47
colour	colourless	colourless	red
crystal system	triclinic	monoclinic	monoclinic
space group	$P\bar{1}$	$P2_1/c$	$P2_1/c$
lattice constants			
a, b, c [Å]	10.1764(7)	10.0911(2)	18.003(4)
	10.9495(8)	11.6290(2)	17.114(3)
	14.2803(9)	15.4981(2)	16.851(3)
α, β, γ [°]	106.262(5)	90.00	90.00
	90.812(5)	96.8210(10)	115.79(3)
	109.592(5)	90.00	90.00
cell volume [Å^3]	1428.79(17)	1805.82(5)	4674.8(16)
Z	2	4	8
density [g · cm^{-3}]	1.117	1.090	1.237
temperature [K]	150(2)	150(2)	150(2)
μ(Mo Kα) [mm^{-1}]	0.068	0.065	0.382
no. of collected rflns	20485	38286	62436
no. of unique rflns	5620	4132	10738
no. of observed rflns	2315	3021	4407
no. of parameters	333	225	484
GOF on F^2	0.603	1.030	0.807
R_1 (I > 2σ(I))	0.0345	0.0494	0.0702
wR_2 (all data)	0.0477	0.1284	0.1875

	20	**21**	**22**
formula	$C_{21}H_{23}N_2Ti$	$C_{41}H_{38}ClHfNP_2$	$C_{34}H_{31}ClNP_2Ti$
F_w [g · mol^{-1}]	351.31	820.60	598.89
colour	green	colourless	green
crystal system	monoclinic	triclinic	triclinic
space group	$P2_1/c$	$P\bar{1}$	$P\bar{1}$
lattice constants			
a, b, c [Å]	14.0456(3)	10.2413(2)	9.3644(4)
	27.7475(6)	11.6123(2)	9.7193(4)
	9.1450(2)	14.9773(3)	17.3054(8)
α, β, γ [°]	90.00	83.569(1)	84.095(4)
	90.2050(10)	87.645(1)	80.708(3)
	90.00	88.005(1)	70.022(3)
cell volume [Å^3]	3564.06(13)	1767.65(6)	1458.92(11)
Z	8	2	2
density [g · cm^{-3}]	1.309	1.542	1.363
temperature [K]	150(2)	150(2)	150(2)
μ(Mo Kα) [mm^{-1}]	0.484	3.147	0.519
no. of collected rflns	81707	59425	27795
no. of unique rflns	7791	8122	7855
no. of observed rflns	6813	7691	5453
no. of parameters	439	389	356
GOF on F^2	1.047	1.056	0.856
R_1 (I > 2σ(I))	0.0298	0.0215	0.0316
wR_2 (all data)	0.0770	0.0563	0.0701

	23-Ti	**23-Zr**	**24**
formula	$C_{38}H_{38}NOP_2Ti$	$C_{45.20}H_{42.80}NP_2Zr$	$C_{34}H_{31}HfNP_2$
F_w [g · mol^{-1}]	634.53	753.16	694.03
colour	green	brown	colourless
crystal system	monoclinic	monoclinic	monoclinic
space group	*Cc*	$P2_1/c$	$P2_1$
lattice constants			
a, b, c [Å]	26.7399(5)	9.0330(2)	8.9746(2)
	16.9826(3)	23.6868(5)	18.1174(4)
	17.4040(6)	18.3998(4)	9.2379(2)
α, β, γ [°]	90.00	90.00	90.00
	126.169(1)	100.376(1)	113.196(1)
	90.00	90.00	90.00
cell volume [Å^3]	6380.2(3)	3872.49(15)	1380.63(5)
Z	8	4	2
density [g · cm^{-3}]	1.321	1.292	1.669
temperature [K]	150(2)	150(2)	150(2)
μ(Mo Kα) [mm^{-1}]	0.400	0.398	3.918
no. of collected rflns	56620	83206	42283
no. of unique rflns	14374	9592	6326
no. of observed rflns	13053	7891	6016
no. of parameters	720	391	283
GOF on F^2	1.018	1.060	1.150
R_1 (I > 2σ(I))	0.0338	0.0386	0.0261
wR_2 (all data)	0.0830	0.1080	0.0592

	25a	**26**	**27a**
formula	$C_{35}H_{31}P_2Ti$	$C_{35}H_{32}P_2Zr$	$C_{35}H_{31}HfClP_2$
F_w [g · mol^{-1}]	561.44	605.77	727.48
colour	blue	light yellow	yellow
crystal system	orthorhombic	triclinic	monoclinic
space group	$P2_12_12_1$	$P\bar{1}$	$P2_1/n$
lattice constants			
a, b, c [Å]	9.8380(1)	9.1876(2)	9.7703(2)
	15.9083(2)	9.9064(2)	18.9793(5)
	17.8806(2)	17.9370(4)	16.0631(4)
α, β, γ [°]	90.00	104.342(1)	90.00
	90.00	91.737(1)	106.139(1)
	90.00	113.795(1)	90.00
cell volume [Å^3]	2798.42(6)	1431.52(5)	2861.25(12)
Z	4	2	4
density [g · cm^{-3}]	1.333	1.405	1.689
temperature [K]	150(2)	150(2)	150(2)
μ(Mo Kα) [mm^{-1}]	0.443	0.519	3.875
no. of collected rflns	35036	30902	43029
no. of unique rflns	6664	6572	6572
no. of observed rflns	6235	6091	5874
no. of parameters	347	351	356
GOF on F^2	1.021	1.071	1.032
R_1 (I > 2σ(I))	0.0248	0.0249	0.0181
wR_2 (all data)	0.0629	0.0598	0.0419

	28-Ti	**29-Ti**	**29-Zr**
formula	$C_{46}H_{50}P_2Ti$	$C_{46}H_{44}P_2Ti$	$C_{49.50}H_{48}P_2Zr$
F_w [g · mol^{-1}]	712.70	706.65	796.04
colour	green	green	green
crystal system	monoclinic	triclinic	monoclinic
space group	$P2_1/c$	$P\bar{1}$	$C2/c$
lattice constants			
a, b, c [Å]	10.1513(2)	11.4225(2)	18.1360(3)
	42.0696(8)	12.4016(2)	12.8709(2)
	17.7599(3)	15.9682(3)	33.6094(6)
α, β, γ [°]	90.00	68.832(1)	90.00
	94.519(1)	73.958(1)	97.837(1)
	90.00	72.245(1)	90.00
cell volume [Å^3]	7561.0(2)	1973.41(6)	7772.1(2)
Z	8	2	8
density [g · cm^{-3}]	1.252	1.189	1.361
temperature [K]	150(2)	150(2)	150(2)
μ(Mo Kα) [mm^{-1}]	0.343	0.328	0.400
no. of collected rflns	114930	42877	79997
no. of unique rflns	17371	9797	8933
no. of observed rflns	14316	7811	7762
no. of parameters	891	442	477
GOF on F^2	1.052	1.063	1.066
R_1 (I > 2σ(I))	0.0416	0.0313	0.0368
wR_2 (all data)	0.1017	0.0809	0.0886

	30a	**33**	**34**
formula	$C_{95.80}H_{87.20}P_4Zr_2$	$C_{68}H_{102}Ni_2O_2P_4$	$C_{23}H_{20}NOTi$
F_w [g · mol^{-1}]	1544.78	1192.80	374.30
colour	orange	black	green
crystal system	triclinic	triclinic	orthorhombic
space group	$P\bar{1}$	$P\bar{1}$	$P2_12_12_1$
lattice constants			
a, b, c [Å]	15.5727(4)	10.2288(2)	9.3339(3)
	15.8919(4)	16.1867(4)	10.7190(4)
	16.9596(4)	19.8900(4)	18.0120(7)
α, β, γ [°]	78.389(1)	98.728(1)	90.00
	68.904(1)	97.499(1)	90.00
	79.209(1)	100.128(1)	90.00
cell volume [Å^3]	3805.35(16)	3162.25(12)	1802.10(11)
Z	2	2	4
density [g · cm^{-3}]	1.348	1.253	1.380
temperature [K]	150(2)	150(2)	150(2)
μ(Mo Kα) [mm^{-1}]	0.407	0.739	4.097
no. of collected rflns	119043	102087	17300
no. of unique rflns	17446	14517	3146
no. of observed rflns	14773	10833	3115
no. of parameters	836	661	223
GOF on F^2	1.034	1.028	1.046
R_1 (I > 2σ(I))	0.0407	0.0412	0.0270
wR_2 (all data)	0.1089	0.1115	0.0719

	35	**36**	**37**
formula	$C_{33}H_{40}NOTi$	$C_{29}H_{32}NOTi$	$C_{18}H_{26}NOZr$
F_w [g · mol^{-1}]	514.56	458.46	363.62
colour	blue	green	colourless
crystal system	monoclinic	monoclinic	monoclinic
space group	$P2_1/n$	$P2_1/n$	$P2_1/n$
lattice constants			
a, b, c [Å]	10.2713(3)	11.3630(11)	13.9518(7)
	18.9809(6)	18.274(2)	8.2467(5)
	14.0637(4)	11.9019(12)	15.4305(8)
α, β, γ [°]	90.00	90.00	90.00
	94.499(2)	106.890(2)	104.166(2)
	90.00	90.00	90.00
cell volume [Å^3]	2733.39(14)	2364.8(4)	1721.39(16)
Z	4	4	4
density [g · cm^{-3}]	1.250	1.288	1.403
temperature [K]	170(2)	173(2)	173(2)
μ(Mo Kα) [mm^{-1}]	0.339	0.383	0.638
no. of collected rflns	54329	27132	14546
no. of unique rflns	5085	6878	5054
no. of observed rflns	3869	5795	4778
no. of parameters	311	333	239
GOF on F^2	1.062	1.038	1.158
R_1 (I > 2σ(I))	0.0461	0.0328	0.0182
wR_2 (all data)	0.1192	0.0855	0.0510

	38	**40a**	**41**
formula	$C_{29}H_{33}NOZr$	$C_{37}H_{41}NOZr$	$C_{29}H_{32}ClNOZr$
F_w [g · mol^{-1}]	502.78	606.93	537.23
colour	colourless	yellow	colourless
crystal system	monoclinic	orthorhombic	orthorhombic
space group	$P2_1/c$	*Pbca*	*Pbca*
lattice constants			
a, b, c [Å]	11.3883(3)	11.7545(9)	18.029(4)
	11.9863(3)	17.1857(14)	14.410(3)
	18.2089(5)	29.603(2)	19.219(4)
α, β, γ [°]	90.00	90.00	90.00
	93.4990(10)	90.00	90.00
	90.00	90.00	90.00
cell volume [Å^3]	2480.9(2)	5980.1(14)	4992.9(17)
Z	4	8	8
density [g · cm^{-3}]	1.346	1.348	1.429
temperature [K]	173 (2)	173 (2)	173(2)
μ(Mo Kα) [mm^{-1}]	0.464	0.398	0.569
no. of collected rflns	23362	301348	29916
no. of unique rflns	7211	9105	6919
no. of observed rflns	5510	7309	5381
no. of parameters	337	406	342
GOF on F^2	1.020	1.123	1.043
R_1 (I > 2σ(I))	0.0362	0.0394	0.0322
wR_2 (all data)	0.0750	0.0853	0.0775

	42	**43**	**44**
formula	$C_{23}H_{20}ClHfNO$	$C_{48}H_{54}N_2O_2Zr_2$	$C_{34}H_{37}ClMgN_4O$
F_w [g · mol^{-1}]	540.34	1564.30	577.44
colour	colourless	colourless	colourless
crystal system	monoclinic	monoclinic	triclinic
space group	$P2_1/c$	$P2_1/c$	$P\bar{1}$
lattice constants			
a, b, c [Å]	10.4156(2)	21.179(1)	9.2425(7)
	13.2134(3)	15.106(1)	9.3328(7)
	14.3417(3)	27.301(1)	19.250(1)
α, β, γ [°]	90.00	90.00	83.431(2)
	96.875(1)	111.175(1)	86.649(2)
	90.00	90.00	73.985(2)
cell volume [Å^3]	1959.59(7)	8144(1)	1584.9(4)
Z	4	4	2
density [g · cm^{-3}]	1.832	1.276	1.210
temperature [K]	150 (2)	173 (2)	100(2)
μ(Mo Kα) [mm^{-1}]	5.472	0.310	0.173
no. of collected rflns	35298	90285	30226
no. of unique rflns	4507	21910	7265
no. of observed rflns	4014	14570	5900
no. of parameters	244	1051	374
GOF on F^2	1.059	1.009	1.034
R_1 (I > 2σ(I))	0.0177	0.0451	0.0387
wR_2 (all data)	0.0371	0.1124	0.0981

6.3. Compounds of this work

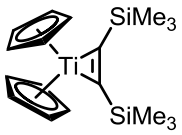

1

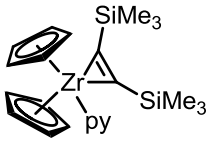

2

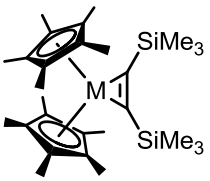

M = Ti, Zr

3-M

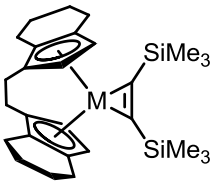

M = Ti, Zr

4-M

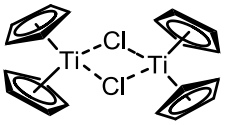

5

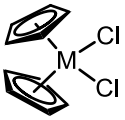

M = Ti, Zr, Hf

6-M

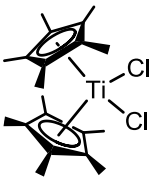

7

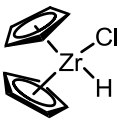

8

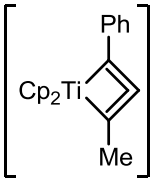

9

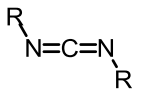

R = Mes, Dipp

10-R-R

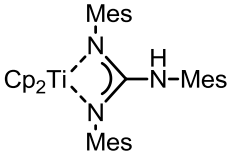

11

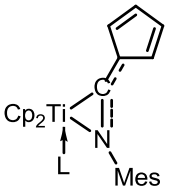

L = CN-Mes

12

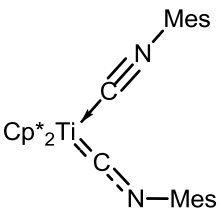

13

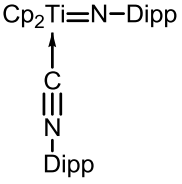

14a

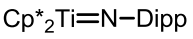

14b

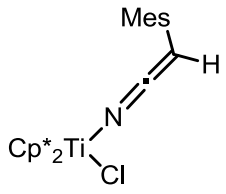

15

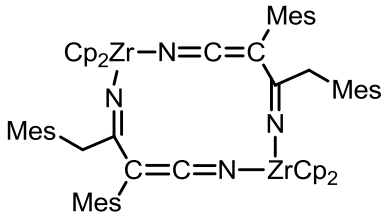

16

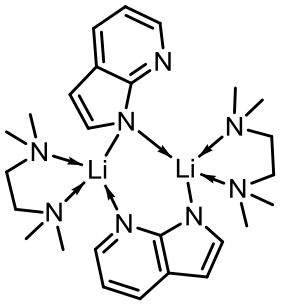

17

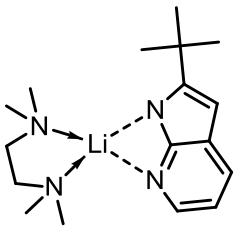

18

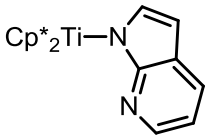

19

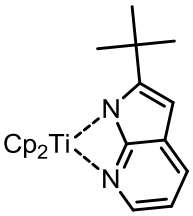

20

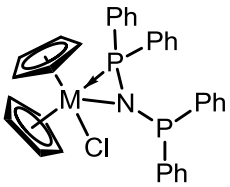

M = Zr, Hf

21-M

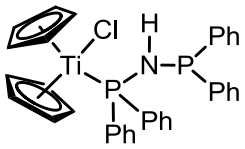

22

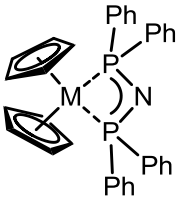

M = Zr, Hf

23-M

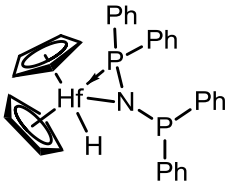

24

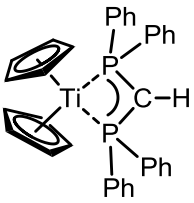

25a

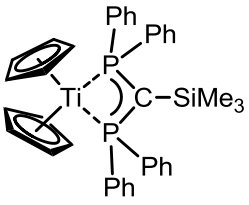

25b

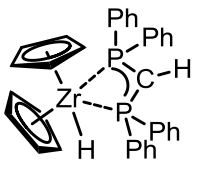

26

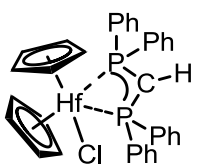

27a

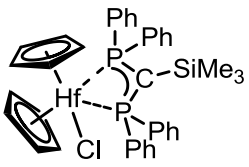

27b

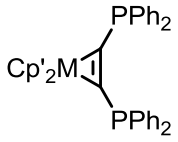

28

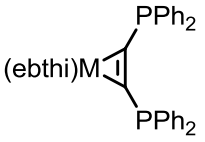

M = Ti, Zr

29-M

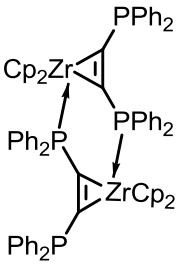

30a

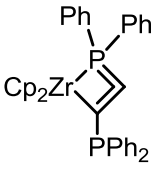

30b

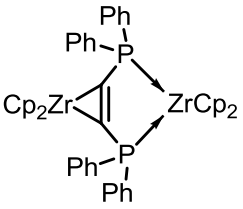

31

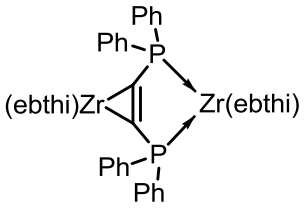

32

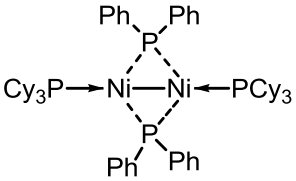

33

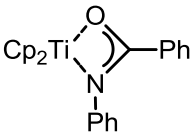

34

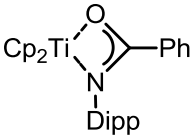

35

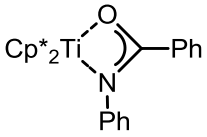

36

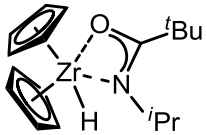

37

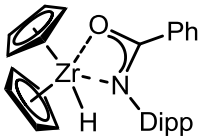

38

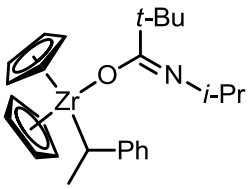

39a

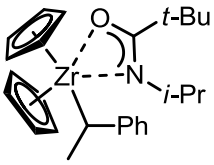

39b

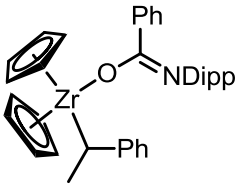

40a

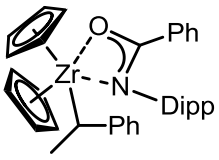

40b

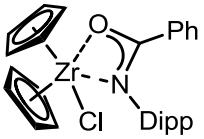

41

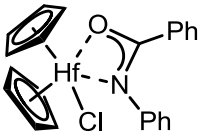

42

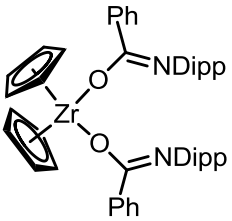

43

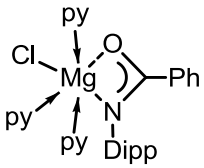

44